NOTE TO USERS

Copyrighted materials in this document have not been filmed at the request of the author.

Figures 3.2 to 3.19, pgs 60 to 77
Figures 4.1 to 4.19 pgs 96 to 114
Figures c.1 to c.19 pgs 175 to 193

This reproduction is the best copy available.

UMI

University of Alberta

Regional Hydrogeological Characterization of the Northeastern Margin in the Williston Basin

by

Daniele Davide Palombi ©

A thesis submitted to the Faculty of Graduate Studies and Research
in partial fulfillment of the requirements for the degree of Master of Science

Department of Earth and Atmospheric Sciences

Edmonton, Alberta

Fall 2008

Library and
Archives Canada

Published Heritage
Branch

395 Wellington Street
Ottawa ON K1A 0N4
Canada

Bibliothèque et
Archives Canada

Direction du
Patrimoine de l'édition

395, rue Wellington
Ottawa ON K1A 0N4
Canada

Your file Votre référence
ISBN: 978-0-494-47385-6
Our file Notre référence
ISBN: 978-0-494-47385-6

NOTICE:
The author has granted a non-exclusive license allowing Library and Archives Canada to reproduce, publish, archive, preserve, conserve, communicate to the public by telecommunication or on the Internet, loan, distribute and sell theses worldwide, for commercial or non-commercial purposes, in microform, paper, electronic and/or any other formats.

The author retains copyright ownership and moral rights in this thesis. Neither the thesis nor substantial extracts from it may be printed or otherwise reproduced without the author's permission.

AVIS:
L'auteur a accordé une licence non exclusive permettant à la Bibliothèque et Archives Canada de reproduire, publier, archiver, sauvegarder, conserver, transmettre au public par télécommunication ou par l'Internet, prêter, distribuer et vendre des thèses partout dans le monde, à des fins commerciales ou autres, sur support microforme, papier, électronique et/ou autres formats.

L'auteur conserve la propriété du droit d'auteur et des droits moraux qui protège cette thèse. Ni la thèse ni des extraits substantiels de celle-ci ne doivent être imprimés ou autrement reproduits sans son autorisation.

In compliance with the Canadian Privacy Act some supporting forms may have been removed from this thesis.

While these forms may be included in the document page count, their removal does not represent any loss of content from the thesis.

Conformément à la loi canadienne sur la protection de la vie privée, quelques formulaires secondaires ont été enlevés de cette thèse.

Bien que ces formulaires aient inclus dans la pagination, il n'y aura aucun contenu manquant.

Canada

Onore, Rispetto, Sacrificio

per

Antonio Palombi & Valentino Vona

ABSTRACT

A hydrostratigraphic framework of 19 aquifers and 13 aquitards has been developed across Saskatchewan and Manitoba in the Williston Basin. Detailed hydrochemical analyses have identified four water compositions: Type 1 (Ca-SO_4) waters, TDS less than 10 g/L, are found in recharge zones; Type 2 (Na-Cl) brines represent evolved waters derived from halite dissolution; Type 3 (Na-HCO_3) waters denote meteoric or subglacial recharge that originates from Ca-HCO_3 compositions; and Type 4 (Na-SO_4) brackish waters represent a mixed composition between meteoric and Na-Cl end-members. The central Williston Basin has horizontal fluid flow traveling up-dip toward the northeast. Vertical flow is evident toward the basin margin. Salt dissolution promotes upward vertical flow and where present the Prairie Evaporite Formation forms a competent barrier between aquifers. Density-dependent flows are found in southern Saskatchewan. Regional hydrogeology is imperative to discern and comprehend the chemical evolution of basinal brines and dynamics of brines during meteoric/subglacial recharge.

ACKNOWLEDGEMENTS

The endeavors and accomplishments of this thesis research can be attributed to a team of people. My supervisor, Dr. Ben Rostron, has provided an environment that facilitated advanced learning and development. I sincerely thank Ben for his enthusiasm, dedication and support of my studies and decisions. His enjoyment of geology and hydrogeology is contagious and I consider learning from Ben and the University of Alberta Hydrogeology Group a fortunate opportunity.

A vital person from early on in my studies until the very end was Dr. Carl Mendoza. Carl introduced me to the science of hydrogeology and is the principal reason as to why I study geology and hydrogeology today. I earnestly thank Carl for his support, reflective knowledge and advice through the years. The understanding of hydrogeology that Carl passes to all of his students provides a foundation upon which to build a successful career.

This research project was funded through teaching assistantships from the Department of Earth and Atmospheric Sciences and grants received by Dr. Rostron from the Economic Innovation and Technology Council (EITC) and the Natural Sciences and Engineering Research Council of Canada (NSERC).

I thank all of the geoscientists and geologists at the Ministry of Energy and Resources and Manitoba Science, Technology, Energy and Mines. The geological framework and data they provided for the Targeted Geoscience Initiatives 2 Project (TGI-2) was fundamental for the hydrogeology completed here. In particular, I specifically thank Kim Kreis, Arden Marsh, Melinda Yurkowski, and Megan Love at the Subsurface Lab in Regina for all their time and persistence toward completing the geology. The geological team at the Petroleum Branch in Manitoba, I equally thank and specifically Greg Keller and Michelle Nicolas for GIS and geological support throughout the project.

I also thank all the support staff in the Department of Earth and Atmospheric Sciences. In particular, Valery Companiytsev I thank for his immediate assistance in database and network issues and Michael Fisher for cartographic support.

To all my colleagues from the Hydrogeology Group, I thank you for friendship and respite. I wholeheartedly thank K. Daniel Khan for the opportunity to work along side him and learn computational geoscience and hydrogeology from an expert. To my friend Gavin Jensen, I thank so much for making it possible to laugh and have a great time through countless evenings while completing our degrees together. I also thank Brian Smerdon for being a pillar upon which many of us relied on for stability. Brian's effort in making time for others is just one reason why all graduate students appreciate him. I thank Brian helping us work, helping us rest, and helping us play. All of the relationships built with graduate students of the past and present, specifically Joe Riddell and Cate Hydeman, will always have that common thread of having endured the hydrogeology program. Finally, I also thank all of my colleagues at the Alberta Research Council who allowed me to pursue my career and still provided solid encouragement while dually working on my thesis.

My family I recognize as the most important element toward the completion of this degree and ultimately my success and happiness in life. My parents, Severino and Rita Palombi, have given me the strength, ability and work ethic to accomplish anything I dream of pursuing. Nothing is impossible if you have the courage and will to sacrifice for a better future. The assistance, patience, and love I received from my wife, Audrey Palombi, I could have not continued without. Audrey dedicated everything toward the success of this degree and demonstrated the exact morals that guide us in a long life of happiness and success. To my family, I specifically acknowledge the patience, understanding and support from Antonio and Jill Palombi, David and Rosa Donovan, and Rosa and Agostino Palombi while completing this phase of my life.

TABLE OF CONTENTS

1.0 INTRODUCTION 1

1.1 BACKGROUND 1

1.2 MOTIVATION 2

1.3 RESEARCH OBJECTIVES 3

2.0 STUDY AREA, GEOLOGY, AND HYDROGEOLOGY 6

2.1 STUDY AREA 6

2.2 GEOLOGICAL OVERVIEW 7

2.2.1 Regional Geologic Setting 7

2.2.2 Lithostratigraphic Framework 8

2.3 REGIONAL HYDROGEOLOGY 19

2.3.1 Hydrostratigraphic Framework 20

2.3.2 Lower Paleozoic Aquifers and Aquitards 21

2.3.3 Mississippian Aquifers and Aquitards 26

2.3.4 Mesozoic Aquifers and Aquitards 27

3.0 HYDROCHEMISTRY: DISTRIBUTION AND COMPOSITION OF FORMATION WATERS 38

3.1 DATA AND METHODOLOGIES 38

3.1.1 Water Chemistry Culling 38

3.1.2 Interval Testing Verification 39

3.2 RESULTS: FORMATION WATER CHEMISTRY 40

3.2.1 Lower Paleozoic Aquifers 41

3.2.2 Mississippian Aquifers........46

3.2.3 Mesozoic Aquifers........49

3.3 MAJOR IONS........51

3.4 FORMATION WATER CLASSIFICATION........55

3.4.1 Type Water Designation........56

4.0 REGIONAL GROUNDWATER FLOW AND DRIVING FORCES ON FORMATION WATERS........81

4.1 DATA AND METHODOLOGIES........81

4.1.1 Pressure Data Culling........82

4.2 RESULTS: POTENTIOMETRIC ANALYSIS AND DRIVING FORCES........82

4.2.1 Lower Paleozoic Aquifers........86

4.2.2 Mississippian Aquifers........88

4.2.3 Mesozoic Aquifers........89

4.3 VERTICAL PRESSURE GRADIENTS........91

5.0 REGIONAL HYDROGEOLOGICAL SYNTHESIS........119

5.1 REGIONAL HYDROCHEMISTRY IN THE NORTHEASTERN CORNER OF THE WILLISTON BASIN........119

5.1.1 Overall Water Types........119

5.1.2 Spatial Distribution of Water Types........122

5.2 SALT DISSOLUTION........125

5.3 DRIVING FORCES ON FORMATION WATERS........126

5.3.1 Vertical Pressure Gradients ... 128

5.3.2 Flow reversals in the northeastern margin of the Williston Basin ... 131

5.4 IMPLICATIONS FOR SUBGLACIAL RECHARGE IN THE BASIN ... 133

5.4.1 Evaporite Dissolution ... 135

5.4.2 Basin Overpressures ... 135

5.4.3 Water Driving Force and Mesozoic Under-pressuring ... 136

5.4.4 Glacial Residence Time ... 137

6.0 CONCLUSIONS AND RECOMMENDATIONS ... 145

6.1 CONCLUSIONS OF THE REGIONAL HYDROGEOLOGICAL CHARACTERIZATION ... 145

6.2 RECOMMENDED AREAS OF FUTURE RESEARCH ... 148

7.0 REFERENCES ... 149

APPENDIX A: WATER CHEMISTRY CULLING ... 169

APPENDIX B: PRESSURE DATA CULLING ... 173

APPENDIX C: FRESHWATER HYDRAULIC HEAD MAPS ... 175

APPENDIX D: CALCULATING DRIVING FORCES ON FORMATION WATERS ... 194

LIST OF TABLES

Table 3.1 Number of chemistry samples and the range of TDS 58

Table 4.1 Number of pressure samples and the range of hydraulic heads 94

Table 4.2 Hydraulic and water driving force gradients 95

LIST OF FIGURES

Figure 1.1 Hydrostratigraphic columns 5

Figure 2.1 TGI-2 study area in the Williston Basin 31

Figure 2.2 Structural cross-section A to A' 32

Figure 2.3 Digital elevation model of the northeast portion in the Williston Basin 33

Figure 2.4a Precambrian to Silurian stratigraphic correlation chart 34

Figure 2.4b Devonian stratigraphic correlation chart 35

Figure 2.4c Mississippian stratigraphic correlation chart 36

Figure 2.4d Triassic to Quaternary stratigraphic correlation chart 37

Figure 3.1 Interval testing of drill stem tests and water sampling intervals 59

Figure 3.2 Total Dissolved Solids in the Cambro-Ordovician Aquifer 60

Figure 3.3 Total Dissolved Solids in the Yeoman Aquifer 61

Figure 3.4 Total Dissolved Solids in the Ordo-Silurian Aquifer 62

Figure 3.5 Total Dissolved Solids in the Winnipegosis Aquifer 63

Figure 3.6 Total Dissolved Solids in the Manitoba Aquifer 64

Figure 3.7 Total Dissolved Solids in the Duperow Aquifer 65

Figure 3.8 Total Dissolved Solids in the Birdbear Aquifer 66

Figure 3.9 Total Dissolved Solids in the Bakken Aquifer 67

Figure 3.10 Total Dissolved Solids in the Souris Valley Aquifer 68

Figure 3.11 Total Dissolved Solids in the Tilston Aquifer 69

Figure 3.12 Total Dissolved Solids in the Alida Aquifer 70

Figure 3.13 Total Dissolved Solids in the Frobisher Aquifer 71

Figure 3.14 Total Dissolved Solids in the Midale Aquifer.........72

Figure 3.15 Total Dissolved Solids in the Ratcliffe Aquifer.........73

Figure 3.16 Total Dissolved Solids in the Poplar Aquifer.........74

Figure 3.17 Total Dissolved Solids in the Jurassic Aquifer.........75

Figure 3.18 Total Dissolved Solids in the Mannville Aquifer.........76

Figure 3.19 Total Dissolved Solids in the Newcastle Aquifer.........77

Figure 3.20 Major Ionic Constituents in the Lower Paleozoic Aquifers.........78

Figure 3.21 Major Ionic Constituents in the Mississippian Aquifers.........79

Figure 3.22 Major Ionic Constituents in the Mesozoic Aquifers.........80

Figure 4.1 Water Driving Force in the Cambro-Ordovician Aquifer.........96

Figure 4.2 Water Driving Force in the Yeoman Aquifer.........97

Figure 4.3 Water Driving Force in the Ordo-Silurian Aquifer.........98

Figure 4.4 Water Driving Force in the Winnipegosis Aquifer.........99

Figure 4.5 Water Driving Force in the Manitoba Aquifer.........100

Figure 4.6 Water Driving Force in the Duperow Aquifer.........101

Figure 4.7 Water Driving Force in the Birdbear Aquifer.........102

Figure 4.8 Water Driving Force in the Bakken Aquifer.........103

Figure 4.9 Water Driving Force in the Souris Valley Aquifer.........104

Figure 4.10 Water Driving Force in the Tilston Aquifer.........105

Figure 4.11 Water Driving Force in the Alida Aquifer.........106

Figure 4.12 Water Driving Force in the Frobisher Aquifer.........107

Figure 4.13 Water Driving Force in the Midale Aquifer.........108

Figure 4.14 Water Driving Force in the Ratcliffe Aquifer........109
Figure 4.15 Water Driving Force in the Poplar Aquifer........110
Figure 4.16 Water Driving Force in the Jurassic Aquifer........111
Figure 4.17 Water Driving Force in the Mannville Aquifer........112
Figure 4.18 Water Driving Force in the Newcastle Aquifer........113
Figure 4.19 Locations of pressure verus depth profiles........114
Figure 4.20 Pressure versus depth profile for block 1........115
Figure 4.21 Pressure versus depth profile for block 2........116
Figure 4.22 Pressure versus depth profile for block 3........117
Figure 4.23 Pressure versus depth profiles for blocks 4-7........118
Figure 5.1 Water types in the Lower Paleozoic aquifers........139
Figure 5.2 Water types in the Mississippian aquifers........140
Figure 5.3 Water types in the Mesozoic aquifers........141
Figure 5.4 Summary of horizontal and vertical flow fields........142
Figure 5.5 Schematic overview of regions where density-flows are significant........143
Figure 5.6 Cross-section B-B' depicting conceptual flow field........144
Figure C.1 Freshwater Hydraulic Head in the Cambro-Ordovician Aquifer........175
Figure C.2 Freshwater Hydraulic Head in the Yeoman Aquifer........176
Figure C.3 Freshwater Hydraulic Head in the Ordo-Silurian Aquifer........177
Figure C.4 Freshwater Hydraulic Head in the Winnipegosis Aquifer........178
Figure C.5 Freshwater Hydraulic Head in the Manitoba Aquifer........179
Figure C.6 Freshwater Hydraulic Head in the Duperow Aquifer........180

Figure C.7 Freshwater Hydraulic Head in the Birdbear Aquifer 181
Figure C.8 Freshwater Hydraulic Head in the Bakken Aquifer 182
Figure C.9 Freshwater Hydraulic Head in the Souris Valley Aquifer 183
Figure C.10 Freshwater Hydraulic Head in the Tilston Aquifer 184
Figure C.11 Freshwater Hydraulic Head in the Alida Aquifer 185
Figure C.12 Freshwater Hydraulic Head in the Frobisher Aquifer 186
Figure C.13 Freshwater Hydraulic Head in the Midale Aquifer 187
Figure C.14 Freshwater Hydraulic Head in the Ratcliffe Aquifer 188
Figure C.15 Freshwater Hydraulic Head in the Poplar Aquifer 189
Figure C.16 Freshwater Hydraulic Head in the Jurassic Aquifer 190
Figure C.17 Freshwater Hydraulic Head in the Mannville Aquifer 191
Figure C.18 Freshwater Hydraulic Head in the Newcastle Aquifer 192
Figure C.19 Freshwater Hydraulic Head in the Judith River Aquifer 193
Figure D.1 Water Driving Force Components 196

1.0 INTRODUCTION

1.1 BACKGROUND

Aqueous fluids migrating in sedimentary basins are important carriers of dissolved metals and petroleum, and often control the formation of exploitable mineral and oil deposits (Garven, 1985; Chapman, 1987; Ge and Garven, 1989; Bethke and Marshak, 1990; Cumming et al., 1990). The Williston Basin hosts an active groundwater flow system and contains many natural resources that are impacted by that flow system. A diverse range of hydrogeologically influenced economic resources such as water, minerals, and hydrocarbons are present within the sediments of the Williston Basin. A clear understanding of regional hydrogeological and hydrochemical processes is essential to accessing and exploiting these resources (Rostron et al., 2002). Comparing hydrochemical compositions and distributions of subsurface waters are fundamental to hydrogeological mapping for delineating patterns of regional flow and basin evolutionary processes (Chebotarev, 1955; Back, 1961; Clayton et al., 1966; Collins, 1975; Tóth, 1984; Hanor, 1994; Lowenstein et al., 2003). Understanding the hydrogeology of the Williston Basin has been hampered due to the fact that several international and provincial/state boundaries partition the basin.

On a basin-wide scale, the regional hydrochemistry of Cambrian to Devonian aquifers has only been conducted by Benn and Rostron (1998). The Nisku Aquifer was characterized across the Western Canada Sedimentary Basin by Alkalali (2002). Jensen (2007) completed a regional assessment of the fluid flow and isotope geochemistry for the Ratcliffe, Midale, and Frobisher Beds in portions of Montana, North Dakota, and Saskatchewan. A detailed cross-border analysis between Saskatchewan and Manitoba, for the complete Phanerozoic, has been completed by Palombi and Rostron (2006; this thesis). On the American side of the basin, previous studies of regional hydrogeology and hydrochemistry have focused primarily on regional water supply assessments by the United States Geological Survey (e.g., Downey, 1984a, b; Neuzil et al., 1982; Bredehoft et al., 1983; Downey et al., 1987; Downey and Dinwiddie, 1988; Berg et al., 1994; Busby et al., 1995; DeMis, 1995; Lefever, 1998). On the Canadian side of the basin, regional hydrogeological mapping has been presented, albeit on a limited set of aquifers, by Hannon (1987) and Bachu and Hitchon (1996). In Saskatchewan, Kreis et al. (1991), Toop and Tóth (1995), and Bernatsky (1998) investigated pieces of the province. In Manitoba, Betcher et al. (1995) conducted groundwater studies discussed in terms of availability, yield, and quality, mainly for domestic and industrial supply. In the northeastern margin, Grasby (2000) and Grasby and Betcher (2002) have sampled saline spring waters along the western shore of Lake Winnipegosis to better understand Pleistocene glaciation and the geochemistry of discharge waters. Khan and Rostron (2004) completed detailed cross-border regional hydrogeological mapping studies between the Canadian and American sides of the basin for Montana, North Dakota and Saskatchewan.

1.2 MOTIVATION

There are five motivations for this thesis research:

1) Despite the previous works, obvious cross-border geological and hydrogeological issues still exist with very few investigations straddling the political boundaries. There are no cross-border hydrogeological/hydrochemical studies completed between Saskatchewan and Manitoba that together form the discharge zone of the Williston Basin.
2) Considerably newer data have become available as a result of deep drilling for petroleum exploration (Haidl et al., 1996) that was not included in previous hydrochemical and hydrogeological studies.
3) The previous studies all lack detail in the hydrostratigraphy and definition of aquifers and aquitards, despite the fact that petroleum geologists have long recognized the geological heterogeneity in the basin. Many formations are incorrectly grouped to form one large aquifer, specifically the Mississippian aquifer and the Carbonate Rock Aquifer (Figure 1.1; Grasby and Betcher, 2002).

4) Many of the previous characterizations utilized automated-culling procedures that were devised for Alberta Basin waters (Hitchon and Brulotte, 1994). Furthermore, these automated procedures were translated to large hydrogeological databases and underlying errors were never clarified or resolved.

5) The estimation of in-situ formation water densities and the calculation of density-corrected driving forces have never been completed for the entire stratigraphic section in the northeastern margin of the Williston Basin.

To answer the obvious cross-border geological correlation issues and to increase the hydrostratigraphic resolution for regional studies, a new geological model would be required. Thus, a joint project between Saskatchewan Industry and Resources (SIR; now Ministry Energy and Resources - MER), Industry Economic Development and Mines (IEDM) of Manitoba (now Manitoba Science, Technology, Energy and Mines - STEM), Natural Resources Canada (NRCan), and the University of Alberta, was initiated. This project was titled "The Williston Basin Architecture and Hydrocarbon Potential Project" (Kreis et al., 2004). As part of NRCan's Targeted Geoscience Initiatives (TGI-2), this project was intended to enhance previous geoscience-framework studies such as the International Energy Agency (IEA) Weyburn CO_2 Monitoring and Storage Project (Whittaker and Gilboy, 2003).

1.3 RESEARCH OBJECTIVES

The overall objective of the thesis study is to characterize the complete regional groundwater flow system in the TGI-2 project area and discharge zone of Williston Basin through high-resolution regional mapping of the hydrochemistry and hydrodynamics for the entire Phanerozoic succession. The synthesis of the regional hydrogeological characterization would lead to new insights of the Williston Basin paleohydrogeology. Characterization in this systematic approach to geology and hydrogeology invariable results in a better understanding of the chemical evolution and dynamics of basinal brines, groundwater flow, the sources of salinity, and the paleohydrogeology of a sedimentary basin.

Specifically, the objectives of this thesis research are to:

1) Define and delineate hydrostratigraphy (aquifers and aquitards) consistently across Saskatchewan and Manitoba using the new lithostratigraphic framework devised for the TGI-2 project.
2) Analyze and interpret the distribution and composition of formation waters.
3) Quantify the regional hydrodynamics and water driving forces using potentiometric surfaces, density-dependent fluid flow analysis and vertical pore-pressure gradients.
4) Synthesize the hydrogeochemistry and hydrodynamics of the northeastern corner of the Williston Basin.

This thesis is an assemblage of six core chapters. Chapter Two provides a comprehensive overview of the study area, geology and hydrogeology of the Williston Basin in reference to the TGI-2 project area and the hydrostratigraphic model devised for this characterization. Chapter Three presents the results of the hydrochemical evaluation describing the distribution and compositions of formation waters. Therein, the data and methodologies are also discussed for both Chapters Three and Four. Chapter Four provides the results of the hydrodynamics and regional groundwater flow regimes including the water driving force analysis. The regional hydrogeological synthesis and interpretations of the findings are contained within Chapter Five. Furthermore, Chapter Five makes the linkages and integrative analysis to the manifestations and implications of the effects of glaciation on the basin hydrodynamics. Finally, a numbered list of the main conclusions of the research is located in Chapter Six.

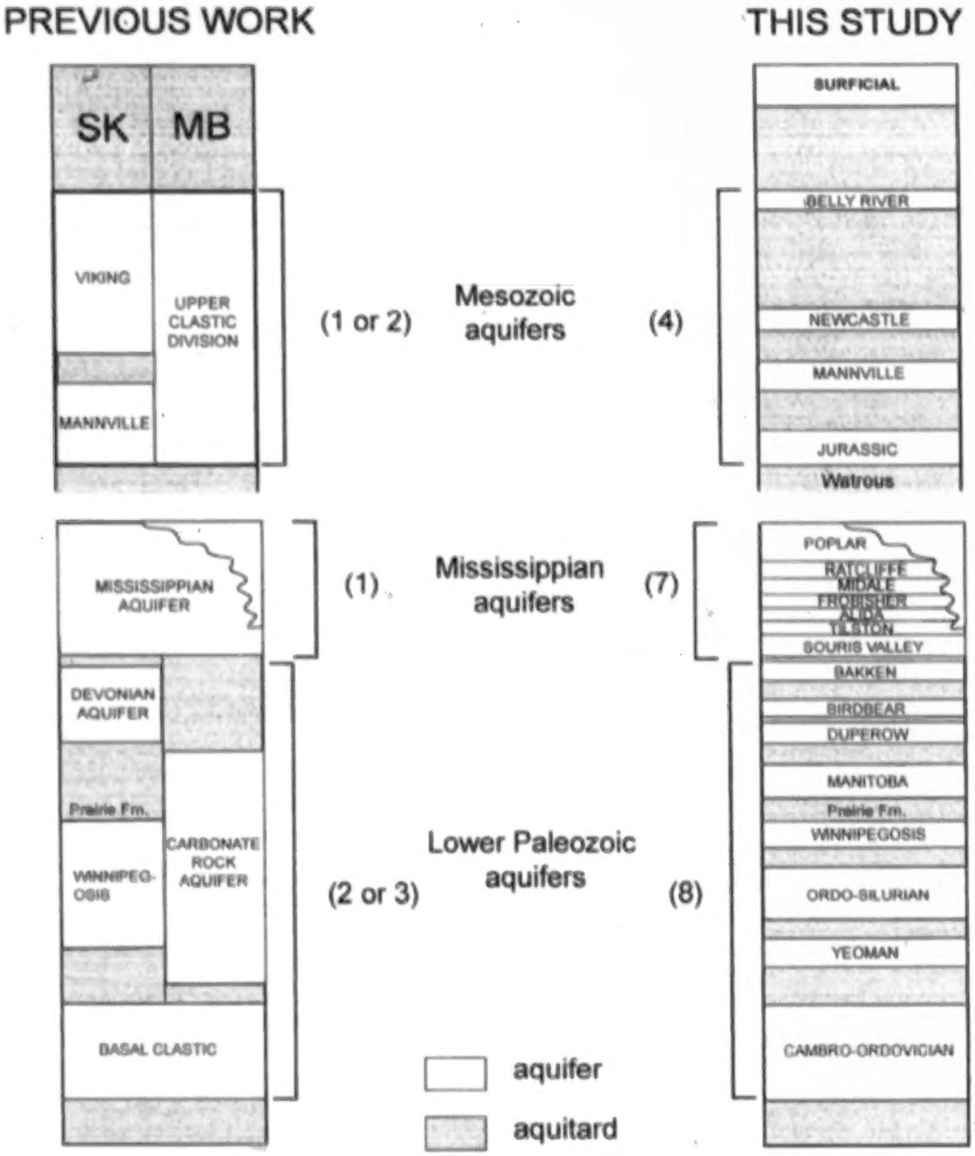
PREVIOUS WORK
THIS STUDY
SK
MB
VIKING
MANNVILLE
UPPER CLASTIC DIVISION
(1 or 2)
Mesozoic aquifers
(4)
SURFICIAL
BELLY RIVER
NEWCASTLE
MANNVILLE
JURASSIC
Watrous
MISSISSIPPIAN AQUIFER
(1)
Mississippian aquifers
(7)
POPLAR
RATCLIFFE
MIDALE
FROBISHER
ALIDA
TILSTON
SOURIS VALLEY
BAKKEN
BIRDBEAR
DUPEROW
MANITOBA
Prairie Fm.
WINNIPEGOSIS
ORDO-SILURIAN
YEOMAN
CAMBRO-ORDOVICIAN
DEVONIAN AQUIFER
Prairie Fm.
WINNIPEG-OSIS
CARBONATE ROCK AQUIFER
BASAL CLASTIC
(2 or 3)
Lower Paleozoic aquifers
(8)
aquifer
aquitard

Figure 1.1. Hydrostratigraphic columns representative of previous research (left-hand side) completed for Saskatchewan and Manitoba individually, compared to the aquifer delineation, integrated across provincial borders, in this study (right-hand side). Notice the number of aquifers recognized in this study versus the previous research.

2.0 STUDY AREA, GEOLOGY, AND HYDROGEOLOGY

2.1 STUDY AREA

The TGI-2 project study area ranges from longitude 106°W through 96°W, is bounded to the south by the 49th parallel, and to the north and northeast by the edge of Phanerozoic cover within the Williston Basin (Figure 2.1). The Williston Basin is an intracratonic sedimentary basin centred in northwestern North Dakota and extending outward into regions of Saskatchewan, Manitoba, South Dakota and Montana (Figure 2.1). This roughly circular area, ranging from about 98.5°W to 108.5°W and 45°N to 51.5°N, covers approximately 518,000 km^2 (Brown and Brown, 1987). This study area encompasses the IEA Weyburn CO_2 Monitoring and Storage Project area in Canada (Figure 2.1).

The area under investigation is a cross-border analysis of Saskatchewan and Manitoba with an emphasis on areas outside the traditional limits of hydrocarbon production and also incorporates the erosional edge of the Williston Basin. The regional hydrogeological characterization is completed on the rocks of lowermost Cambrian to uppermost Cretaceous periods and reaches a maximum thickness of approximately 3300 m offset slightly north of the basin's depocentre (Figure 2.2).

The basin is bounded by high relief features in the south and southwest, mainly the Black Hills of South Dakota, Bighorn Mountains, Beartooth Mountains and Little Rocky Mountains of Montana, by the Canadian Shield in the north and northeast, and bordered to the east by the Sioux Arch of the Dakotas and southeastern Manitoba (Figure 2.1; Sloss, 1987; Kent and Christopher, 1994). Topography across the study area is highest on the southwestern corner of Saskatchewan at approximately 900 metres, and the topographic low around Lake Winnipeg in Manitoba is roughly 220 metres (Figure 2.3).

2.2 GEOLOGICAL OVERVIEW

The regional geology of the Williston Basin has been extensively examined previously in the United States (Gerhard et al., 1982; Peterson and MacCary, 1987; Gerhard and Anderson, 1988) and Canada (Mossop and Shetsen, 1994) due to hydrocarbon exploration. More recent geological characterizations (Whittaker et al., 2004; Christopher et al., 2006; Halabura, 2006; Kreis et al., 2006; Nicolas, 2006), have focused on the definition of a regional stratigraphic framework and geometry for selected parts (i.e. northeastern margin) of the basin in fulfillment of CO_2 storage, stratigraphy, natural gas and petroleum studies in the provinces. These compilations and revised mapping, largely completed by SIR and IEDM for the Weyburn CO_2 (Whittaker et al., 2004) and TGI-2 (Kreis et al., 2004) projects, has resulted in a succinct and consistent interpretation for the study area described in the following sub-sections.

2.2.1 Regional Geologic Setting

Only a summary of the geology will be described here in context and applicability to this regional hydrogeology investigation. For further descriptions refer to Mossop and Shetsen (1994), Whittaker et al. (2004), and more recent geological characterizations (e.g., Christopher et al., 2006; Halabura, 2006; Kreis et al., 2006; Nicolas, 2006).

Initial development phases of the Williston Basin began during the Late Cambrian to Early Ordovician periods and continued episodically until the Late Cretaceous period (Kent and Christopher, 1994). Regional tectonism was dominated by foreland evolution associated with the Laramide orogeny along the western margin of the North American craton (Kent and Christopher, 1994). The Phanerozoic succession in the basin begins with the basal sandstones of the Cambrian and Early Ordovician and concludes with the Quaternary glacial drift packages (Figures 2.4a-d). Whittaker et al. (2004) subdivided the rocks of the basin into three broad packages for description and analysis: 1) Lower Paleozoic strata ranging from the basal Deadwood Formation to the uppermost Bakken Formation (Three Forks Group) are composed primarily of carbonates, evaporates, and minor sandstones and shales; 2) Mississippian strata ranging from the lowermost Souris Valley Formation (Lodgepole Formation equivalent in Manitoba) to the uppermost Poplar Beds (Charles Formation) consisting largely of expansive shallow and deep platform carbonates; and 3) Mesozoic strata ranging from the Watrous Formation (Triassic-Jurassic periods) to the Judith River Formation (Upper Cretaceous period). The upper package is volumetrically-dominated by thick, basin-fill shales encasing sandstones and siltstones. Important hiatuses existing in the lithostratigraphic framework are the unconformities that stratigraphically represent periods of geologic change in the evolution and generation of the Williston Basin (Figures 2.4a-d).

2.2.2 Lithostratigraphic Framework

One of the main objectives for the TGI-2 project was to integrate the geology across the provincial border. SIR and IEDM focused on developing a consistent framework that would be utilized for this cross-border analysis (Figure 2.4a-d). Previous stratigraphic isolation between the provinces (Kent 1968; McCabe, 1980; Barchyn, 1982; Haidl, 1988; Christopher, 2003) would be overcome by the generation of an integrated framework bringing the geology and nomenclature into a seamless model. Williston Basin nomenclature issues and stratigraphic inconsistencies have persisted over many years of geological studies. Consistency in the stratigraphic correlations was attempted by having individual researchers focus on specific packages of rocks. A major focus in developing the lithostratigraphic framework was to further develop a geological database to be later utilized for establishing a well-defined hydrostratigraphic model. The hydrogeology portion of the TGI-2 project was designed to correlate with the geological model.

As previously defined, the three packages of rock (Lower Paleozoic, Mississippian and Mesozoic systems) will serve as a grouping to discuss the geology and hydrogeology of this thesis. The next three sections describe the lithological and sedimentological characteristics for the formations. For all hydrogeologically-mapped formations the spatial extents, outcrop locations, and subcrop edges can be found within the maps of Chapters Three and Four.

Lower Paleozoic Strata

Cambrian-aged sandstones and shales are the first of the Phanerozoic strata to reflect the existence of the Williston Basin (LeFever et al., 1987; Peterson and MacCary, 1987). The Deadwood Formation thickens westward and in the east represents a nearshore sandstone body from a Precambrian shield source (Kent, 1994; Potter, 2006). In the centre of the basin, LeFever et al. (1987) report a thickness of more than 270 m, and describe the formation as composed primarily of siliciclastic rocks of quartz arenites, quartz wackes, siltstones, and lesser amounts of carbonate rocks, with textures from mudstones to grainstones (Paterson, 1988). Deadwood Formation strata are overlain unconformably by the Winnipeg Formation (Ordovician in age) representing a global drop in sea level (Kent and Christopher, 1994).

The Winnipeg Formation is opposite to that of the Deadwood Formation in that it wedges out westward from Manitoba along an irregular, northerly-oriented edge eventually overlapping the Deadwood Formation in western Saskatchewan (Norford et al., 1994; Potter, 2006). Vigrass (1971) suggested that the Winnipeg Formation is an infill of a topographic depression on an eroded Deadwood Formation. In Saskatchewan it reaches a thickness of 67 m and eastward into Manitoba it progressively thins to 24 m and then outcrops along the islands and shores of the southern part of Lake Winnipeg (Figure 2.3; Porter and Fuller, 1959). Lithologically, it is comprised of well sorted quartz sandstone in the lower part and grading upward it consists of waxy shales interbedded with thin sandstones (Porter and Fuller, 1959). For further detail, Potter (2006) describes the relationships of the Cambro-Ordovician stratigraphy to the paleotopography on the basement.

Strata of the Red River Formation overlie shales and sandstones of the Winnipeg Formation sharply and with slight unconformity (Kendall, 1976). The thickness and distribution of the Red River Formation can be correlated throughout the Williston Basin. However, in the study area it varies from approximately 215 m in the central part of the basin to 150 m at the southern end of the outcrop belt (McCabe, 1980). The lithology of the Red River Formation varies with distribution but in the central area of the Manitoba outcrop belt the lower Red River Formation is comprised of a basal fossiliferous, mottled dolomitic limestone, overlain by a cherty dolomite. This is overlain by a second sequence of fossiliferous, mottled, dolomitic limestones (McCabe, 1980). In Saskatchewan and Manitoba, the lower member of the Red River Formation is termed the Yeoman Formation and the upper portion is referred to as the Herald Formation (Figure 2.4a; Haidl et al., 1996).

The Stony Mountain Formation, that is Ordovician-aged, overlies the Red River Formation sharply and extends throughout the basin. All of the Lower Paleozoic formations thin to the north and east toward the limit of Phanerozoic deposition. Near the United States border the Stony Mountain Formation is approximately 45 m thick and successively thins northeastward. Towards the centre of the basin, the formation consists dominantly of Gunn Member calcareous shales and highly fossiliferous limestones. Penitentiary Member dolomites overlie this and are followed by the dolomites of the Gunton Member that become progressively denser towards the north (Kendall, 1976).

The Stonewall Formation spans from the Late Ordovician to Early Silurian. In the Stonewall Formation, the thickness varies from approximately 15 to 34 m in the Manitoba outcrop belt and towards the basin centre (Kendall, 1976). Smith (1964) describes that it consists largely of finely crystalline dolomite with the lower member containing more sandy-dolomite. A nodular anhydrite, defined as the "Stonewall Anhydrite" (Porter and Fuller, 1959; Kendall, 1976), occurs toward the base of the formation and averages three metres thick.

Grading into the Lower and Upper Silurian, the Interlake Formation extends throughout the basin and ranges from about 50 to 110 m in the Manitoba outcrop belt to 335 m in North Dakota (Haidl, 1987, 1988; Osadetz and Haidl, 1989). The mineralogy of the Interlake Formation consists largely of very finely crystalline to sublithographic dolomites, interbedded with coarse fossil fragments of oolitic, stromatolitic and biohermal interbeds (Haidl, 1987). The Interlake Formation is overlain by the Ashern Formation (Devonian period) with a gentle angular unconformity (Osadetz and Haidl, 1989). Details of the stratigraphy and hydrocarbon potential of the Silurian-Interlake strata in southeastern Saskatchewan can be found in Haidl et al. (2006).

The Ashern Formation marks the onset of a more diverse Devonian period involving deposition in a northwesterly, elongated Elk Point Basin that extends from northwestern Alberta to the Williston Basin in the Dakotas (Kent and Christopher, 1994). In the subsurface, the Ashern Formation's thickness ranges up to nearly 55 m in North Dakota, while in the Manitoba outcrop belt it is variable and thin ranging from three to five metres (Kendall, 1975). Both in outcrop and in the subsurface, the Ashern Formation consists of slightly silty, argillaceous dolomite to dolomitic shale with only the colour changing (Kendall, 1975).

The seaway expanded during the Middle and Late Devonian, and sedimentation during this time is characterized by cyclic carbonates and evaporites (Kent and Christopher, 1994). Beginning with the Winnipegosis Formation, the platform carbonates have a fairly constant thickness of around 13 m, whereas the overlying banks are up to 100 m thick (Fuzesy, 1975, 1980). The composition of the banks, reefs and platforms are generally mottled dolomite with laminated bituminous carbonates. Fossils are common in the banks often with excellent porosity (Fuzesy, 1975, 1980).

Above the carbonate platform of the Winnipegosis Formation many evaporite units are present in the stratigraphy of the Williston Basin. The most significant of these evaporites is the Prairie Evaporite Formation. It is the best developed evaporite sequence in the basin and is mined for salts (potash). It forms an aquitard that is the most competent in the basin (Kendall, 1975; Bachu and Hitchon, 1996; Whittaker et al., 2004). Mineralogically it is composed of halite, carnallite and sylvite, with frequent seams of dolomitic mudstone and some anhydrite. The Prairie Evaporite Formation can be 200 m thick but in locations of major salt dissolution it is absent (Figure 3.5; Kendall, 1975; Reinson and Wardlaw, 1972; Gerhard and Anderson, 1988; Kreis et al., 2003).

Overlying the Prairie Evaporite Formation is the Dawson Bay Formation that is comprised of dolomitic mudstone at its base overlain by fossiliferous limestone capped by anhydrite and dolomite (Dunn, 1975). Its thickness is uniform, 40 to 50 m, from outcrop to west-central Saskatchewan (Dunn, 1975).

The upper Devonian sediments of the Williston Basin were deposited in a shallow seaway and as a result, cyclic ordering of stratal types from shelf carbonates to evaporites is the norm (Kent and Christopher, 1994). Above the Dawson Bay Formation are the rocks of the Souris River Formation. They consist of several shale-limestone-evaporite cycles composed largely of calcareous shales, fossiliferous argillaceous limestone, and dolomite and dolomitic limestone (Sandberg and Hammond, 1958). In Manitoba, this formation ranges from 67 to 85 m while in Saskatchewan it is generally about 120 m thick (Kent, 1968).

Shallowing upward cycles continue in the rocks of the Duperow Formation. The parasequences are defined by calcareous claystone grading into wackestone and near reef colonies, capped by laminated dolomites and a layered anhydrite finishing up the sequence (Kent and Christopher, 1994). The Duperow Formation ranges from 120 m in Manitoba to about 300 m in western Saskatchewan and is also present throughout the entire Williston Basin (Dunn, 1975).

Adjacent to the Duperow Formation is the Birdbear Formation. The Birdbear Formation is approximately 30 to 45 m thick and consists of two members. A lower member comprised of non-argillaceous limestones and dolostones, and an upper member of mainly dolomites with interbedded evaporites (Kent, 1968; Halabura, 1982).

From the Birdbear Formation the strata transition into the Torquay Formation (Figure 2.4b). The Torquay Formation is dominantly dolomite and shale with lesser amounts of anhydrite, compared to the Birdbear Formation, and a consistent thickness of 45 to 50 m (Christopher, 1961; Kent, 1968).

By the end of the Devonian period sediments became dolomitic and evaporitic, and eventually were succeeded by argillaceous sandy strata transitioning into the basal formations of the Mississippian (Christopher, 1961).

Mississippian Strata

Mississippian strata at the base of the succession are represented by the Bakken Formation. The Bakken Formation (Exshaw Formation lateral equivalent in Alberta) is found entirely across the Williston and Alberta basins. It is Late Devonian to Early Mississippian in age and varies in thickness from about three metres to 40 m (Christopher, 1961). The Bakken Formation consists of three members: 1) a basal organic rich shale; 2) a middle quartzose sandstone and siltstone with ripples, cross-bedding and flaser bedding that are cemented together with calcite; and 3) another black organic rich shale (Christopher, 1961). Currently, the Bakken Formation and underlying Devonian-aged Torquay Formation are the focus of extensive hydrocarbon exploration. More details of this can be found in Kreis and Costa (2005) and Kreis et al. (2006).

Kent and Christopher (1994) describe the Mississippian carbonate facies distribution above the Bakken Formation as being controlled by the Williston Basin paleobathymetry. Kent et al. (2004) show two broad phases of deposition influencing the fabric of the Mississippian rocks: 1) an earlier progradational phase represented by the basin-fill deposits of the Souris Valley, Tilston and Alida Beds and 2) an aggradational phase resulting in one or more shallowing or brining upward cycles in the Frobisher, Midale, Ratcliffe and Poplar Beds. A sequence stratigraphic approach to the Mississippian of southeastern Saskatchewan can be found in Halabura (2006).

The first of these parasequences is the Souris Valley Beds (Lodgepole Formation in Manitoba). It is a thin-bedded basin-type sequence of argillaceous limestones, calcareous shales, and chert (Kent et al., 2004). The Souris Valley Beds range from 122 to 170 m in Saskatchewan and Manitoba progressively eroded in the north and eastern margins of deposition (Figures 3.10 and 4.9; Edie, 1958; Fuller, 1956; Kent et al., 2004). Detailed lithofacies of the Souris Valley Beds in southeastern Saskatchewan are discussed in Miller and Krause (2006).

Above the Souris Valley Beds are the sediments of the Tilston Beds that make up the second parasequence of the Mississippian strata. These rocks were originally subdivided by Thomas (1954) into the MC1 and MC2 intervals (Figure 2.4c). The MC1 division consists of oolitic-pisolitic and crinodial grainstones and packestones. Towards the west, a facies change occurs in the MC1 to cherty-finely crystalline limestones with localized dolomite (Kent et al., 2004). Above the MC1, an argillaceous and silty limestone or dolomitic limestone with shale makes up the MC2 division (Kent et al., 2004). The entire thickness of the Tilston Beds varies from 49 to 80 m (Kent et al., 2004) and its erosional edge in this study is shown in Figures 3.11 and 4.10.

The Alida Beds form the last parasequence in the earlier progradational phase of the Mississippian period. It is composed largely of crinoidal limestones and averages 52 m in thickness (Kent et al., 2004). The subcrop of the Alida Beds is depicted in Figures 3.12 and 4.11. The top of the Alida Beds marks the depositional limit of the lower basin-fill deposits in the Mississippian. This horizon is also marked by the Kisbey Sandstone unit and helps delineate the top of the Alida Formation (Kent et al., 2004).

Directly overlying the Alida Beds and Kisbey Sandstone unit are the Frobisher Beds. The Frobisher Beds mark the beginning of the aggradational phase in the Mississippian that creates shallowing upward sequences. The Frobisher Evaporite includes a variety of sub-aqueously deposited and supratidal anhydrites that may reach nine metres in thickness providing for a very competent seal in the Mississippian (Kent et al., 2004). The shallowing upward sequences consist mainly of oolitic and pisolitic carbonates, as well as argillaceous and fossiliferous, silty limestones and interbedded silty, sandy dolomite and dolomitic limestones (Kent et al., 2004). The Frobisher Beds vary in thickness from about 43 to 70 m and lie beneath the Frobisher Evaporite of the Midale Beds (Kent et al., 2004).

The Midale Beds consist of two lithological intervals known as the "Midale Vuggy" and the "Midale Marly" (Kent et al., 2004). The lower portion contains the Frobisher Evaporite and the upper portion varies from oolitic-pisolitic and skeletal grainstones and packestones that in places have well developed vuggy porosity. In addition, the Midale Beds contain dolomites and dolomitized burrow-mottled limestones that have intercrystalline porosity (Kent et al., 2004). The zero erosional edge of the Midale Beds is shown in Figures 3.14 and 4.13. The thickness varies considerably from the subcrop edge to a maximum of 45 m in the Canadian portion of the Williston Basin (Kent et al., 2004). Capping the Midale Beds is the Midale Evaporite that formed during the last phase of the brining-upward sequence related to the deposition of the Midale Beds and the beginning of deposition for the Ratcliffe Beds (Whittaker et al., 2004).

The Ratcliffe Beds form dense dolomites and mudstones interlayered with three distinctive anhydrite intervals. They vary in thickness from zero to 46 m and the subcrop edge is indicated in Figures 3.15 and 4.14 (Kent et al., 2004). The maximum northerly extent of the subcrop parallels the Midale Beds and also the trend of the sub-Mesozoic unconformity (Kent et al., 2004).

Capping the entire Mississippian succession (Figure 2.4c) are the limestones, argillaceous dolomites and evaporites of the Poplar Beds (Kent et al., 2004). The Poplar Beds are widespread in the interior of the basin; however, in Canada their areal extent reaches only into southern Saskatchewan (Figures 3.16 and 4.15). The Poplar Beds in Saskatchewan have a maximum thickness of 200 m (Kent et al., 2004).

At the top of the Mississippian succession, there is an alteration zone that occurs along the subcrop region of the Poplar, Ratcliffe, Midale, Frobisher, and Alida Beds lying subjacent to the sub-Mesozoic unconformity. Directly overlying the sub-Mesozoic unconformity is the Lower Watrous Member (Figure 2.4d).

Mesozoic Strata

The Jurassic period is represented by the Watrous (Amaranth Formation equivalent in Manitoba), Gravelbourg, Shaunavon, Rierdon, and Masefield formations. Middle Jurassic-aged strata feature a stratigraphic transition from the restricted-basin evaporites of the upper Watrous Formation to open-marine fossiliferous limestones and shales of the Gravelbourg, Shaunavon, Rierdon, and Masefield formations (Reston, Melita, and Waskada formations in Manitoba) (Kent and Christopher, 1994).

Spanning the periods of the Jurassic and Triassic, the Watrous Formation was partly deposited in Saskatchewan but dominantly in Manitoba where it is separated into two members. The lower member is typified by red shales and mudstones, with thin and irregularly interbedded anhydrite (Barchyn, 1982). In southern Saskatchewan, the basal Watrous Formation is marked by sandstone, conglomerates, and locally can be found to contain cherty anhydrite, dolomite, and shale (Barchyn, 1982). Massive anhydrites that are several metres thick overlie the lower beds and form the Upper Watrous Formation that reaches a maximum thickness of 110 m along the border (Barchyn, 1982).

The lower portion of the Gravelbourg Formation contains dolomitic limestone and dense shale whereas veins and bands of chalcedonic chert occur over its lower half (Peterson, 1972). The upper member consists mostly of fossiliferous shale, that in southeastern Saskatchewan is interbedded with minor amounts of quartzose sand and argillaceous limestone (Peterson, 1972). While in southwestern Manitoba, the Gravelbourg Formation thins to 18 m and towards the basin centre it can reach up to 60 m (Peterson, 1972).

There are two members that constituent the Shaunavon Formation. The lower unit is a microcrystalline limestone with a thickness of up to 32 m and the upper unit is a heterogeneous package, up to 30 m thickness, of calcite-cemented quartzose sandstone, oolitic limestone, dolomite, and shale (Christopher, 1984a; Poulton, 1984).

The marine depositional environments of the Jurassic period terminated in the Late Jurassic, represented by the shales of the Rierdon and Masefield formations, and in the Early Cretaceous by the progressive uplift of the Precambrian shield (Christopher, 1984b). Cretaceous seas encroached on the Williston Basin and massively drowned the region (Kent and Christopher, 1994). The sediment supply was dominantly clastic and was directly related to the uplift and erosion of the flanking Rocky Mountains (Kent and Christopher, 1994).

The Mannville Group contains the Pense, Cantuar, and Success formations that generally consist of interbedded sands and shales overlain by a thin, nonmarine calcareous member that is further overlain by marine shales and glauconitic sands (Christopher, 1984b). Thickness for the Pense Formation ranges from less than six metres near the basin margin and approaches 36 m towards western Saskatchewan (Christopher, 1984b). However, the underlying Cantuar Formation ranges from zero to 120 m not including the lowermost, discontinuous member of the Mannville Group, the Success Formation (Christopher, 1984b).

The Colorado Group provides evidence of a significant transgressive event and as a result, massive shales encasing less extensive sandstone formations define the Colorado Group.

In the Lower Cretaceous, the Joli Fou (Skull Creek Member in Manitoba) Formation is thick (61 m), dark noncalcareous shale with minor interbedded sandstone lenses (Simpson, 1975). Directly overlying this shale unit are the sandstones of the Newcastle Formation. The clean sandstones reach a thickness of 40 m in southeastern Saskatchewan and are equivalent to the sandstones of the Ashville Formation in southern Manitoba (Simpson, 1979; Simpson and O'Connell, 1979).

The regional Niobrara Formation and all its members form the uppermost formation within the Colorado Group (Figure 2.4d). In Manitoba and Saskatchewan, the Niobrara Formation consists of black, carbonaceous, chalk-speckled calcareous shale (Christopher, 1984b). It is regionally a very diverse and heterogeneous formation with a maximum thickness of 73 m in southern Manitoba, before thinning along the Manitoba Escarpment down to 15 m (Figure 2.3; Christopher et al., 2006).

The top of the Colorado Group is a major unconformity that separates the overlying Late Cretaceous sediments from the remainder of the Mesozoic strata being studied for this thesis.

The regionally extensive shales of Lea Park Formation correlate with the shales of the Pierre Formation in Manitoba and extend throughout most of the Williston Basin (Williams and Burk, 1964). It is composed of dark grey shale with minor amounts of silt thinning westward and can exceed 270 m in Saskatchewan and Manitoba (Williams and Burk, 1964).

Concluding the stratigraphic section under analysis is the Judith River Formation that is contained between the underlying Lea Park Formation, and overlying Bearpaw Formation. The Judith River Formation in Saskatchewan is predominantly mudstone, with varying proportions of siltstone and sandstone (Christopher, 2003). The last Mesozoic-aged shale formation is the regional and extensive Bearpaw Formation. Clays, claystones, silty claystones, shales, silts and siltstones, and minor amounts of sandstones are the principal lithologies of the Bearpaw Formation (Williams and Burk, 1964). Thicknesses are variable because of its wedge-like form generally decreasing northwards and westwards. However, in south Saskatchewan an average representative value of 350 m is conservative (Williams and Burk, 1964). In Saskatchewan, the Bearpaw Formation thins westward and undergoes facies changes between its lowest and uppermost beds of marine silty clays and sands; however, it loses definition and becomes part of the Pierre Formation in the region of the eastern plains of Saskatchewan and the Mesozoic Escarpment (Figure 2.3; Williams and Burk, 1964).

The objectives of this thesis do not include any analysis on Quaternary or Tertiary-aged strata. This investigation will not incorporate any "shallow groundwater" or local scale aquifer systems and therefore their geology is not discussed.

2.3 REGIONAL HYDROGEOLOGY

Previous studies have interpreted that the regional flow system is perceived to have meteoric waters enter the basin in the uplifted recharge areas (Figures 2.1 and 2.2) and are gravity-driven to depth. This has been identified with comparatively fresh formation waters in the Paleozoic aquifers (Hannon, 1987; Busby et al., 1995; Hitchon, 1996; Benn and Rostron, 1998) containing meteoric isotopic signatures (Rostron and Holmden, 2003). Previous regional mapping studies have all identified that formation waters generally flow from SSW to NNE across the basin (Downey, 1984a, b; Hannon, 1987; DeMis 1995; Bachu and Hitchon, 1996). The edge of Phanerozoic cover marks the depositional limit of Williston Basin sediments (Figure 2.3). Along the shield, low-elevation Paleozoic outcrop belts discharge formation brines (Downey et al., 1987; Grasby and Chen, 2005) (Figure 2.2). The discharging waters are thought to be refluxing Pleistocene-age glacial meltwater, mixed with basin brines and result in the saline springs of Manitoba (Grasby and Betcher, 2002; Grasby and Chen, 2005). However, the flow regime is not that simple due to the presence of the brines.

Dense basinal brines are recognized in the central portion of the basin with peak hydrodynamics occurring in the early Tertiary time (DeMis, 1995), displacing the brines up-dip on the northeastern margin of the basin (Downey, 1984a, b; 1986). The "brine slug" may have been displaced northeasterly; however, studies suggest that a large component of recharging waters preferentially flowed around the deep basin brines dissolving thick evaporite formations (Chipley and Kyser, 1991; Busby et al., 1995) and migrated towards the flanks of the basin (Downey et al., 1987; Hannon, 1987; Jensen, 2007).

Early works recognized the brines, but did little quantifications on the hydrochemistry and density-dependent fluid flow effects in the basin. New studies carried out by the University of Alberta Hydrogeology Group (Alkalali, 2002; Iampen, 2003; Khan, 2006; Jensen, 2007), have included them and presented revised interpretations of the paleohydrogeology in the Williston Basin.

2.3.1 Hydrostratigraphic Framework

The process of taking a stratigraphic column, based on lithology, and identifying similar hydraulic properties for each stratum is referred to as delineating a hydrostratigraphic framework. Unifying and delimiting geology on the basis of its observable hydrologic characteristics creates a hydrostratigraphic unit (Seaber, 1988).

Most importantly, the hydrostratigraphic units are based on the rocks porosity and permeability. The generation of a hydrostratigraphic column incorporates detailed stratigraphic data and requires identification of hydraulically-similar flow units that are relatively transmissive (aquifers) versus those of relatively low permeability (aquitards) (Khan, 2006). The classification of a stratum or a group of strata as either an aquifer or an aquitard is based largely on the purpose of study and the timescales of the processes under consideration (Tóth, 1995).

A hydrostratigraphic column consisting of 19 major aquifers and 13 major aquitards was established for this work. Aquifers were delineated by using drill-stem tests and water chemistry data that tracked laterally persistent and permeable formations. This framework is further combined into three major groups for discussion here: 1) Lower Paleozoic Aquifers, 2) Mississippian Aquifers, and 3) Mesozoic Aquifers (Figure 1.1). The TGI-2 framework was based mostly on that devised for the Weyburn CO_2 Project (Whittaker et al., 2004; Khan, 2006) which is consistent given the partial overlap of the study areas (Figure 2.3).

The Tertiary and Quaternary aquifers present above the Lea Park Formation are not addressed here. For the purposes of this regional hydrogeological characterization, the shallower horizons are considered to have negligible effects on the regional flow fields. The uppermost aquitard in this assessment is the Bearpaw Aquitard (Section 2.3.4). The thickness of the Bearpaw Aquitard in Saskatchewan is estimated to be approximately 350 m (Christopher, 2003). This aquitard serves as a regional barrier to flow considering the scale of this study.

2.3.2 Lower Paleozoic Aquifers and Aquitards

The hydrostratigraphic framework for the Lower Paleozoic (Figure 2.4a, b) builds upon that devised by Benn and Rostron (1998), and used in subsequent studies by Iampen and Rostron (2000), Iampen (2003), Rostron and Holmden (2003), and Khan

(2006). Eight major aquifers have been mapped (Figure 1.1) within what has been previously considered thick confining aquitards (Downey, 1984a, b; 1986; Downey et al., 1987; Busby et al., 1995), undifferentiated aquifer systems (Bachu and Hitchon, 1996), the carbonate rock aquifer (Grasby and Betcher, 2002; Grasby and Chen, 2005), and the basal Winnipeg Aquifer (Ferguson et al., 2007). The subdivision is also supported by isotopes (Rostron and Holmden, 2003; Jensen, 2007) and high resolution hydrogeological mapping (Khan, 2006). These hydrostratigraphic aquifer units have many intervening aquitards of variable composition ranging from the Winnipeg Aquitard comprised of marine shales and siltstones, to the thick salt of the Prairie Evaporite Formation that is one of the most effective aquitards in the basin.

Cambro-Ordovician Aquifer

The Precambrian basement forms the underlying contact with both the Deadwood and Winnipeg formations. Basal clastic units of the Deadwood Formation (Cambrian-aged) and Winnipeg Formation (Middle Ordovician-aged) have been combined into a thick clastic aquifer forming the largest areal expansive aquifer in the study. This aquifer ranges from approximately 300 m thick in the centre of the basin to its erosional edge and outcrop limit in the north and northeastern margins of Saskatchewan and Manitoba respectively. The contact between the shales of the Icebox Member (Winnipeg Formation) and the sandstones of the Black Island Member (Winnipeg Formation) are taken as the upper bounding surface for the Cambro-Ordovician Aquifer (Figure 2.4a).

Winnipeg Aquitard

Capping the Cambro-Ordovician Aquifer and separating it from the overlying Yeoman Aquifer is the Winnipeg Aquitard. The Winnipeg Aquitard is defined as the marine shales and siltstones belonging to the Icebox Member of the Winnipeg Formation. The thickness of the aquitard varies from 43 m in the central portion of the basin and thins outward to approximately 29 m in southeast Saskatchewan (Paterson, 1988).

Yeoman Aquifer

The Yeoman Aquifer combines the formations of the mottled-dolomitic limestones of the Yeoman and Red River formations. Minor anhydrite layers, namely the Lake Alma and Coronach members are within this aquifer (Figure 3.3); however, they are not regionally persistent across the study area to form a barrier to flow. The upper bounding surface is taken as the base of the Stony Mountain Formation and depending on location it is either, the basal Gunton Member, Gunton Anhydrite, Gunn Member shale, and/or the Hartevan Member subgroups (Figure 2.4a).

Stony Mountain Aquitard

The Stony Mountain Aquitard is lithologically heterogeneous and is made up of mixed carbonates and shales belonging to the Gunton and Hartevan Members, the Gunton Anhydrite, and the Gunn Member respectively. This aquitard is uniform in thickness (maximum 22 m) throughout the basin and generally thickens toward the north and northeast.

Ordo-Silurian Aquifer

The Ordo-Silurian Aquifer is made up of two petroleum bearing units: 1) Stonewall Formation (Late Ordovician- to Silurian-aged), and 2) Interlake Formation (Silurian-aged). A paucity of data in the Stonewall Formation and the lack of a consistent barrier between the two warranted grouping the formations. This is a thick aquifer with a thickness of over 320 m in the study area. The basal boundary is taken as the top of the Gunton and Gunn Member shales with the upper contact marked by the Ashern Formation (Lower Devonian-aged).

Ashern Aquitard

The Ashern Aquitard is made up of the Ashern Formation and it caps the Ordo-Silurian Aquifer. It consists of low permeability argillaceous and dolomitic shale strata.

Although locally thin and variable in the Manitoba outcrop belt, it is regionally extensive.

Winnipegosis Aquifer

Carbonate platforms and reef build-ups of the Winnipegosis Formation form the Winnipegosis Aquifer. As previously mentioned (Section 2.2.2), its thickness is extremely variable as a function of the pinnacle reef growth versus the platform upon which they grew (Fuzesy, 1975).

Prairie Aquitard

The Prairie Aquitard consists of the Prairie Evaporite Formation. It is dominantly composed of halite and its thickness varies from greater than 150 m down to zero where the salt has been removed (Kreis et al., 2003). The trace of the formation edge is shown is Figures 3.5 and 4.4. This indicates where major dissolution has occurred and is recognized in the west, north, and northeast portions of the TGI-2 project area. The Prairie Evaporite Formation forms one of the most competent sealing horizons and aquitards in the basin. This geological configuration has lead to the Winnipegosis Formation being a significant hydrocarbon producer in the Williston Basin (Fuzesy, 1975).

Manitoba Aquifer

The Manitoba Aquifer consists of the Dawson Bay and Souris River formations. These two formations are largely limestone with lesser amounts of dolomite and anhydrite. The Manitoba Aquifer can be up to 125 m thick in Manitoba, whereas in Saskatchewan it can reach 170 m (Dunn, 1975).

Souris River Aquitard

Between the Manitoba and Duperow aquifers are the shale-limestone-evaporite cycles of the Souris River Aquitard. It is the Hatfield and Wymark Members that combined form nearly 180 m of lower permeability calcareous shales and carbonates.

The Hatfield Member varies from 30 to 60 m and the Wymark Member is up to 120 m thick. This aquitard is present throughout most of the Williston Basin (Kent, 1968).

Duperow Aquifer

Limestones and dolostones comprise the lithology of the Duperow Aquifer. It consists entirely of the Duperow Formation that ranges in thickness from 120 m in Manitoba to over 160 m in the Saskatchewan study area. Similar to the Winnipegosis Aquifer, the Duperow Formation is also productive in both the Canadian and American portions of the basin.

Seward Aquitard

The Seward Member forms the Seward Aquitard (Kent, 1968). Its lithology is micro- to crypto-crystalline limestone cycles of carbonate and evaporite sedimentation capped by an anhydrite layer (Wilson, 1967). It is laterally persistent and maintains a thickness of roughly 50 m (Wilson, 1967). The Seward Member shales cap the Duperow Aquifer and form the base of the overlying Birdbear Aquifer.

Birdbear Aquifer

Both the lower and upper members of the Birdbear Formation make up the Birdbear Aquifer. The lower member consists of limestones and dolostones and the upper member is dolomites and interbedded evaporites. On average the Birdbear Aquifer is 45 m thick and has very transmissive intervals across the study area (Halabura, 1982). The upper contact in this aquifer is taken as the top of the Birdbear Formation.

Three Forks Aquitard

The Birdbear Aquifer is overlain by a package of rocks consisting of low permeability carbonates and shales of the Torquay and Big Valley formations as well as the Lower Bakken Member. These formations are all Upper Devonian in age and together form the Three Forks Aquitard. The Three Forks Aquitard forms an effective barrier for flow to the overlying Upper Devonian/Mississippian-aged Bakken Aquifer with a consistent thickness of 45 to 50 m. In addition, the Torquay Formation has been found to be an aquifer when it is associated with the productive Middle Bakken Member (Kreis et al., 2006).

Bakken Aquifer

The Middle Bakken Member is encased by black organic rich shales of the lower and upper members. The Bakken Aquifer is made up of the Middle Bakken Member that consists of clean sand. It is of variable thickness across the study area from zero in the north to a regional maximum of 25 m in the south. The Bakken Aquifer can be up to 44 m thick in known areas of salt dissolution (Kreis et al., 2006). The Bakken Aquifer is capped by the black shales of the Upper Bakken Member that reach a maximum thickness of approximately nine metres in the south of Saskatchewan.

2.3.3 Mississippian Aquifers and Aquitards

The Mississippian system has long been mapped, hydrogeologically, as a single aquifer system (e.g., Downey, 1984a, b; Downey et al., 1987; Toop, 1992; Hannon, 1987; Berg et al., 1994; Demis, 1995; Bachu and Hitchon, 1996). Previous hydrogeological studies have mapped the Mississippian strata as one aquifer for a couple reasons: 1) it contains an extreme abundance of pressure and chemistry data that make differentiating aquifer tests a daunting task, and 2) on a basinal-scale, the chemistries and hydraulic heads appear similar with no major differences. However, more recent investigations (Khan, 2006; Jensen, 2007) have shown that subdividing the Mississippian aquifers is necessary using an updated geological framework. Upon subdividing the Mississippian based on the geology, significant differences in the groundwater flow directions and hydrochemistry are recognized in the individual aquifers.

Given the new stratigraphic framework for the TGI-2 project (Whittaker et al., 2004; Christopher and Yurkowski, 2005; Christopher et al., 2006; Nicolas, 2006), a revised and detailed Mississippian hydrostratigraphy was created here. The Mississippian system was divided into seven aquifers (Figure 2.4c). Primary evaporites and argillaceous layers of low porosity and permeability straddle these Mississippian porous carbonates. There are distinct porous and permeable units separated by thick evaporites and claystone sequences within the Mississippian. Also, all of the Mississippian aquifers are beneath the Watrous Formation (Kent et al., 2004). The Mississippian aquifers used here are also consistent with what was mapped in the Weyburn CO_2 project (Khan, 2006).

Mississippian aquifers for this study, in ascending order, are the Souris Valley, Tilston, Alida, Frobisher, Midale, Ratcliffe, and Poplar aquifers (Figure 2.4c). The individual Mississippian aquifers were subdivided to reflect the sequences and parasequences identified geologically (Section 2.2.2). Therefore, given the similar nature by which they are defined, they will not be described here individually.

2.3.4 Mesozoic Aquifers and Aquitards

The Mesozoic aquifer system overlies the sub-Mesozoic unconformity, separating it from the underlying Mississippian system. For this study, the Mesozoic aquifers encompass all rock units below the top of the Bearpaw Formation shales (Pierre Formation shale equivalent in Manitoba).

Four aquifers were identified and mapped within this succession (Figure 2.4d) as described in the proceeding sections.

Watrous Aquitard

Shales and mudstones of the Watrous Formation (Amaranth Formation equivalent in Manitoba) comprise the Watrous Aquitard. In Saskatchewan, the lower and upper

Watrous Formation are typified by red shales and mudstones; however in Manitoba, the Watrous Formation has been found to contain sandstone and conglomerates forming the main sand unit within the Lower Red Beds Member (Christopher, 1984a). Typically, the Watrous Aquitard is about 100 m but it ranges from 40 to 200 m across the study area. The Watrous Aquitard was identified as the main aquitard in the Weyburn CO_2 project (Khan, 2006).

Jurassic Aquifer

The Gravelbourg and overlying Shaunavon formations are grouped together to form the Jurassic Aquifer. Dominantly carbonates and sandstones make up this aquifer and its thickness ranges from 80 to 100 m across the study area. The top of this aquifer is the contact with the overlying shales of the Masefield and Waskada formations.

Masefield-Waskada Aquitard

This aquitard caps the Jurassic Aquifer with shales of the Rierdon, Masefield and Waskada formations (Figure 2.4d). The Masefield-Waskada Aquitard nomenclature is used here because the Masefield and Waskada formations are lateral equivalents in Saskatchewan and Manitoba respectively. This aquitard is regionally extensive and thick at up to 100 m in the Williston Basin-centre (Christopher, 1984b).

Mannville Aquifer

Interbedded sandstones and shales of the Pense, Cantuar, and Success formations (Mannville Group) make up the Mannville Aquifer. This is the highest permeability aquifer in the section with effective permeabilities estimated to be greater than 10,000 millidarcy (Khan, 2006). In addition, this aquifer can be thick, up to 150 m of high transmissivity sandstones. The base of the overlying Joli Fou Formation is defined as the top of this aquifer.

Joli Fou Aquitard

The Joli Fou Formation and Skull Creek Member (Manitoba lateral equivalent) combined form the Joli Fou Aquitard. This massive shale formation separates the underlying Mannville Formation from the overlying Newcastle Aquifer. The Joli Fou Aquitard is reasonably thick at approximately 60 m and is widespread across the Williston Basin (Christopher, 2003).

Newcastle Aquifer

Encased within the massive shales of the Colorado Group are the comparatively thin sandstones of the Newcastle (Ashville Formation equivalent in Manitoba) Formation. The sands of the Newcastle Formation make up the Newcastle Aquifer. They have a maximum thickness of approximately 40 m and are overlain by the remaining Colorado Group formations. The shales of the Lea Park and Pierre formations create an effective seal to the overlying Upper Cretaceous rocks (Simpson, 1975; Christopher et al., 2006).

Colorado-Lea Park Aquitard

The Colorado-Lea Park Aquitard is formed by the lower and upper Colorado Group rocks comprised of the Belle Fourche through the Niobrara formations (Figure 2.4d), and the Lea Park Formation and equivalent Millwood Member (Pierre Formation) of Manitoba. This aquitard is composed of dark grey shale and can exceed 300 m across the study area (Christopher et al., 2006).

Judith River Aquifer

The last aquifer in this section is that formed by the sandstones and siltstones of the Judith River Formation (Belly River Formation in Alberta). The Judith River Aquifer is situated between the underlying Lea Park Formation and overlying shales of the Bearpaw Formation. The aquifer thickness can be up to 360 m but thins toward its depositional edge in central Saskatchewan (Christopher, 2003).

Bearpaw Aquitard

The extremely thick shales of the Bearpaw and Pierre formations define the Bearpaw Aquitard in this study. The Bearpaw Aquitard is estimated at a conservative value of 350 m in southern Saskatchewan; however, it contains several interbedded layers of silt and sand that inherently form minor discontinuous aquifers. The shallower horizons above the Lea Park Formation are not being considered in this study.

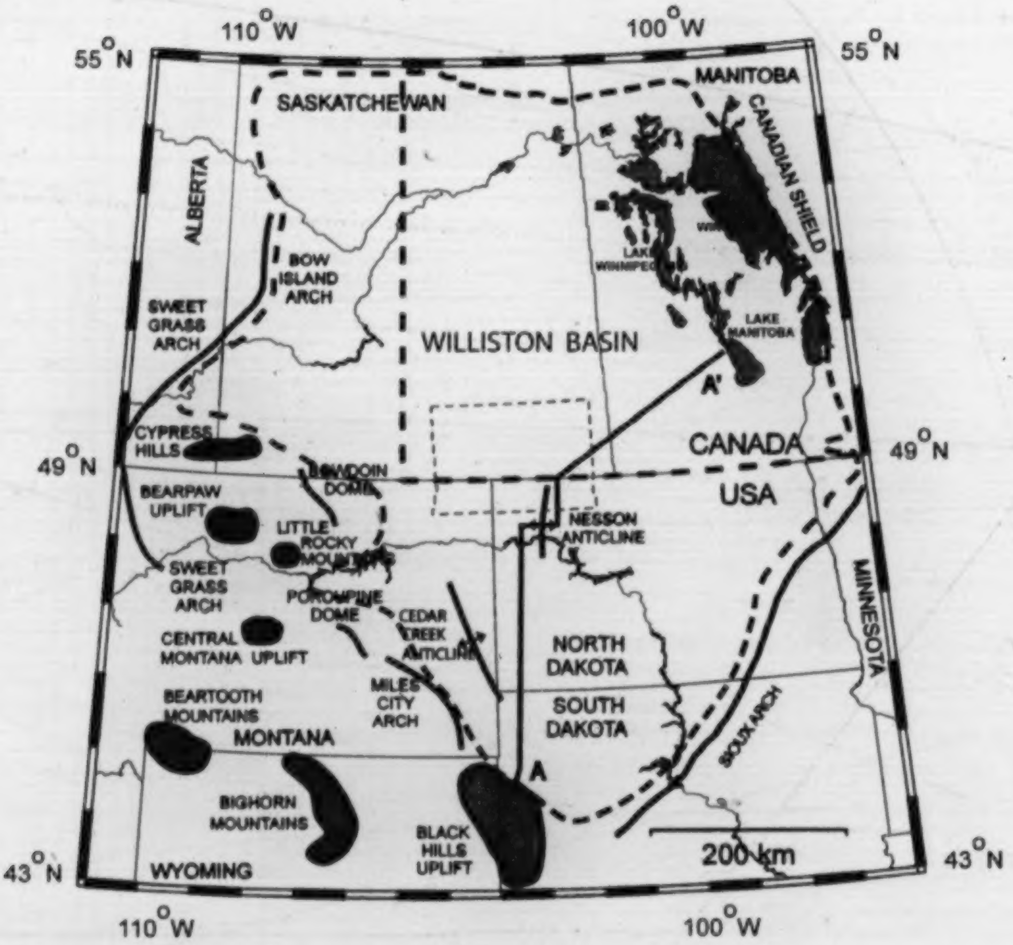
110°W
100°W
55°N
55°N
MANITOBA
SASKATCHEWAN
CANADIAN SHIELD
ALBERTA
LAKE WINNIPEG
BOW ISLAND ARCH
SWEET GRASS ARCH
LAKE MANITOBA
WILLISTON BASIN
A'
CYPRESS HILLS
CANADA
49°N
49°N
BOWDOIN DOME
USA
BEARPAW UPLIFT
NESSON ANTICLINE
LITTLE ROCKY MOUNTAINS
SWEET GRASS ARCH
PORCUPINE DOME
CEDAR CREEK ANTICLINE
MINNESOTA
CENTRAL MONTANA UPLIFT
NORTH DAKOTA
MILES CITY ARCH
SOUTH DAKOTA
BEARTOOTH MOUNTAINS
MONTANA
SIOUX ARCH
A
BIGHORN MOUNTAINS
BLACK HILLS UPLIFT
200 km
43°N
WYOMING
43°N
110°W
100°W

Figure 2.1. TGI-2 study area in dashed black line. Williston Basin boundary shown in a dashed green line with significant physiographic features (modified after Benn and Rostron, 1998). Recharge zones are filled orange and the discharge zone is signified by the lakes in Manitoba. The IEA Weyburn CO_2 Monitoring and Storage project area is also shown in a thin dashed grey line. The location of cross-section A to A' (Figure 2.2) is identified.

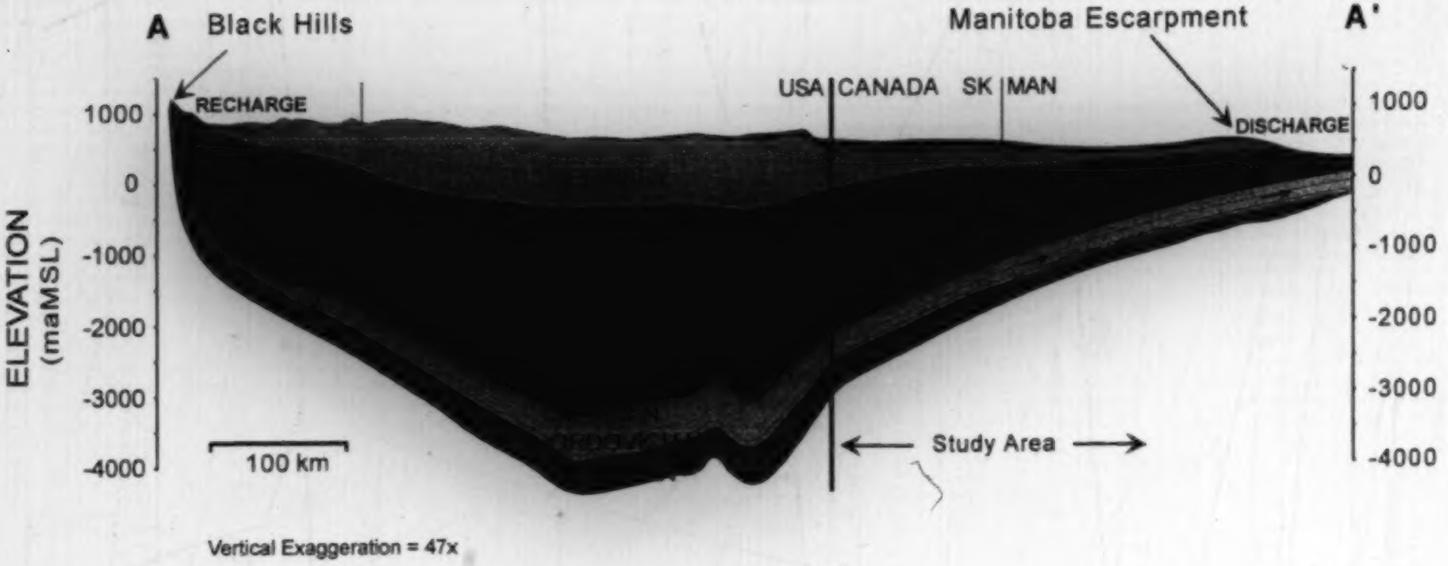
A
Black Hills
RECHARGE
Manitoba Escarpment
A'
USA
CANADA
SK
MAN
DISCHARGE
ELEVATION (maMSL)
1000
0
-1000
-2000
-3000
-4000
100 km
Study Area
Vertical Exaggeration = 47x

Figure 2.2. Structural cross-section A to A' through the line of section shown in Figure 2.1 (modified after Benn and Rostron, 1998). The hydrogeological characterization includes rocks from the Cambrian to uppermost Cretaceous systems. This study spans from the USA-CANADA border and continues to the edge of Phanerozoic deposition (beyond this section). Recharge is thought to enter the basin in the Black Hills of South Dakota and up-dip discharge to the northeast of the Manitoba Escarpment.

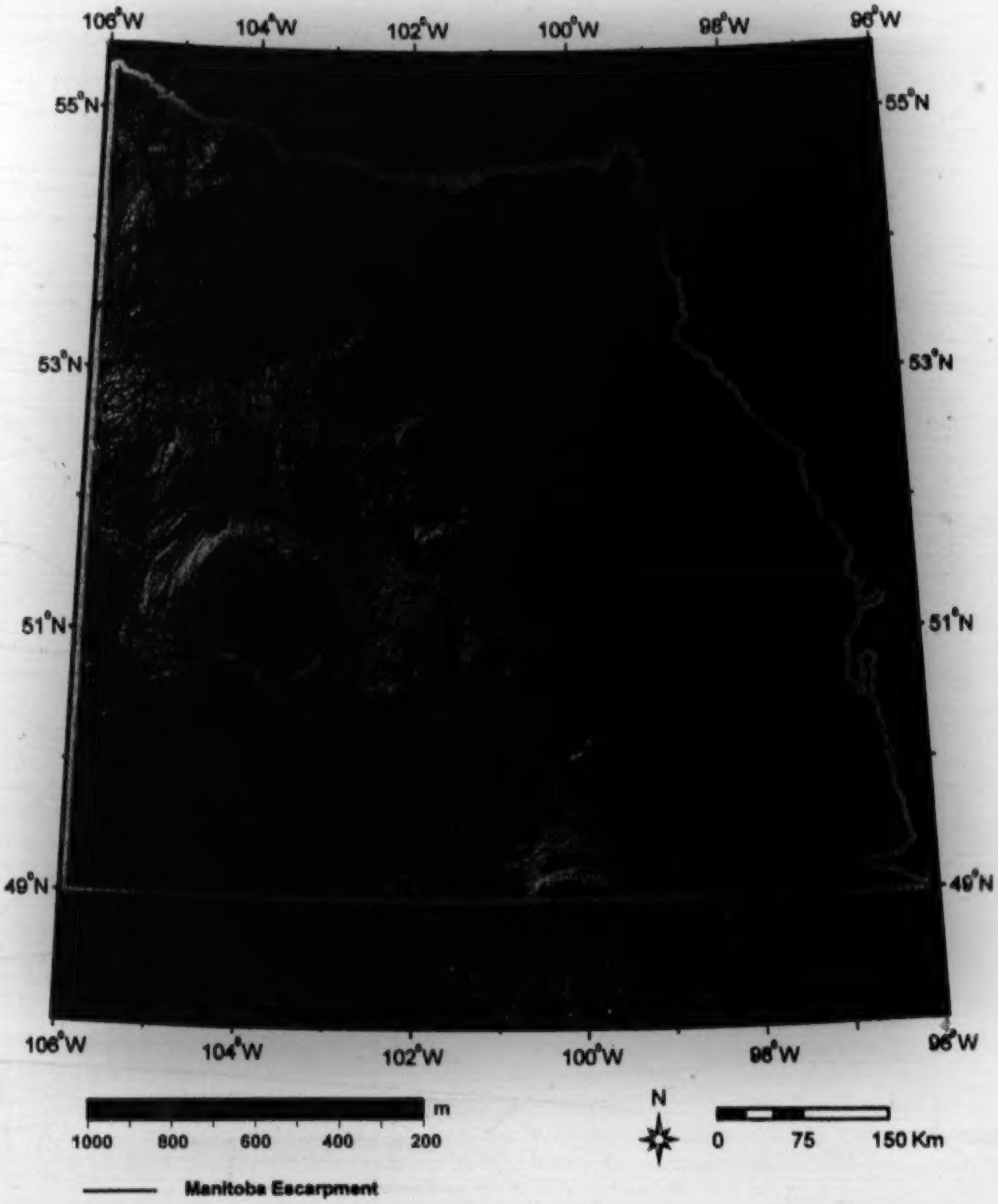
106°W
104°W
102°W
100°W
98°W
96°W
55°N
53°N
51°N
49°N
m
1000
800
600
400
200
N
0
75
150 Km
Manitoba Escarpment

Figure 2.3. Digital elevation model of the northeast portion in the Williston Basin (modified after Kreis et al., 2004). The TGI-2 project area is outlined in pink. The IEA Weyburn CO_2 Monitoring and Storage project area is outlined in a thin black line.

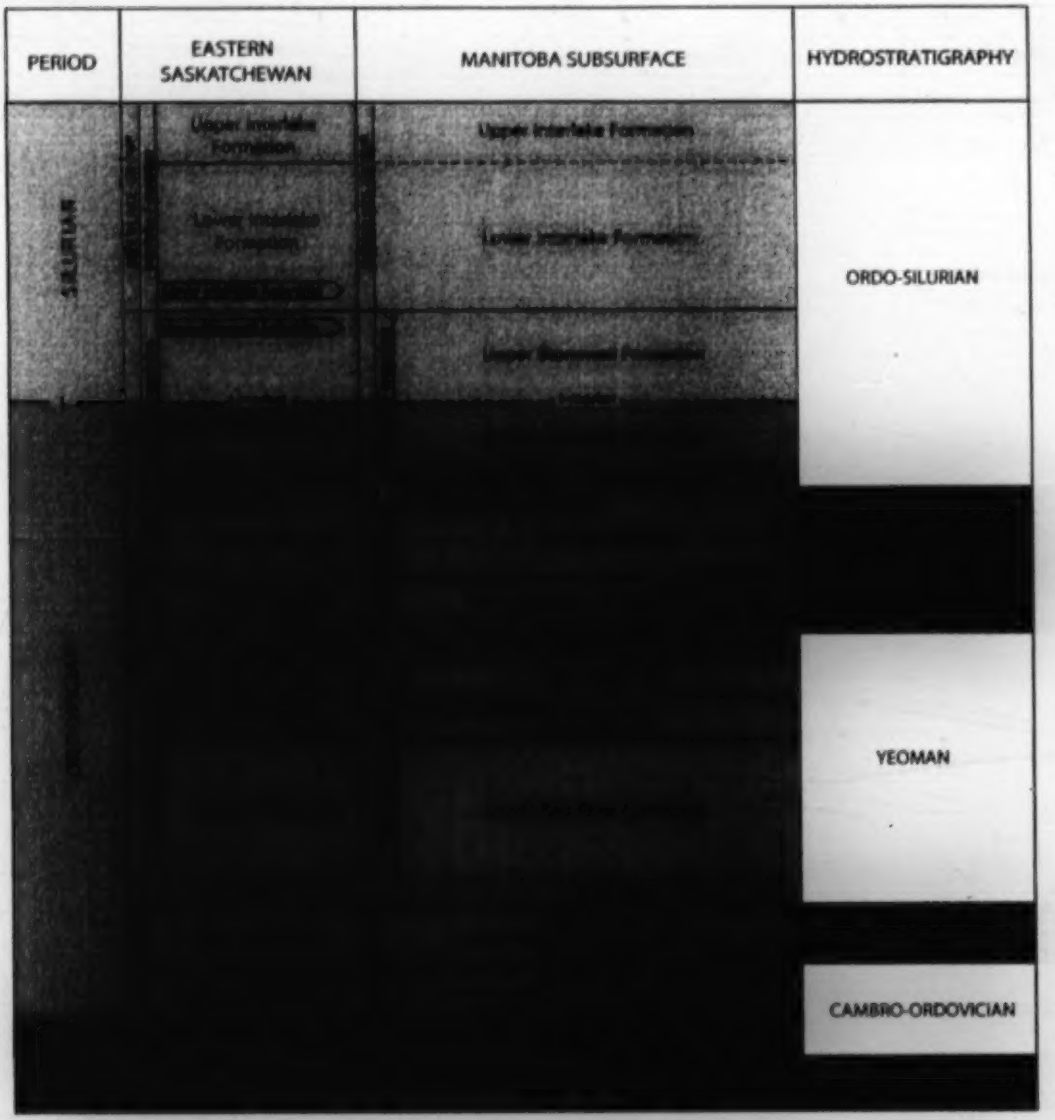

Figure 2.4a. Precambrian to Silurian stratigraphic correlation chart for Eastern Saskatchewan and Manitoba incorporating the hydrostratigraphic framework adopted for the TGI-2 project (modified after Nicolas, 2007).

☐ AQUIFER
■ AQUITARD

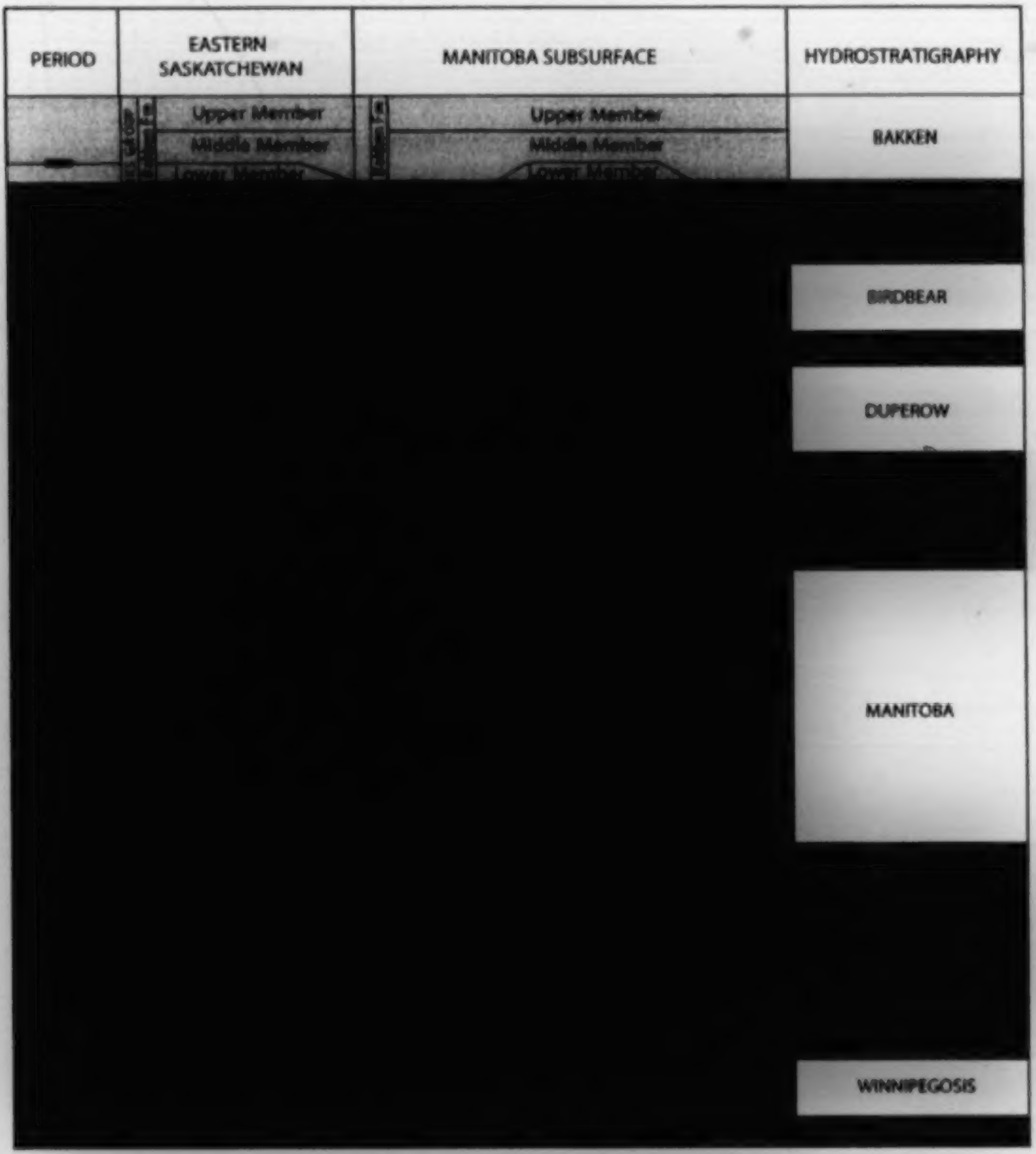

Figure 2.4b. Devonian stratigraphic correlation chart for Eastern Saskatchewan and Manitoba incorporating the hydrostratigraphic framework adopted for the TGI-2 project (modified after Nicolas, 2007).

☐ AQUIFER

■ AQUITARD

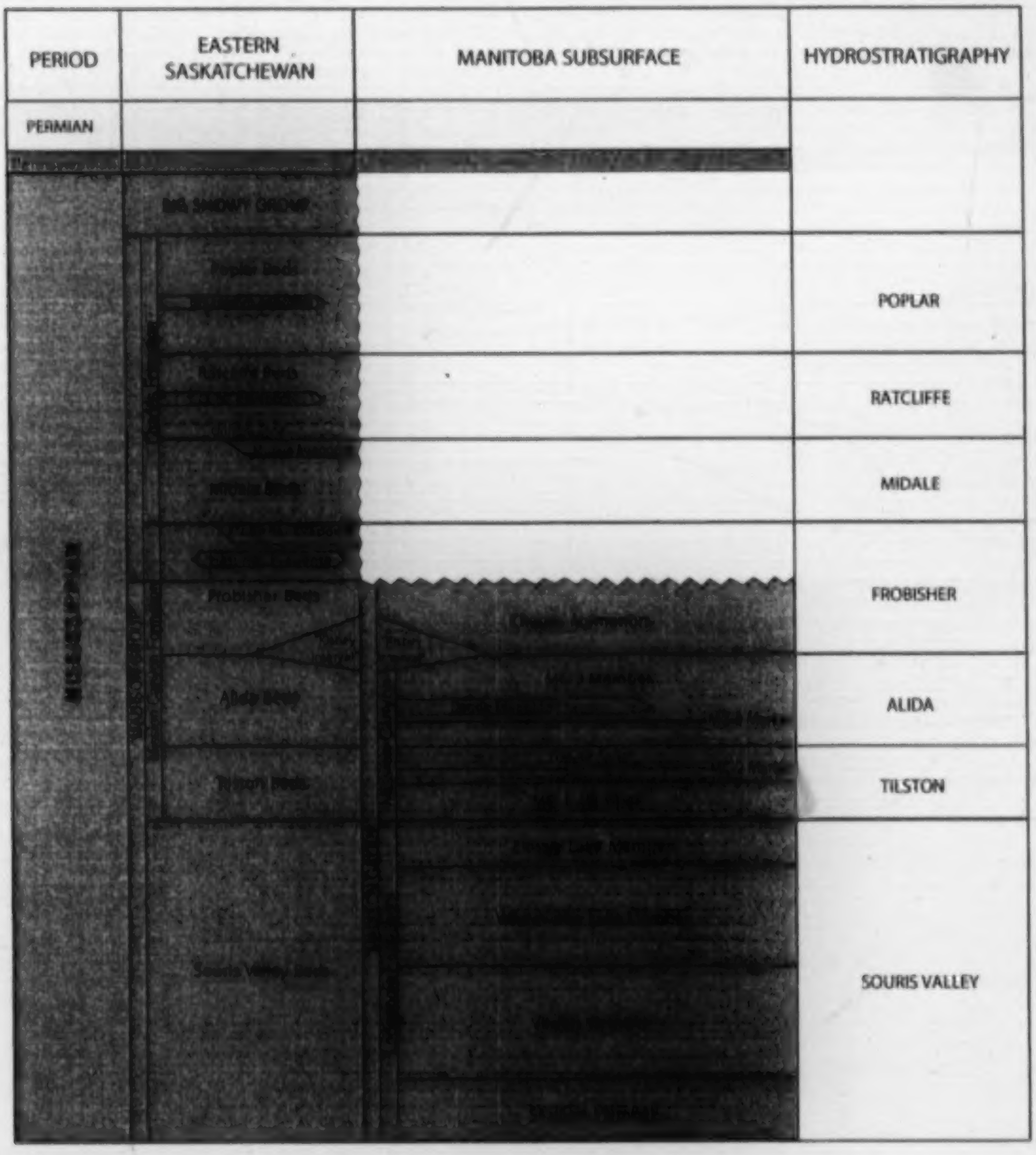
PERIOD
EASTERN SASKATCHEWAN
MANITOBA SUBSURFACE
HYDROSTRATIGRAPHY
PERMIAN
Big Snowy Group
Poplar Beds
Ratcliffe Beds
Midale Beds
Frobisher Beds
Alida Beds
Tilston Beds
Souris Valley Beds
POPLAR
RATCLIFFE
MIDALE
FROBISHER
ALIDA
TILSTON
SOURIS VALLEY

Figure 2.4c. Mississippian stratigraphic correlation chart for Eastern Saskatchewan and Manitoba incorporating the hydrostratigraphic framework adopted for the TGI-2 project (modified after Nicolas, 2007).

☐ AQUIFER

■ AQUITARD

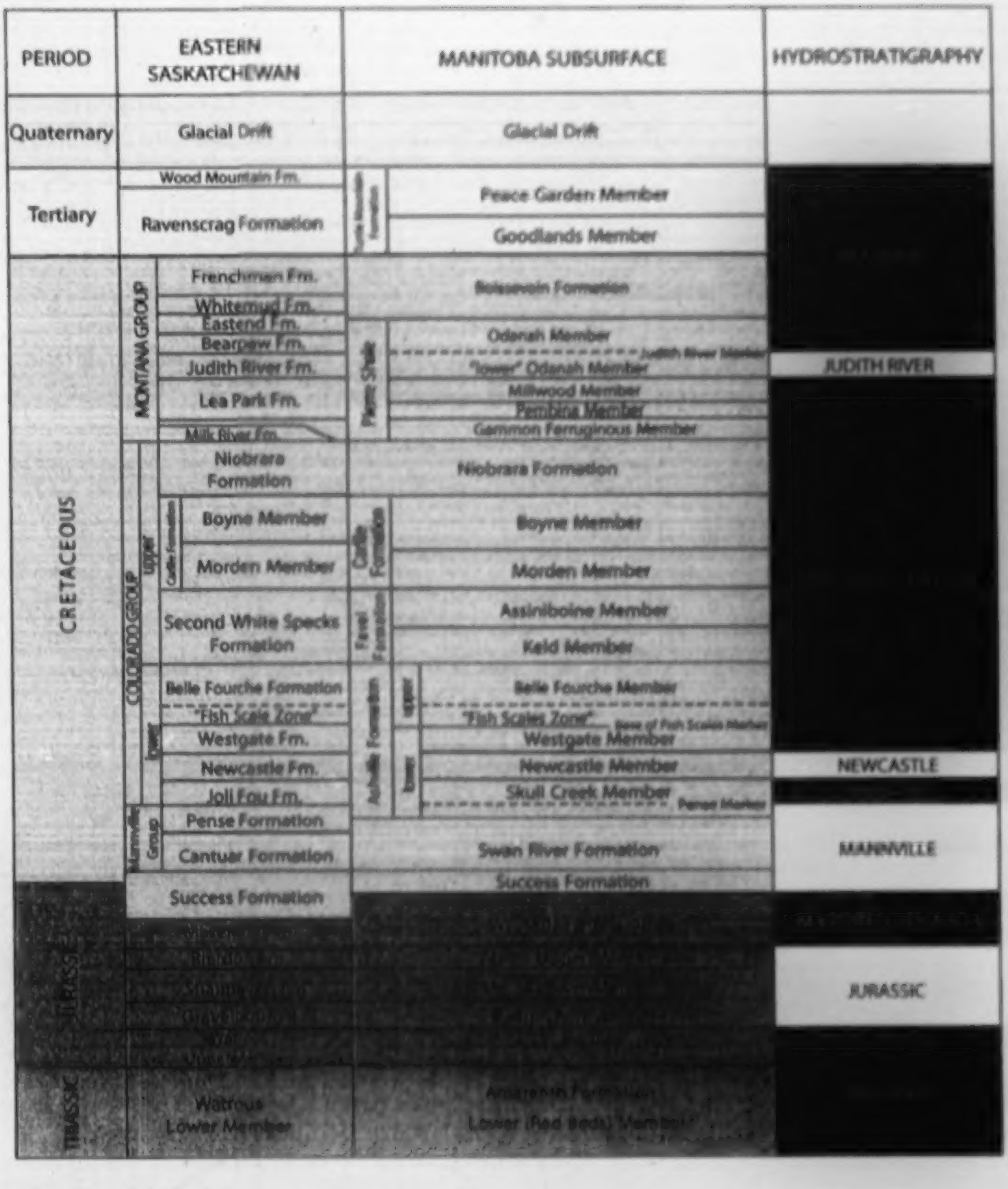

PERIOD
EASTERN SASKATCHEWAN
MANITOBA SUBSURFACE
HYDROSTRATIGRAPHY
Quaternary
Glacial Drift
Glacial Drift
Tertiary
Wood Mountain Fm.
Ravenscrag Formation
Peace Garden Member
Goodlands Member
CRETACEOUS
MONTANA GROUP
Frenchman Fm.
Whitemud Fm.
Eastend Fm.
Bearpaw Fm.
Judith River Fm.
Lea Park Fm.
Milk River Fm.
Boissevain Formation
Pierre Shale
Odanah Member
Judith River Marker
"lower" Odanah Member
Millwood Member
Pembina Member
Gammon Ferruginous Member
JUDITH RIVER
COLORADO GROUP
Niobrara Formation
Niobrara Formation
upper
Carlile Formation
Boyne Member
Morden Member
Carlile Formation
Boyne Member
Morden Member
Second White Specks Formation
Favel Formation
Assiniboine Member
Keld Member
Belle Fourche Formation
"Fish Scale Zone"
lower
Westgate Fm.
Newcastle Fm.
Joli Fou Fm.
Ashville Formation
upper
lower
Belle Fourche Member
"Fish Scales Zone"
Base of Fish Scales Marker
Westgate Member
Newcastle Member
Skull Creek Member
Pense Marker
NEWCASTLE
Mannville Group
Pense Formation
Cantuar Formation
Swan River Formation
MANNVILLE
Success Formation
Success Formation
JURASSIC
JURASSIC
TRIASSIC
Watrous Lower Member
Amaranth Formation
Lower (Red Beds) Member

Figure 2.4d. Triassic to Quaternary stratigraphic correlation chart for Eastern Saskatchewan and Manitoba incorporating the hydrostratigraphic framework adopted for the TGI-2 project (modified after Nicolas, 2007).

☐ AQUIFER

■ AQUITARD

3.0 HYDROCHEMISTRY: DISTRIBUTION AND COMPOSITION OF FORMATION WATERS

3.1 DATA AND METHODOLOGIES

A water chemistry database of approximately 12,200 formation water analyses was assembled for the entire Phanerozoic succession in the study area. In order to compile this database, both public and private sources were referenced. First, the Rakhit Petroleum Consulting Ltd. (now Canadian Discovery Ltd.) database called "Geofluids" was queried. This database represents the digital version of water analyses reported to the Energy Resources Conversation Board (Geofluids is now entirely owned by IHS Inc.). Secondly, previous studies and field sampling completed by the University of Alberta's Hydrogeology Group was also utilized in this study (Toop and Tóth, 1995; Benn and Rostron, 1998; Rostron et al., 1999; Iampen and Rostron, 2000; Jensen et al., 2006). The third data source came from the Manitoba Energy and Mines Petroleum (now Manitoba Science, Technology, Energy and Mines) literature, where formation water analyses available in previous work and data records for the province are reported (McCabe, 1983; Betcher et al., 1995). Cumulatively, these water analyses are from a variety of sampling procedures such as drill stem tests (DSTs), production samples, wellhead samples, or spring water samples taken in Manitoba (Grasby et al., 1999). A majority of the samples used in these analyses are from DSTs and require quality control procedures to ascertain what the representative formation water chemistry is for a particular aquifer.

3.1.1 Water Chemistry Culling

Water analyses obtained during the drilling or completion of oil and gas wells have a high risk of becoming contaminated with the drilling fluids (Hitchon, 1996). However, the extent or degree of contamination between the drilling and completion fluids is variable and can be discerned. The water chemistry culling procedures to identify only representative formation water samples are based generally on data culling criteria set forth in previous studies (Hitchon and Brulotte, 1994; Block, 2001). Khan (2006) modified these standard procedures to accommodate Williston Basin waters that are compositionally different than Alberta Basin waters. Differences in fresh Ca-Na-SO_4 waters having low Na/Ca and high Na/Cl ratios, and the presence of high K contents in the Williston Basin can result in the removal of otherwise quality data (Khan, 2006). The data culling process is iterative and largely manual due to the variability of formation waters present in the basin at this scale of study. Moreover, this data culling procedure in combination with successive mapping of water chemistry, albeit iterative, produces the best representation of the hydrochemical composition, classification, and distribution of subsurface waters in the basin (Khan, 2006).

The details of the water chemistry culling criterion set forth for every aquifer can be found in Appendix A. Ionic charges of the cations and anions will be left off for clarity.

The combination of the culling criteria and available information about recovery, sampling location, and test details must be used to ascertain representative water samples. Contamination of formation water analyses through drilling and completion is large, approximately 65% are unusable (Hitchon, 1996), and using this form of water analyses poses challenges. However, with a rigorous water chemistry culling procedure as defined here, it is possible to attain a representative distribution and composition of formation waters throughout the basin.

3.1.2 Interval Testing Verification

To resolve the problem of unassigned formations and to verify the correct formation that is being sampled, a new technique known as "Interval Testing" was created (Figure 3.1; Khan, 2006). Precise sampling locations within thick aquifers and/or identifying the sample formation within a series of thin-bedded stacked carbonates are just some motivations to specifically identify the testing location.

Previous studies (Alkalali, 2002; Khan, 2006) have utilized a geological framework (similar to this project) to generate structural grids of each stratigraphic horizon to determine largely anomalous tests. Residual mapping of structural surfaces and the "imaginary" surfaces of the respective tops and bases of the sampling intervals can indicate whether testing locations are largely out of place (above or below structural top). The interval testing procedure is often a lengthy process that can be adversely affected by gridding algorithms. In addition, the results of residual subtraction can be subjective where data are sparse. For the present study, the method was found to be most accurate when the residual surface (amount that a particular sample is outside of the testing formation) was more than five metres.

In this study, the "Interval Testing" technique described above was used. However, the geological model developed for TGI-2 was of such high resolution that a more accurate and simpler method was developed and used (when required). A geological database in Microsoft Access was generated with all of the geological tops for the entire stratigraphic column. In conjunction with the hydrogeological mapping, one of the first steps was to query the geological database to attain the total vertical depths for the aquifer tops and bases. The results of the queries were exceptional with all but a few wells matching for many of the aquifers. With this method, it was possible to exactly determine the testing locations with respect to the aquifer tops and bases. This method proved to be effective and precise, enabling the assignment of each sample to its hydrostratigraphic unit.

3.2 RESULTS: FORMATION WATER CHEMISTRY

The hydrochemistry of each aquifer unit was analyzed using maps of Total Dissolved Solids (TDS) shown in figures 3.2-3.19, individual major ions (Figures 3.20-3.22), and the cationic fraction of Ca. TDS is the summation of all ionic constituents measured in a groundwater sample indicating the quantity of dissolved material (Porges and Hammer, 2001). The chemical interaction between formation waters and the rock framework has long been studied using TDS to qualitatively evaluate the relationship of groundwater chemistry to flow systems and lithology (Chebotarev, 1955; Tóth, 1984).

Formation waters with TDS less than 10 g/L have been classified as fresh waters, waters ranging from greater than 10 to 100 g/L are brackish to saline respectively, and over 100 g/L waters are brines (Carpenter, 1978). Given the enormous range in TDS across the study area (2 to 470 g/L; Figures 3.20-3.22), a variable contour interval was chosen to map TDS and is set to illustrate significant changes in composition across the isoconcentration lines (Khan, 2006).

The following section describes the TDS distributions for each aquifer. The number of water chemistry samples, original and after culling, and the minimum and maximum TDS measured for each aquifer is summarized in Table 3.1.

3.2.1 Lower Paleozoic Aquifers

The Lower Paleozoic aquifers (Cambrian to Bakken; Figure 2.4a, b) exhibit a lower salinity signature in the west with salinity increasing gradationally towards the basin centre (Figures 3.2-3.9). The salinity systematically decreases, with the exception of the Ordo-Silurian, Winnipegosis, and Birdbear aquifers, toward the north and northeast approaching the edge of Phanerozoic cover. The geochemical gradient in many cases is steep. Fresh water incursion zones are prevalent to the west, north and northeast of the study area.

Cambro-Ordovician Aquifer

Formation waters broadly classified as brines (> 100 g/L) make up the dominant spatial extent of this aquifer (Figure 3.2). The TDS map for the basal Cambro-Ordovician Aquifer ranges from 3 g/L in northern Saskatchewan to 350 g/L located in eastern Saskatchewan adjacent to the Manitoba border. Regions of high TDS (> 300 g/L) occur in southern Saskatchewan just north of the basin centre. Another region of high TDS is located straddling the Saskatchewan-Manitoba border around Township 20 and is coincident with the erosional edge of the Deadwood Formation as well as the Rocanville potash mine. There is a systematic trend of decreasing TDS from the deepest portion of the study area toward the zero edge of the Cambro-Ordovician Aquifer. Three regions having low TDS are in the west, north and northeast. The low feature in the west, supported by only one data point, is honoring a fresh water incursion tongue present to the west of the study area depicted in Benn and Rostron (1998). The remaining two fresh water signatures present to the north and northeast are relatively close to the aquifer zero edge and are part of a freshening geochemical gradient existing on the flank of the basin defined by a brackish transition zone (25-100 g/L; blue to purple zones).

Yeoman Aquifer

Yeoman Aquifer TDS ranges from 3 g/L in northern Saskatchewan (consistent with the Cambro-Ordovician Aquifer), to 330 g/L in south-central Saskatchewan (TWP 1 R12 W2) (Figure 3.3). The TDS gradationally decreases toward the west, north and northeast of the study area similar to that of the Cambro-Ordovician Aquifer. Data points confirming the position of the brackish mixing zone (25-100 g/L) are found in Manitoba (TWP 45 R25 and TWP 23 R12); however, in the Yeoman Aquifer the brackish mixing zone is broader and larger displacing higher TDS brine toward the basin centre. The overall areas of fresh water (< 10 g/L) are consistent with the underlying aquifer with some localized differences. The Lake Alma Anhydrite (shown in a dashed orange line) is present both in Saskatchewan and Manitoba. Where data are present, the contour line of 100 g/L brine compositions tracks the Lake Alma Anhydrite edge. In Manitoba (around TWP 8 R7) the dissolution edge parallels the isoconcentration lines of brackish-saline waters. Toward the basin centre, the Coronach Anhydrite is only present south of TWP 12 in Saskatchewan. Also of interest in the north and northeast is the outcrop belt of the Red River Formation (outlined in dark green).

Ordo-Silurian Aquifer

In the Ordo-Silurian Aquifer the Interlake Formation is the dominant aquifer. Regions of high TDS in the Ordo-Silurian Aquifer occur around TWP 20 and the provincial border, as well as in southern Saskatchewan where the high TDS plume is coincident with the deepest part of the aquifer (Figure 3.4). Significant anhydrites are also present within this aquifer and they are the Basal and Upper Stonewall anhydrites. Figure 3.4 shows the Stonewall Basal Anhydrite in a dashed light green line existing only south of TWP 15 and dominantly in Saskatchewan. The outcrop belts of the Stony Mountain, Stonewall and Interlake formations are shown in the north and northeast. The occurrence of 60 g/L waters at TWP 45 R25 (near the Mafeking Quarry) highlights the northerly extent of saline waters and the wide brackish mixing zone adjacent to the outcrop area. This transitional mixing zone of 25 to 100 g/L waters has encroached further into the middle of the study area as compared to underlying aquifers. In the west and north well developed, and data supported, freshwater incursion zones are more prevalent than any deeper aquifers.

Winnipegosis Aquifer

TDS content of the Winnipegosis Aquifer is shown in Figure 3.5. The distribution of TDS is similar to that of the Cambro-Ordovician and Yeoman aquifers, ranging from 5 g/L located in the far north of Saskatchewan (TWP 50 R23 W2) to 340 g/L near the centre of the high TDS plume (TWP 4 R9 W2). The region of brine with TDS greater than 300 g/L is larger than any of the underlying units, but does not extend as far north as in the Cambro-Ordovician and Ordo-Silurian aquifers. The distribution of brine greater than 200 g/L is significantly different, spanning much greater distances across the study area toward the northwest rather than the northeast as previously observed. Subtle increases in TDS near the western margin (TWP 36 R28 W2) are likely from formation waters outside of the study area (Benn and Rostron, 1998).

Also of interest in the Winnipegosis Aquifer is the presence of the fresh water recharge zones. The TDS low in the west observed in the Cambro-Ordovician Aquifer, and increasing up-section, is now more prevalent in the Winnipegosis Aquifer and seemingly influences the higher TDS composition present across much of Saskatchewan. Fresher waters are observed along the northern flank of the basin as far south as Township 30. Observed within this aquifer, the dissolution edge of the Prairie Evaporite Formation (Figure 3.5) coincides very closely with tongues of low TDS (topic of discussion in Section 5.2).

Manitoba Aquifer

The Manitoba Aquifer has a TDS range of 5 to 330 g/L (TWP 46 R9 W2 and TWP 27 R17 W2 respectively), similar to that of other aquifers mapped (Figure 3.6). The areas of high TDS brines are not as prominent in southern Saskatchewan as found in the lower aquifers, but formation waters of greater than 200 g/L have increased in distribution and occur as far north as TWP 40. The fresher water incursion from the west is more prominent with brackish waters inferred to exist as far as 51°N. In Manitoba, the brackish mixing zone is wider along the northeast flank of the basin. The mixing zone in the Manitoba Aquifer has a strong SW-NE trend (mildly depicted in the Cambro-Ordovician Aquifer) that extends south to around TWP 6 R12 W1. Lastly in the Manitoba Aquifer, the Davidson Member Salt (Figure 3.6) is present as outlined on the TDS map. It is one of four significant salt beds in this aquifer (Figure 2.4b). The Davidson salt dissolution edge correlates closely with greater than 200 g/L saline waters in central Saskatchewan, the location of high TDS brines (TWP 27 R17 W2 and TWP 24 R10 W2), and very closely with the fresh water tongue encroaching from the west starting around TWP 17 R29 W2.

Duperow Aquifer

Geochemical trends in the Duperow Aquifer are observed and supported by 86 sample points that cover a majority of the aquifer (Figure 3.7; Table 3.1). TDS variations within the Duperow Aquifer are consistent with many of the Lower

Paleozoic aquifers ranging from 5 g/L in northern Saskatchewan (TWP 46 R9 W2) to 330 g/L in southern Saskatchewan (TWP 6 R8 W2). Systematically, the spatial distribution of TDS is changing up-section, and the Duperow Aquifer best exemplifies this overall. It has similar characteristics to the Manitoba Aquifer, but with the areal coverage of water having TDS greater than 200 g/L diminishing. The brackish zone in the west is as far east as Range 19 W2, progressively displacing higher TDS waters. In the northwest, the brackish mixing zone is where the Manitoba Aquifer has waters greater than 100 g/L. The continual "invasion" and in particular an overall freshening upwards is noted also in the Duperow Aquifer supported by the northeast geochemical gradient subsequently found closer to the basin centre. The Flat Lake Salt is plotted on the TDS map (dashed orange line) and albeit largely dissolved in the west, it is noticed that the remaining salt edge mimics the overall shape of the intruding freshwater tongue and distribution of the greater than 200 g/L isoconcentration line in central Saskatchewan.

Birdbear Aquifer

The Birdbear Aquifer has TDS that ranges from 4 to 300 g/L (TWP 8 R26 W2 and TWP 6 R11 W2 respectively; Figure 3.8). Overall, the TDS decreases upward in the Lower Paleozoic and this pattern remains consistent in the Birdbear Aquifer. High TDS brine is absent within the Birdbear Aquifer. In contrast to the Manitoba Aquifer below where formation waters were generally greater than 200 g/L, within the Birdbear Aquifer they are between 50-100 g/L. Congruently, the western fresh-water tongue has become increasingly larger and encroaches toward the centre of the study area. Also worth mentioning is the fresh water incursion from the northeast is no longer present and brine of salinity greater than 100 g/L reaches the subcrop edge with a low of 19 g/L in the southeast corner.

Bakken Aquifer

TDS ranges from 25 to 280 g/L (TWP 5 R27 W2 and TWP 4 R14 W2 respectively; Figure 3.9) in the Bakken Aquifer. The Bakken Aquifer does not appear to mimic the underlying aquifers as compared to all the other Lower Paleozoic aquifers and it also has the lowest maximum TDS (Table 3.1). Nevertheless, the spatial distribution of the brines greater than 200 g/L has remained consistent with the underlying Birdbear Aquifer. The main difference is the brackish waters (25 to 50 g/L) occupy the northern area of the Bakken Aquifer. The waters ranging from 50 to 100 g/L extend no further than TWP 13 (data supported) in comparison to the Birdbear Aquifer where they are measured as far north as TWP 30 (Figure 3.8).

3.2.2 Mississippian Aquifers

The geochemical gradient in the Mississippian aquifers is oriented northwest to southeast (Figures 3.10-3.16). The Mississippian flow units have a significant reduction in the presence of high TDS brines (greater than 300g/L and only found within the Frobisher and Midale aquifers) and less dense formation waters occur in the northwestern margin of the study area. From the Alida Aquifer (Figure 3.12) to the uppermost Poplar Aquifer (Figure 3.16), there no longer is a brackish-freshwater composition in the north or northeast as previously noted in the underlying units. In general, the Tilston and Souris Valley aquifers (Figure 3.11, 3.10 respectively) have spatial TDS distributions that resemble that of the Bakken and Birdbear aquifers (Figure 3.9, 3.8 respectively). Up-section, it is observed that the plume of salinity ranging from 200-300 g/L (yellow scale) migrates eastward and is nearly completely gone in the uppermost Ratcliffe and Poplar aquifers (Figure 3.15, 3.16 respectively). As in the Lower Paleozoic aquifers the gradients are often steep, but in the Mississippian freshwater zones are only present in the north and northwest margins and high TDS brines in this system are limited.

Souris Valley Aquifer

The Souris Valley Aquifer has a TDS distribution that ranges from 15 g/L in the northwest portion of the aquifer (TWP 19 R28) to 280 g/L in southern Saskatchewan (TWP 2 R14) (Figure 3.10). There is a region of greater than 200 g/L waters in southern Saskatchewan and in Manitoba. Waters ranging from 100-200 g/L make up the southern half of the aquifer. In general, the southern portion of this aquifer is saline (greater than 100 g/L) while the north is composed of fresh-brackish water compositions. The Souris Valley Aquifer is characterized by a broad trough of fresh to brackish waters originating from the west and spanning across the entire aquifer into Manitoba. This large plume seems to cross-cut waters toward the north, south and east (TDS ranging from 50-100 g/L). The freshwater recharge zone to the west is prevalent and fresh to brackish waters make-up approximately 50% of the spatial distribution in this aquifer.

Tilston Aquifer

In the Tilston Aquifer, the range of TDS is similar to that in the Souris Valley Aquifer (Figure 3.11). The western portion of the map at TWP 3 R22 has a TDS value that is approximately 18 g/L. The highest value was found in southeastern Saskatchewan, TWP 5 R3 W2, and is approximately 260 g/L. The TDS distribution in this aquifer is characterized by a systematic decrease from southeastern Saskatchewan toward the margins of the Tilston Formation zero edge. The dominant geochemical gradient is orientated from northwest to southeast and a brackish composition exists along the northeast subcrop edge. The brackish-saline zone (50-100 g/L: purple area) along the northeast subcrop edge of the Tilston Aquifer correlates with the same zone as in the Souris Valley Aquifer.

Alida Aquifer

TDS in the Alida Aquifer ranges from 4 to 284 g/L (Figure 3.12). The low TDS waters are situated in the western portion of the map and specifically the lowest value is found in TWP 9 R23. High TDS waters in the Alida Aquifer are located in southern Saskatchewan and the highest value is in TWP 1 R9. In comparison to the underlying Tilston Aquifer (Figure 3.11), the Alida Aquifer is host to lower TDS waters but generally the same spatial extent of TDS less than 25 g/L exists between the two. The plume of water with TDS between 100 and 200 g/L is larger in the Alida Aquifer and brackish water does not exist along the subcrop edge as was apparent in the Tilston Aquifer. Overall, the Tilston and Alida aquifers have similar TDS distributions.

Frobisher Aquifer

TDS distributions in the Frobisher Aquifer have a large variation from as low as 10 g/L in the northwest to as high as 355 g/L in southeastern Saskatchewan (Figure 3.13). The highest TDS brine is located in TWP 2 R4 and progresses south into the US portion of the Williston Basin where brines with TDS greater than 300 g/L form a larger extent of the aquifer than recognized in Canada (Khan, 2006). The lowest TDS in the Frobisher Aquifer is found in TWP 9 R21 and is part of a large low in the northwest. This confirms the progressive invasion of low salinity waters documented in all underlying aquifers (Figures 3.10-3.12). There is no correlation with the Frobisher Evaporite (shown in a dashed orange line) and the TDS distribution. Overall, the TDS distribution is not starkly different than the Alida Aquifer.

Midale Aquifer

Formation waters in the Midale Aquifer show strong similarities to those established in the underlying aquifers (Figure 3.14). The variation in TDS is between 4 and 305 g/L (TWP 3 R28 and TWP 3 R6 respectively). The freshwater incursion zone covers the northwestern margin of the Mississippian aquifers with freshwaters also found in the southwest of the Midale Aquifer. In terms of higher TDS waters, the Midale Aquifer has just two samples that are slightly over 300 g/L and the distribution of waters over 200 g/L has diminished. The Midale Aquifer is not present in Manitoba and it is also noted that the well control is almost entirely dictated by the outline of the Midale Evaporite. No correlation between the Midale Evaporite and TDS is found.

Ratcliffe Aquifer

TDS distribution in the Ratcliffe Aquifer is from 5 to 290 g/L and is similar to the Midale Aquifer, but does not exceed 300 g/L (Figure 3.15). Freshwaters are dominant in the northwest and are the lowest in TWP 1 R28. Brines having a salinity between

200 to 300 g/L are present but minimal in proportion to all underlying aquifers in the south. The highest TDS sample is located in TWP 1 R15 and is consistent with the results to the south of the basin (Khan, 2006). Overall, the upper Mississippian aquifers have a reduction in TDS greater than 200 g/L.

Poplar Aquifer

The Poplar Aquifer contains a paucity of data with only 15 samples defining the TDS map (Figure 3.16); however, the coverage is sufficient to confirm the uniform freshening upward trend observed in the Mississippian aquifers. Deviation in the TDS is from 5 to 250 g/L and nearly mimics the locations in the Ratcliffe Aquifer (TWP 1 R28 and TWP 1 R17 respectively). Continued influx of freshwaters is identified in the northwest and the most saline brines are edging into the Canadian portion of the Williston Basin.

3.2.3 Mesozoic Aquifers

The Mesozoic aquifer system is separated by the Watrous Aquitard from the underlying Mississippian system. Three aquifers are mapped, out of the four identified, within the Mesozoic stratigraphy (Figures 3.17-3.19). There was insufficient data control to produce a TDS map of the Judith River Aquifer. Results indicate that the Watrous Aquitard forms a competent seal across the majority of southern Saskatchewan. The composition and distribution of formation waters is significantly different than both the Lower Paleozoic and Mississippian aquifers. Waters with TDS less than 50 g/L are predominant with freshwater zones characterizing the succession. An overall freshening-upward trend is recognized, albeit the patterns of TDS in the aquifers are distinctive. The Jurassic Aquifer (Figure 3.17) contains the only minor occurrence of saline waters with TDS over 100 g/L. Both the Jurassic and Mannville aquifers have higher TDS plumes in the northwest and all aquifers have considerable freshwater zones originating from the west.

Jurassic Aquifer

TDS in the Jurassic Aquifer is lowest in TWP 10 R25 W2 and is centred within one of two large freshwater regions (Figure 3.17). High TDS formation water (greater than 100 g/L) is also found in two regions: 1) in the northwestern region, with ample control to confirm its presence, and 2) in southwestern Manitoba (TWP 1 R26 W1), albeit only supported by one data point. Regionally formation waters with less than 50 g/L TDS prevail across the study area. Overall, there is a band of lower TDS running east-west with fresher waters found on the margins of the aquifer.

Mannville Aquifer

The Mannville Aquifer TDS distribution shows geochemical trends that are considerably different than the underlying aquifers (Figure 3.18). Minimum TDS is approximately 3 g/L in TWP 1 R27 W1 and is consistent with underlying aquifers. Two areas of low TDS occur in southwestern Manitoba and Saskatchewan. The highest TDS sample (77 g/L) is located in the west-central portion of the aquifer (TWP 32 R29 W2). There is an overall large-scale area of brackish waters entering the aquifer from the northwest consistent with higher TDS waters found in the Jurassic Aquifer. The TDS distribution and resultant gradient in the Mannville Aquifer is significantly different than the Jurassic Aquifer (Figure 3.17).

Newcastle Aquifer

The Newcastle Aquifer has a different TDS distribution and gradient than any others in the succession (Figure 3.19). The lowest TDS sample is located within an outlier at TWP 39 R29 W1. This sample, measured at 3 g/L, is not within the most predominant freshwater region. The largest freshwater zone occurs in the southwestern margin and this is consistent with many underlying aquifers. A TDS of 45 g/L defines the upper limit in the southeastern corner of the aquifer. This brackish water region was previously an area of fresher water in the underlying Mannville Aquifer (Figure 3.18).

3.3 MAJOR IONS

The analysis and classification of formation water samples must involve an illustration of their major individual ionic constituents. The standard major ions reported in formation water analyses are: Na, K, Ca, and Mg, Cl, SO_4, and HCO_3.

Principal chemical compositions of formation waters were identified and classified using major ion chemistry (Section 3.4). Predictable relationships have been observed in datasets from sedimentary basins worldwide (Hanor, 1994), and can be indicative in deciphering the chemical evolution and flow path in a regional scale flow system (Tóth, 1995). For the purposes of identifying major trends between ionic constituents and TDS in formation water compositions, the Lower Paleozoic, Mississippian and Mesozoic aquifers have been amalgamated. Major-ions and TDS are plotted for the cations of Na, K, Mg, and percent cationic Ca, and for the anionic percent of SO_4 and HCO_3 (Figures 3.20-3.22).

Lower Paleozoic Aquifers

For the Cambro-Ordovician through Bakken aquifers the major cation plots of Na, K, Mg, and percent cationic Ca, and the anionic percent of SO_4 and HCO_3 are graphed versus TDS (Figure 3.20).

There is a strong positive linear relationship between Na and TDS up to approximately 200 g/L where Na concentrations begin to drop out of solution and form a cluster on the graph (Figure 3.20a). Around 300 g/L there is a greater frequency of samples that have Na concentrations dropping sharply in the Lower Paleozoic aquifers. The Yeoman, Ordo-Silurian, Winnipegosis, and Manitoba aquifers have the greatest decrease in Na concentrations as described above.

Potassium (K) and Magnesium (Mg) both exhibit an exponential trend with increasing TDS (Figures 3.20b, c). Potassium (K) values increase steadily as TDS increases up to approximately 250 g/L where they rise sharply beyond 300 g/L (Figure 3.20b). With respect to Mg concentrations (Figure 3.20c), the trend is similar to that of potassium but with greater frequency and less scatter (formation water sample reports often list concentrations of Na and K together and therefore fewer data points are observed for K). The steep rise (positive association) commencing at approximately 200 g/L in both K and Mg mimics that of the decrease in Na. Again the Yeoman, Ordo-Silurian, Winnipegosis, and Manitoba aquifers have the greatest increase in K and Mg trends as described above.

Calcium can be a dominant cation in both formation waters with less than 25 g/L and brines in excess of 300 g/L (Figure 3.20d). The Lower Paleozoic aquifers have a characteristic "U-shape" correlation between Ca and TDS. In formation waters with less than 25 g/L, Ca accounts for up to 60% of the total cations (negative association with TDS) and drops to approximately 10% in waters having a TDS ranging from 50-200 g/L. After 200 g/L, the %Ca begins to increase again and a dominant spike occurs in brines having a TDS of 300 g/L and alternatively a positive association (Figure 3.20d). The characterization of water types to the variability in the cationic fraction of calcium will be discussed in the following section (Section 3.4).

The anionic fractions of both SO_4 and HCO_3 have strong negative exponential correlations with TDS (Figures 3.20e, f). Saline waters having TDS greater than 200 g/L have less than 5% SO_4 (Figure 3.20e). With decreasing TDS, SO_4 exponentially increases (up to 80% of the total anions) forming a negative association with TDS. Sulfate can be a dominant anion in waters with TDS less than 25 g/L and remains characteristically elevated in these waters. Bicarbonate has similar characteristics to that of SO_4, and can form up to 30% of the total anions in formation waters with less than 25 g/L (Figure 3.20f). All aquifers, albeit with significantly different magnitudes, display these SO_4 and HCO_3 relationships.

Mississippian Aquifers

For the Souris Valley through Poplar aquifers the major cation plots of Na, K, Mg, and percent cationic Ca, and the anionic percent of SO_4 and HCO_3 are graphed versus TDS (Figure 3.21).

The relationship between Na and TDS for the Mississippian aquifers is a strong positive linear correlation throughout the entire range of TDS (Figure 3.21a). Other than a few data points noticed individually in the Poplar Aquifer, the characteristic "downward" hook observed in the Lower Paleozoic aquifers (Figures 3.20a) does not exist.

Potassium and magnesium relationships are again different in the Mississippian as compared to the Lower Paleozoic aquifers (Figures 3.21b, c). The distinctive rise in K and Mg around 250 g/L is no longer present. Essentially, K shows a gentle exponential increase overall (Figure 3.21b) and greater scatter in the data. Moreover, Mg (Figure 3.21c) has neither sharp increase nor exponential rise but rather a strong positive linear correlation.

The cationic percent Ca relationship in the Mississippian aquifers (Figure 3.21d) is in contrast to the Lower Paleozoic aquifers (Figure 3.20d). The characteristic "U-shape" dependence with TDS no longer exists but rather a strong negative exponential correlation. TDS in excess of 25 g/L never exceeds 20% calcium, with the exception of one sample in the Ratcliffe Aquifer. It is apparent that lower TDS waters between the Mississippian and Lower Paleozoic aquifers have a similarity in elevated levels of Ca, but high TDS brines in the Mississippian have low percentage Ca in their composition.

Anionic fractions of both SO_4 and HCO_3 in the Mississippian aquifers (Figures 3.21e, f) are nearly indistinguishable to those in the Lower Paleozoic aquifers (Figures 3.20e, f). Sulfate and bicarbonate have the same negative exponential correlation and maximum SO_4 concentrations are even comparable. High percentages of SO_4 are still found below 25 g/L and form a positive association with calcium as in the freshwaters of the Lower Paleozoic aquifers. Bicarbonate alternatively still has the negative exponential correlation but never forms greater than 20% of the total anions (Figure 3.21f).

Mesozoic Aquifers

For the Jurassic through Newcastle aquifers the major cation plots of Na, K, Mg, and percent cationic Ca, and the anionic percent of SO_4 and HCO_3 are graphed versus TDS (Figure 3.22).

As observed in the Mississippian aquifers (Figure 3.21), the correlation between Na and TDS for the Mesozoic aquifers is again a strong positive linear relationship (Figure 3.22a). Noticeably different though is the range of TDS in the Mesozoic aquifers, having a considerably lower range in comparison to all underlying aquifers (Figures 3.20, 3.21).

Potassium and magnesium concentrations for the Mesozoic aquifers form minor constituents of the water composition (Figures 3.22b, c). Essentially, a cluster forms at low TDS values and as TDS increases a linear increase in K and Mg is observed.

Calcium concentrations in the Mesozoic aquifers are less than 15% (Figure 3.22d). However, there are three outliers in the Jurassic Aquifer that did not warrant culling and are considerably higher (Figure 3.22d). In general, these Ca-deficient fresh waters in the Mesozoic aquifers are unlike the freshwaters in the Mississippian and Lower Paleozoic aquifers.

The anionic percent of SO_4 in the Mesozoic aquifers has a predictable distribution (Figure 3.22e). The lower range of TDS in these aquifers creates a near vertical line and can be described as SO_4 having a negative association with TDS (low TDS equals higher SO_4). Sulfate values are measured up to approximately 80% of the total anions, when the TDS is less 25 g/L, but interestingly only the Jurassic Aquifer has SO_4 values over 30% (not shown). This observation then draws a comparison of the Jurassic Aquifer to some of the underlying two deeper aquifer groups and segregates the Mannville and Newcastle aquifers exclusively in the Mesozoic succession.

Water compositions between the Jurassic and overlying Mannville and Newcastle aquifers are distinguishable. When compared together, the graph of HCO_3 and TDS forms an "L" shape with lower TDS waters having a higher percentage of HCO_3 (Figures 3.22f). In the Mesozoic aquifers, the anionic percentage of total HCO_3 is up to 35%. However, greater than 15% HCO_3 is only recognized in the Mannville and Newcastle aquifers. The Jurassic Aquifer's HCO_3 composition is less than 15%, further distinguishing the compositional differences between the three Mesozoic aquifers.

3.4 FORMATION WATER CLASSIFICATION

Previous hydrochemistry investigations in the Williston Basin have defined distinct water compositions (Benn and Rostron, 1998; Iampen, 2003; Khan, 2006; Jensen, 2007). Khan's (2006) water classification for the basin will be used here.

The following type waters define the principal chemical compositions observed in this study area. There are four end-member water compositions that were identified using major ion chemistry (see Section 3.3 and Figures 3.20-3.22):

Type 1: Ca-SO_4

This Type 1 water is characterized by Ca in excess of 40% the total cations, SO_4 having greater than 50% of the total anions concentration, and a corresponding low TDS that is less than 10 g/L. Type 1 waters using Back's (1960, 1961) hydrochemical facies would actually be referred to as Calcium-Sodium-Chloride-Sulfate waters.

However for clarity, the dominant and prevalent sodium and chloride components have been left off.

Type 2: Na-Cl

Type 2 waters are Na-Cl dominant and span the complete range of TDS mapped in this study (Table 3.1). The Ca and SO_4 concentrations account for less than 10% of their respective cationic and anionic fractions defining this type water.

Type 3: Na-HCO_3

Type 3 waters have a composition that is comparatively elevated with respect to HCO_3 and deficient in cationic Ca concentrations. This fresh water has a TDS less than 10 g/L, HCO_3 levels greater than 20% of total anions, and the Ca component less than approximately 10% total cations.

Type 4: Na-SO_4

Sodium-sulphate type waters have an intermediate and mixed composition that represents the chemistries found in the brackish water transition zone (Khan, 2006). These waters occur approximately between the TDS contours of 25-100 g/L but never exceeding 100 g/L. In addition, it was interpreted by Khan (2006) that this type water is likely a result of mixing between Type 1 fresh waters and Type 2 brines.

3.4.1 Type Water Designation

Principal chemical compositions of formation waters were identified and classified into water types using major ion chemistry. The proceeding section describes the distribution and compositional similarities and differences between the aquifers.

Lower Paleozoic Aquifers

All of the Lower Paleozoic aquifers have Type 2 (Na-Cl) brines and Type 4 (Na-SO_4) mixed/intermediate composition formation waters. The lower three aquifers

(Cambro-Ordovician, Yeoman, and Ordo-Silurian aquifers) have Type 2 and 4 waters, but also have Type 3, Na-HCO_3 fresh waters. Furthermore, the Duperow and Birdbear aquifers are compositionally unique in the Lower Paleozoic system because they contain Type 1 Ca-SO_4 fresh waters.

Mississippian Aquifers

The Mississippian aquifers also contain Type 2 and Type 4 waters as compared to the Lower Paleozoic aquifers. The Na-SO_4 waters for the Mississippian vary significantly. In the Souris Valley and Tilston aquifers, the anionic SO_4 composition never exceeds 40% (also found in Bakken Aquifer). The Alida through Poplar aquifers all have samples that contain greater than 50% SO_4. The Ratcliffe and Poplar aquifers also have Type 1 fresh waters that compositionally differentiate them from any other aquifers in the Mississippian.

Mesozoic Aquifers

The Mesozoic aquifers are compositionally distinct when compared to both underlying aquifer groups. Type 2 brines are much lower in TDS and are only observed in a small region of the Jurassic Aquifer (Figure 3.17). Also, the Jurassic Aquifer contains Type 1 waters, only previously observed in the Poplar, Ratcliffe, Duperow and Birdbear aquifers. This makes the Jurassic Aquifer compositionally similar to the underlying units and different to both of the overlying aquifers. Fresh to brackish waters dominate the Mannville and Newcastle aquifers with Type 3 and Type 4 waters making up the principal water types. Type 3 waters are also found in the Cambro-Ordovician, Yeoman and Ordo-Silurian aquifers.

Aquifer	Number of Water Chemistry Samples		TDS Range (g/L)	
	Raw	Mapped	Min	Max
Judith River	7	1	N/A	N/A
Newcastle	155	42	3.0	45.0
Mannville	234	53	3.0	77.0
Jurassic	739	74	4.0	130
Poplar	163	15	5.0	250
Ratcliffe	710	61	5.0	290
Midale	2220	177	4.0	305
Frobisher	3053	488	10	355
Alida	471	144	4.0	284
Tilston	527	175	18	260
Souris Valley	1002	226	15	280
Bakken	110	35	25	280
Birdbear	432	192	4.0	300
Duperow	230	86	5.0	330
Manitoba	235	70	5.0	330
Winnipegosis	575	117	5.0	340
Ordo-Silurian	193	85	3.0	471
Yeoman	428	75	3.0	330
Cambro-Ordovician	202	81	3.0	350

Table 3.1. Number of water chemistry samples and the range of TDS measured in each aquifer.

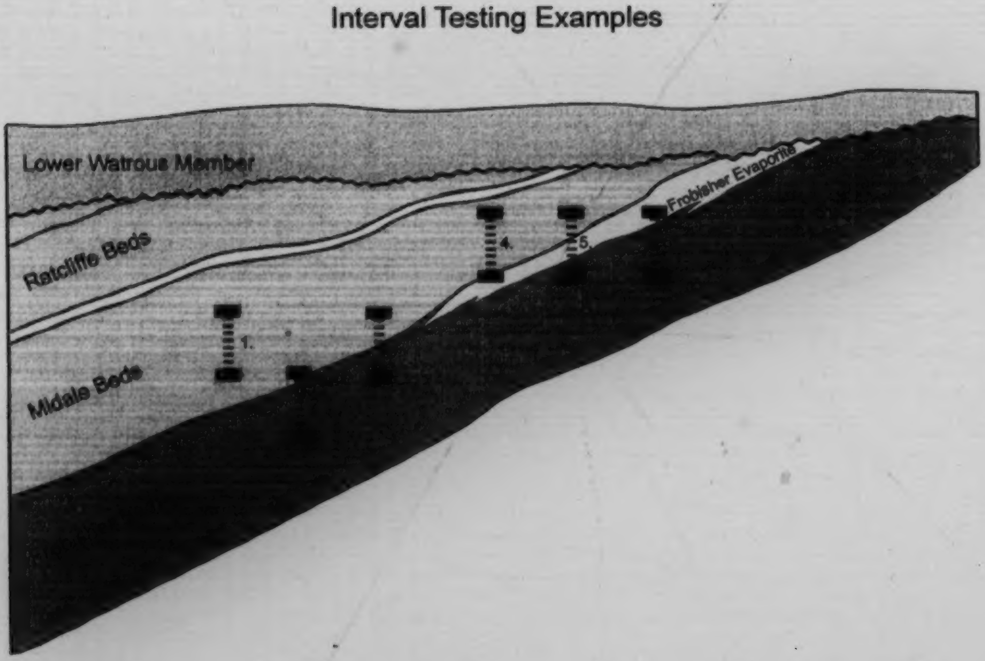
Interval Testing Examples

1. Midale test - database correctly reports Midale
2. Frobisher test - database erroneously reports Midale
3. Midale/Frobisher test - database reports only Midale
4. Midale test - database correctly reports Midale test where bottom packer is identified to be in the Frobisher evaporite
5. Midale/Frobisher test - database reports Frobisher evaporite and erroneously concludes that the test must be in Frobisher Beds based on an assumption that the top packer is seated in the evaporite unit.
6. Frobisher test - database reports Frobisher evaporite, correctly concludes that test must be in Frobisher Beds.

Figure 3.1. Interval testing of drill stem tests and associated water sampling intervals with respect to Mississippian structure and stratigraphy (modified after Rostron and Khan, 2005). This identifies the common discrepancy between formations reported in the oil and gas databases versus determining the precise intervals tested using the interval testing procedure.

The Figures 3.2 to 3.19 (pages 60 to 77) have been removed at the request of the Faculty of Graduate Studies and Research at the University of Alberta. These tabloid sized maps will not be included in the microfilming version of this dissertation.

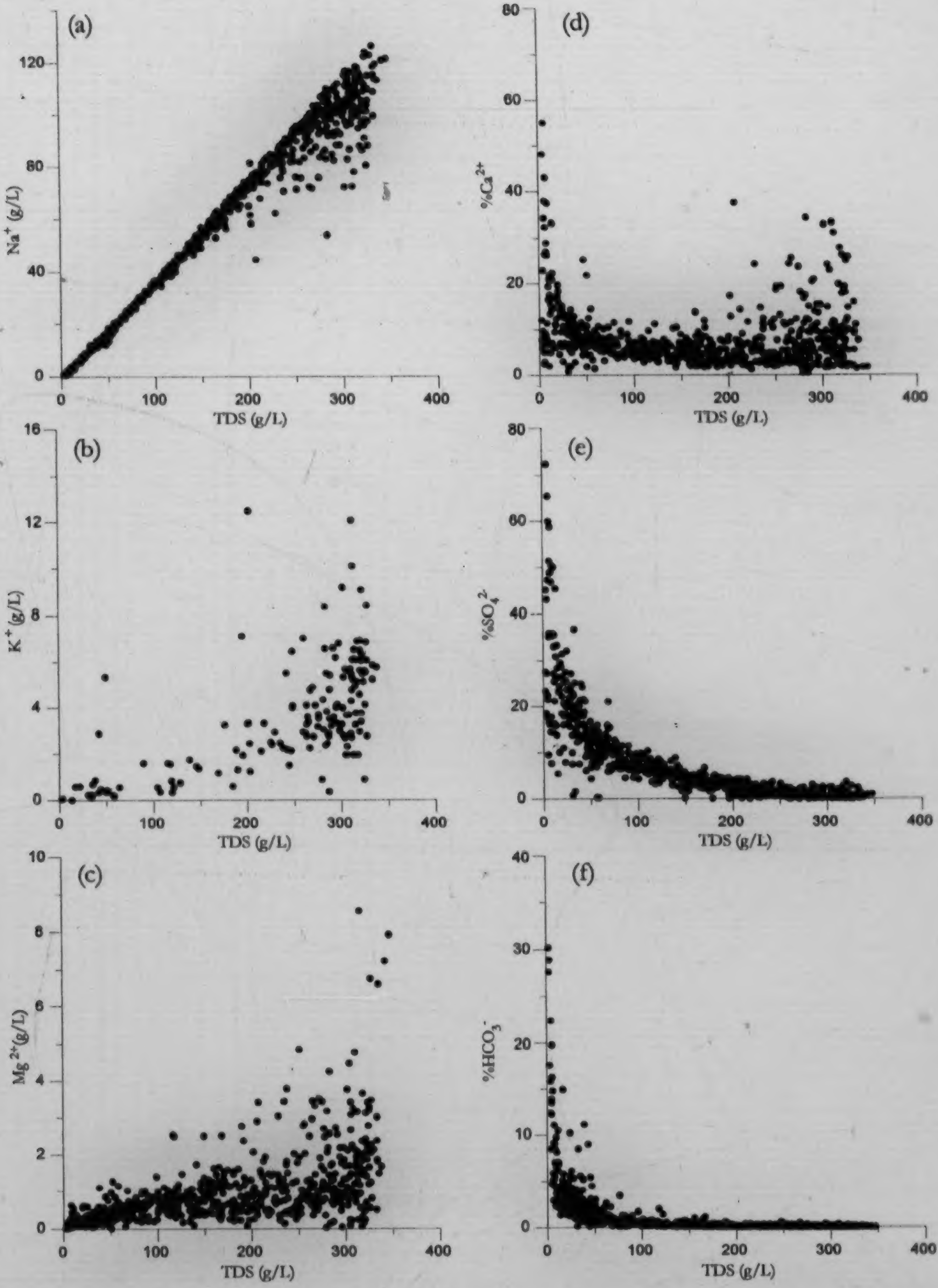

Figure 3.20. Major cation plots of Na (a), K (b), Mg (c), and percent cationic Ca (d), and the anionic percent of SO_4 (e) and HCO_3 (f) are plotted versus Total Dissolved Solids for the Lower Paleozoic aquifers.

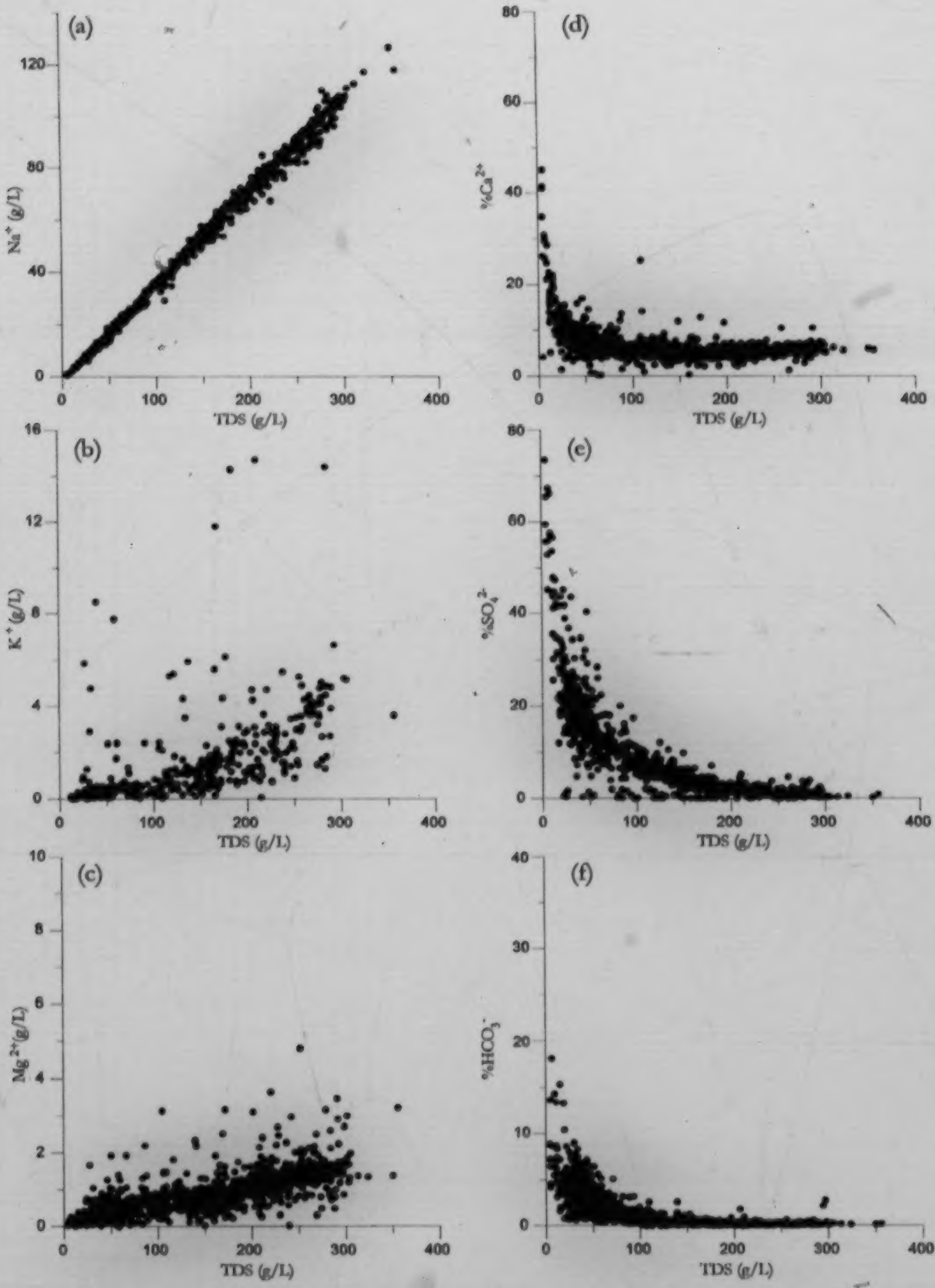

Figure 3.21. Major cation plots of Na (a), K (b), Mg (c), and percent cationic Ca (d), and the anionic percent of SO_4 (e) and HCO_3 (f) are plotted versus Total Dissolved Solids for the Mississippian aquifers.

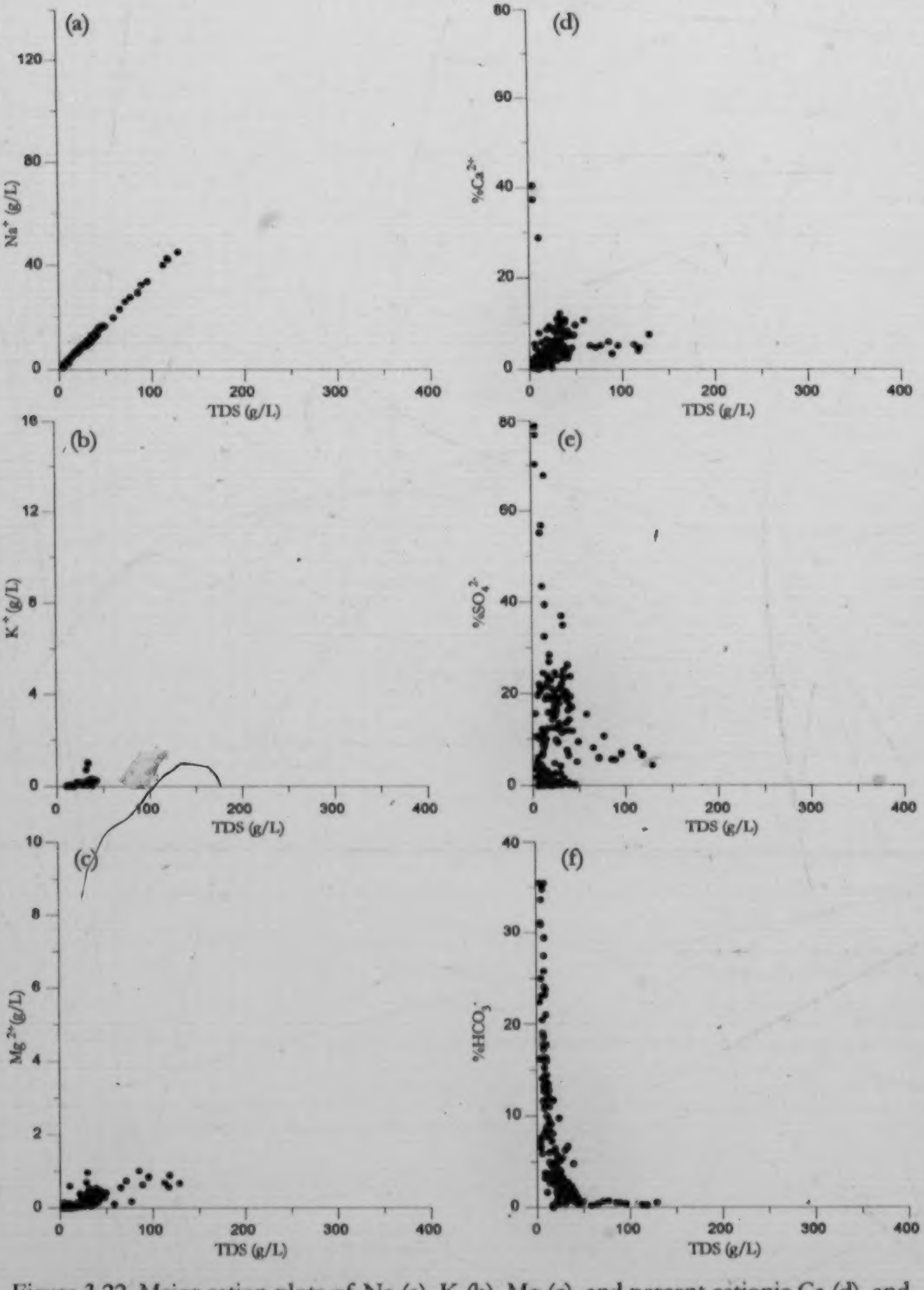

Figure 3.22. Major cation plots of Na (a), K (b), Mg (c), and percent cationic Ca (d), and the anionic percent of SO_4 (e) and HCO_3 (f) are plotted versus Total Dissolved Solids for the Mesozoic aquifers.

4.0 REGIONAL GROUNDWATER FLOW AND DRIVING FORCES ON FORMATION WATERS

4.1 DATA AND METHODOLOGIES

A fluid pressure, formation temperature, and production database was assembled for each well in the entire Phanerozoic succession. The fluid pressure database was assimilated from drill-stem tests that measure reservoir conditions such as fluid types, pressures, flowrates, and down-hole temperatures. A drill-stem test (DST) is essentially a temporary well completion that records pressures as a function of time and collects a fluid sample. DSTs are used to determine the potential productivity of oil or gas reservoirs by measuring reservoir pressures and flow capacities (Dahlberg, 1994).

Public pressure data was sourced from three databases. First, Geoscout (Geologic Systems Ltd.) was assessed to compile DST data. The pressure data available in Geoscout was taken from Hydrofax Resources, a company that specializes in updating and generating digital pressure databases from historic oil and gas exploration data for the Western Canada Sedimentary Basin (WCSB). Second, digital data from the Canadian Institute of Formation Evaluation (CIFE) were available. These two datasets were compared and one comprehensive hydrogeological database was generated. Finally, on an individual aquifer basis, Accumap (IHS Inc.) was queried to fill in any remaining gaps between the two previously mentioned data sources. Accumap could not be directly used because its data is stored as images, rather than in digital form. Thus, it requires digitizing before any calculations can be completed. Further, extrapolations (Horner, 1951) to arrive at reliable virgin-reservoir pressures are not readily available in Accumap. Over 4300 fluid pressures, fluid recoveries, and formation temperatures have been compiled (Table 4.1).

4.1.1 Pressure Data Culling

All pressure data, similar to the water chemistry data (see Section 3.1.1), were carefully screened using both automated and manual techniques to remove inaccurate or non-representative fluid pressures. A number of parameters must be analyzed to ensure only quality pressure samples are used to calculate hydraulic heads for all the aquifers. In addition to examining the individual DSTs for their flow and shut-in periods, calculations must be completed to determine the influence of production and injection within the reservoir.

To examine the influence of production and injection drawdown on the aquifers/reservoirs, the method of Cumulative Interference Index (CII) was employed (Tóth and Corbet, 1986; Barson, 1993; Rostron, 1994; Alkalali, 2002). For each pressure, a quantitative index was calculated accounting for radial proximity of a DST to production and/or injection wells and the duration of production and/or injection. To facilitate these calculations, the Visual Basic Code developed by Alkalali (2002) was utilized. After calculating a CII for each pressure measurement, manual examination of the actual DST was performed. Quality control was assessed by a number of criteria. Details of the culling procedures used are discussed in Appendix B. The pressure data culling procedure arrives at the best possible representation of undisturbed formation pressures in an aquifer and resultant approximation of the potentiometric surface.

4.2 RESULTS: POTENTIOMETRIC ANALYSIS AND DRIVING FORCES

The flow of formation waters is deduced from distributions of freshwater hydraulic heads. The dominant driving force effecting the movement of formation fluids is the fluid potential gradient. Water will flow from high to low fluid potential assuming no groundwater density variations exist in the aquifer. According to Hubbert (1940, 1953):

$$\Phi = g\,z + \frac{p}{\rho} = g\,h \tag{1}$$

re-arranging and solving for h

$$h = z + \frac{p}{\rho g} \tag{2}$$

where: Φ is fluid potential, h is the hydraulic head, z is the elevation of the pressure recorder, p is the fluid pressure, ρ is the fluid density, and g is the acceleration due to gravity. In equation (2), z represents elevation head and $\frac{p}{\rho g}$ represents pressure head.

Maps of freshwater hydraulic heads are traditionally used to infer flow directions travelling perpendicular to equipotential lines. Freshwater hydraulic head represents a column of freshwater in equilibrium with pore pressure at the point of measurement (Tóth, 1978). Fluid potential gradients imparted by topographic elevation differences between the recharge and discharge zones often dominate the fluid driving force regime in sedimentary basins (e.g. Tóth, 1978; Garven, 1995).

Potentiometric surface maps provide an estimation of the hydraulic gradient component acting on the formation fluids and overall direction of groundwater flow. These maps have been created and are found in Appendix C. They use a contour interval of 40 m because this is the accuracy of the pressure recorders used during the DSTs (Alkalali, 2002). However, density variations of the formation fluids influence the flow fields and gradients.

TDS variations both across and within all aquifers have been observed and delineated in Chapter 3. The effects of groundwater density variations on lateral groundwater flow can have local variations that influence the net driving force on formation fluids given the favorable hydrodynamic and basin conditions.

Variable density groundwater flow and its effects on a regional scale have been previously addressed in the WCSB (Davies, 1987; Bachu, 1995; Alkalali, 2002; Bachu and Michael, 2002; Alkalali and Rostron, 2003; Khan, 2006). Early investigations focused largely on the delineation and adjustment of uncertainty imposed by strictly analyzing freshwater hydraulic head distributions. Density-dependent flow of brines in the Williston Basin was originally hypothesized by Downey (1984a, b; 1986) and Downey et al. (1987) with quantitative analyses of density-flows recently completed for the Nisku Aquifer across the WCSB by Alkalali (2002) and a Cambrian-Cretaceous study around the Weyburn CO_2 project area by Khan (2006).

The density-dependent driving force analysis completed here follows the methodology and conceptual model of Khan (2006) and utilizes the computer program presented by Alkalali and Rostron (2003). Details on the methodologies used to calculate the in-situ formation water densities and the water driving force vectors are provided in Appendix D.

In summary, to calculate the in-situ brine density across the regional aquifers the equation of state was used (Appendix D). Discretized grids of TDS and formation temperatures were required as input for the calculations. Hydraulic gradients were computed from the potentiometric surface maps (Appendix C). Structure gradients were calculated from structure maps generated for the base of the aquifer under analysis (not shown). The structural gradients are required to calculate the Water Driving Force (WDF).

The following sections describe the mapping and analysis for groundwater flow (potentiometric surfaces and density-dependent driving forces). The precise location of the pressure measurements, obtained from DSTs, was determined using the procedure outlined in Section 3.1.2 "Interval Testing Verification".

The WDF vector maps (Figures 4.1-4.18) quantify the apparent hydraulic gradient (Table 4.2) and horizontal orientations of groundwater flow. They also have the equipotentials (Appendix C) overlain on the map to show the direction of flow inferred from the potentiometric surface. The azimuthal difference between the density-dependent water driving force (black arrows) and the hydraulic gradient driving force (grey arrows) vectors are indicated by the coloured contours ranging from light orange to dark orange as the angle between the two components increases respectively (Appendix D; Figure D.1). Directions and magnitudes of formation water flow are quantified by the density-dependent water driving force vectors (black arrows). Important observations to notice in the WDF maps are the presence of black arrows diverging from the orthogonal direction to the equipotentials, and their angle of divergence. Magnitudes are also important and are shown by the size of the vector arrows (see legend for scale). Complete flow reversals are recognized as regions that are shaded darker orange representing a greater than 90 degree azimuthal difference in WDF and hydraulic gradient. For clarity, the control points used to calculate hydraulic heads have been left off the WDF maps; however, their exact locations are on the "Freshwater Hydraulic Head" maps in Appendix C.

The following sections describe the results of the WDF maps with the exception of the Judith River Aquifer (Freshwater Hydraulic Head map found in Appendix C) that has insufficient data to produce a TDS map.

The number of pressure control points, original and after culling, and the minimum and maximum hydraulic heads for each aquifer are summarized in Table 4.1. The hydraulic and density-corrected gradients are found in Table 4.2.

4.2.1 Lower Paleozoic Aquifers

The Lower Paleozoic aquifers (Cambro-Ordovician to Bakken aquifers) have formation fluids traveling up-dip towards the northeast outcrop and subcrop locations (Figures 4.1-4.8). East-northeast flow in the western margin of the study area is found in the Ordo-Silurian, Manitoba, Duperow and Birdbear aquifers (Figures 4.3, 4.5-4.7). The potentiometric surfaces as a group are generally similar, but local and regional scale variations are observed.

Areas of significant density-corrected water driving force are found easily by regions contoured in dark orange. Density effects can increase up to a complete "flow reversal" when the combined dominant driving force is orientated 180 degrees opposite to that of the driving force caused by the hydraulic gradient alone.

Overall, the aquifers contain some regions of considerable density-driven flow effects. Considering the high formation water densities found in the Lower Paleozoic aquifers (Section 3.2.1) this is expected. The Cambro-Ordovician and Yeoman aquifers (Figures 4.1-4.2) both have down-dip "flow reversals". These flow reversals are in different regions of southern Saskatchewan and it is observed that the density-dependent water driving force vectors (black arrow) are pointing in significantly opposing directions with considerably lower magnitudes. High potentiometric zones observed around Lake Manitoba are clearly identified by the regions of larger arrows in the Cambro-Ordovician and Yeoman aquifers. The Yeoman Aquifer (Figure 4.2) has a region in southeastern Saskatchewan that has strong down-dip preferential flow. Furthermore, the Yeoman, Ordo-Silurian and Manitoba aquifers have some of the highest gradients (both hydraulic and density-corrected) calculated for the Lower Paleozoic aquifers (Table 4.2).

In the Ordo-Silurian Aquifer (Figure 4.3) the Water Driving Force (WDF) analysis identifies an interesting feature. There is a complete orthogonal departure of flow directions, in comparison to that inferred from the equipotentials, within the first five townships of southern Saskatchewan. The density-corrected flow direction is actually from west to east in this zone, rather than the ubiquitous up-dip flow directions. Also, the Ordo-Silurian Aquifer has a southeast-northwest trend found between the equipotentials of 350 and 390 m that appears again up-section in the Winnipegosis and Manitoba aquifers (Figures 4.4, 4.5). On a local scale the divergence is quite minimal, but on a regional scale the effects and correlation between the reduction in hydraulic gradient and the resulting buoyancy effect is important.

Equipotentials in the Winnipegosis Aquifer are planar, like the others, and overall lower heads are found (Table 4.1). The Winnipegosis Aquifer has significant density-flows in southern Saskatchewan (Figure 4.4) when compared to the Duperow and Birdbear aquifers (Figures 4.6, 4.7). In addition, regions where the WDF is of significance, the Winnipegosis Aquifer also has the lowest calculated hydraulic and water driving force gradients of the Lower Paleozoic aquifers (Table 4.2). No distinct perturbation in the pressure field is correlated to the dissolution edge of the Prairie Evaporite Formation in the northeastern margin (Figure 4.4 dashed orange line). However, in the southwestern corner, increased gradients and higher hydraulic heads evidently coincide with the dissolution edge.

The Manitoba Aquifer (Figure 4.5) has a large region in southern Saskatchewan that exhibits marked flow reversals also with considerable magnitude. In fact, the Manitoba Aquifer has the largest WDF gradients (Table 4.2) in comparison to all others in the Lower Paleozoic aquifers but fluid potentials remain consistent with the underlying aquifers.

The Duperow and Birdbear aquifers (Figures 4.6, 4.7), in southern Saskatchewan, have buoyancy effects that result in azimuthal differences between the WDF and the hydraulic gradient; however, the gradients are low and highlight a quasi-stagnant zone. The Bakken Aquifer (Figure 4.8) has a delineated zone in southern Saskatchewan that indicates east-southeast flow inferred from the WDF. This region is roughly the first five townships in Saskatchewan, and in Manitoba the density-controlled flow continues along the subcrop edge.

4.2.2 Mississippian Aquifers

Potentiometric surfaces, hydraulic gradients, and water driving force gradients for the Mississippian aquifers are shown in Figures 4.9-4.15. Overall, hydraulic heads in the Mississippian aquifers are higher than the Lower Paleozoic aquifers (Figures 4.1-4.8, Appendix C). In comparison to the Lower Paleozoic aquifers, flow directions exhibit noticeable differences with the exception of the Souris Valley Aquifer (Figure 4.9). Principal flow directions in the Mississippian aquifers, except the Poplar Aquifer described below, are up-dip from west to east. Moreover, hydraulic gradients in the Mississippian aquifers, for example the Frobisher and Midale aquifers (Table 4.2), are lower as shown by increased equipotential spacing in south-central Saskatchewan (Figures 4.12, 4.13).

The uppermost Poplar Aquifer (Figure 4.15) has a potentiometric surface that contrasts both other Mississippian and the entire Lower Paleozoic aquifers. The Poplar Aquifer not only has the highest hydraulic heads calculated throughout the entire Phanerozoic succession (Table 4.1), but also has a dominant northward flow direction with steep hydraulic gradients (Figure 4.15).

The Mississippian aquifers exhibit both local-scale variability in buoyancy-controlled flows and have the highest average hydraulic and WDF gradients in the Frobisher Aquifer (Figure 4.12; Table 4.2). In addition, the directly adjacent Midale Aquifer (Figure 4.13) has the lowest calculated minimum and maximum hydraulic and WDF gradients in the entire study (Table 4.2). Throughout the Mississippian aquifers, density-dependent water driving force is largely found in southeastern Saskatchewan as in depicted in Figures 4.9-4.15 (eastern margins of the aquifers).

The Souris Valley Aquifer has a potentiometric surface that mimics the Lower Paleozoic aquifers and in particular the directly adjacent Bakken Aquifer (Figures 4.9 and 4.8 respectively). The Souris Valley Aquifer has the lowest indication of density effects in the Mississippian. Flow directions are predominantly controlled by hydraulic gradients and are up-dip toward the northeast (Figure 4.9). Flow-reversals are evident in approximately the same spatial locations for the Tilston and Alida aquifers (Figures 4.10, 4.11).

WDF maps in the Frobisher and Midale aquifers are shown in Figures 4.12 and 4.13. Flow directions are still from east-northeast and hydraulic heads are increasing up-section (Table 4.2). Density-controlled flows are significant in the Frobisher and Midale aquifers. The Frobisher Aquifer has local flow-reversals occurring along the northeastern subcrop edge and hydraulic gradients are much less, in the eastern margin of the aquifer, in comparison to the WDF vectors (Figure 4.12). The Midale Aquifer, in the eastern margin, has the largest down-dip flow-reversals than any other aquifer in the Mississippian (Figure 4.13 and Table 4.2).

Density-dependent flows are similar in the Ratcliffe and Poplar aquifers (Figures 4.14, 4.15). The western margin of the Poplar Aquifer is dominated by a convergent zone that is a result of a potentiometric low. This region is controlled by the hydraulic gradient driving force. However, the black WDF arrows are only seen because the two vectors are completely parallel indicating no difference in azimuth or magnitude.

4.2.3 Mesozoic Aquifers

Potentiometric surfaces for the Mesozoic aquifers beginning with the lowermost Jurassic Aquifer and ending with the uppermost Judith River Aquifer are shown in Figures 4.16 to 4.18 and Appendix C respectively. Local and regional scale variations exist between the Mesozoic aquifers and the underlying aquifer systems. Overall, hydraulic heads within the Mesozoic aquifers are lower than both major underlying aquifer systems (Lower Paleozoic and Mississippian). Flow directions in the Jurassic Aquifer (Figure 4.16) are similar to the underlying Mississippian units, while the Mannville and Newcastle aquifers show significant differences (Figures 4.17, 4.18). The Jurassic Aquifer has generally east-northeast flow directions that are similar to the Tilston and Alida aquifers, albeit with a different magnitude.

Flow patterns in the Mannville, Newcastle and Judith River aquifers have unique hydraulic patterns (Figures 4.17, 4.18 and Appendix C). Large-scale focused flow is evident in the Mannville Aquifer. Fluid potentials appear to be reacting to large north-south trending channels of thick sands within the Mannville Aquifer (Christopher, 2003). Overall, groundwater flow is dominantly north-northeast in the Newcastle and Judith River aquifers.

The absence of dense brines in the Jurassic, Mannville and Newcastle aquifers warrants the use of strictly potentiometric surfaces to infer flow directions. Nevertheless, the WDF maps (Figures 4.16-4.18) for these aquifers provide useful quantification of the magnitudes and directions of formation water flow. These maps are also quite useful in determining areas of divergent and convergent flows controlled by potentiometric highs and lows that would otherwise not be as evident. For example, the Jurassic Aquifer (Figure 4.16) in southwestern Manitoba has a region where divergent flow exists. Flow is directed outward towards the escarpment and potentiometric low in southeastern Saskatchewan. Table 4.2 displays the hydraulic and water driving force gradients for the Mesozoic aquifers. The gradients systematically decrease, leaving the Newcastle Aquifer with the lowest gradients in the Mesozoic and on average in the entire Phanerozoic succession (note that the Midale Aquifer actually has lower minimums and maximums than any other aquifer).

4.3 VERTICAL PRESSURE GRADIENTS

To determine the presence of any vertical variations in fluid potential and hydraulic gradients, indicating any upward or downward movement of groundwater and existence of hydraulic continuity in the stratigraphic succession, the analysis of pore pressures versus depth (p(d) profiles) (Tóth, 1978) was employed. Density-corrected driving forces and potentiometric surface mapping reflects the horizontal gradients acting within the aquifers; however, determining whether the aquifers are under-pressured, normally-pressured, or over-pressured quantifies the vertical flow and hydraulic communication.

Three regions have been chosen for pressure-depth analysis exemplifying conditions where vertical gradients may or may not be of significance in the northeastern margin (Figures 4.19-4.22). The results are integrated with those from Khan (2006) and are discussed further in Chapter 5 (Figure 4.19 and 4.23, identified in hatched-grey blocks). Ideal block sizes, corresponding to regions where topographic elevation differences are negligible and adequate data are present, was sought in local areas to minimize the effects of aquifer heterogeneity and topographic relief (Tóth and Almasi, 2001).

In the west-central portion of the study area (Figure 4.20; Block 1), pressure data were available for p(d) analysis spanning the Yeoman through Birdbear and Mannville aquifers. The Paleozoic and Mesozoic aquifers have pore-pressure measurements that all plot closely along the nominal hydrostatic gradient. This indicates that in the west-central region there is predominantly horizontal flow. Interestingly, the Mannville Aquifer in this region exemplifies slight under-pressuring and is consistent with most samples above the Prairie Evaporite Formation (Figure 4.20). Directly south of this region in Khan's (2006) investigation (Figure 4.19, Block 7) a significant upward component to flow in the Paleozoic aquifers was found (Figure 4.23; Block 7).

Super-hydrostatic pressure conditions exist in a region straddling the provincial border around TWP 20, block 2 (Figures 4.19 and 4.21). This region is under-pressured from the Cambro-Ordovician through Mannville aquifers. Cambro-Ordovician through Winnipegosis aquifers are on a different pressure gradient than the overlying Manitoba through Mannville aquifers. The deeper Cambro-Ordovician to Winnipegosis aquifers fall on the same super-hydrostatic gradient of 14.4 kPa/m. This vertical pressure profile demonstrates there is vertical hydraulic communication between the Cambro-Ordovician through Winnipegosis aquifers and likely a component of upward flow is present. Furthermore, towards the basin margin, it would be expected that the net saturated flow of groundwater be directed upward as the dynamic pressure will be greater than the static weight of the overlying column of fluid.

The overlying pressure data in block 2 (Figure 4.21) comes from the Manitoba to Mannville aquifers and also plots along a single super-hydrostatic gradient. As mentioned above, because all the data in this region falls along a super-hydrostatic gradient of 11.1 kPa/m, it suggests that there is vertical hydraulic continuity and upward flow between the Manitoba, Duperow, Birdbear, Bakken and Mannville aquifers. There appears to be a hydraulic separation and discontinuity between these two packages of aquifers (Figure 4.21) and this can be explained by the competent Prairie Evaporite Aquitard (structure top at approximately 1091.5 m). In block 2, the Prairie Evaporite Formation is up to 80 m thick and forms the barrier between the lower and upper super-hydrostatic gradients depicted here.

Also of interest in block 2 is the under-pressuring of all the Mannville Aquifer samples along this hydrostatic gradient (Figure 4.21; 387 – 444 m depth). This was previously mentioned in the potentiometric surface analysis and is confirmed in the pressure-depth profile.

Block 3 is located in southwestern Manitoba (Figures 4.19 and 4.22) and contains pressure data from the Cambro-Ordovician through Ordo-Silurian, Manitoba, Birdbear, Souris Valley, Tilston, Jurassic and Mannville aquifers. Two pressure depth gradients are evident in this region; one lower super-hydrostatic pressure gradient that fits the Cambro-Ordovician to Birdbear aquifers (12.5 kPa/m), and a second normally-pressured regime (9.9 kPa/m) for the overlying Mississippian and Mesozoic aquifers. The lower super-hydrostatic gradient indicates that for the Cambro-Ordovician through Birdbear formations there is vertical hydraulic continuity and upward flow across the Lower Paleozoic and Devonian formations. This is contrasting what was observed in block 2 (Figure 4.21) where the Prairie Evaporite Formation created a hydraulic barrier to any vertical fluid potential. In block 3, the Prairie Evaporite Formation has been dissolved providing the pathway for vertical continuity between the Birdbear and Manitoba aquifers to the underlying Ordo-Silurian, Yeoman and Cambro-Ordovician aquifers.

The shallower aquifers in block 3 appear to be normally to slightly super-hydrostatic. It is possible to fit one single normal to super-hydrostatic gradient (9.9 kPa/m) for the basal Mississippian and Mesozoic strata. The Souris Valley, Tilston, Jurassic and Mannville aquifers have predominantly horizontal flow in this locality with the potential for upward flow. It is believed that this region is host to super-hydrostatic gradients with Mississippian flow upward into the basal Jurassic Aquifer (geochemical evidence exists; Figure 3.17) but evidence in this p(d) profile is not conclusive.

Geological (Christopher, 1987) and hydrogeological (Khan, 2006) data that support communication between the basal Mississippian, Devonian and Jurassic aquifers to the north of the TWP 10 in Saskatchewan has been recognized (Figure 4.19). Khan (2006) found that all of the data spanning the interval between the Newcastle down to the Birdbear aquifers were under-pressured and plotted along a super-hydrostatic gradient (Figure 4.23, block 6); thus, indicating that an upward flow of formation waters across the Watrous Aquitard is occurring (Figure 4.19).

Aquifer	Number of Pressure Samples		Minimum Hydraulic Heads (m)		Maximum Hydraulic Heads (m)	
	Raw	Mapped	Min	Location	Max	Location
Judith River	22	6	524	TWP 20 R23 W2	712	TWP 5 R26 W2
Newcastle	72	30	384	TWP 9 R25 W1	617	TWP 7 R8 W2
Mannville	105	56	343	TWP 35 R8 W2	679	TWP 2 R 19 W2
Jurassic	112	44	298	TWP 4 R11 W1	750	TWP 8 R28 W2
Poplar	26	12	821	TWP 4 R21 W2	978	TWP 1 R28 W2
Ratcliffe	53	23	586	TWP 1 R2 W2	872	TWP 7 R29 W2
Midale	269	44	660	TWP 4 R9 W2	879	TWP 3 R 228 W2
Frobisher	686	45	512	TWP 3 R32 W1	896	TWP 2 R29 W2
Alida	385	28	517	TWP2 R30 W1	915	TWP 2 R29 W2
Tilston	382	38	459	TWP 12 R9 W2	870	TWP11 R28 W2
Souris Valley	566	29	374	TWP 22 R1 W2	874	TWP 3 R28 W2
Bakken	119	69	355	TWP 30 R10 W2	868	TWP 4 R26 W2
Birdbear	355	101	332	TWP 23 R27 W1	889	TWP 1 R28 W2
Duperow	169	72	328	TWP 34 R6 W2	889	TWP 7 R28 W2
Manitoba	205	64	233	TWP 13 R15 W1	895	TWP 11 R28 W2
Winnipegosis	274	99	283	TWP 34 R26 W1	865	TWP 10 R26 W2
Ordo-Silurian	126	62	234	TWP 5 R8 W1	920	TWP 17 R29 W2
Yeoman	176	69	268	TWP 45 R25 W1	903	TWP 4 R23 W2
Cambro-Ordovician	226	55	238	TWP 24 R3 W1	936	TWP 1 R27 W2

Table 4.1. Number of pressure samples, and range and location of hydraulic heads for the aquifers.

Aquifer	Hydraulic Gradient (m/km)			Water Driving Force (m/km)		
	Min	Max	Average	Min	Max	Average
Newcastle	0.01	2.8	0.25	2.0E-03	2.8	0.24
Mannville	5.0E-03	3.5	0.46	5.0E-03	3.5	0.45
Jurassic	0.07	3.7	0.65	0.01	3.7	0.61
Poplar	0.01	4.1	0.44	0.01	4.0	0.41
Ratcliffe	8.0E-03	4.2	0.69	7.0E-03	4.2	0.66
Midale	7.7E-04	2.3	0.41	2.0E-03	2.3	0.43
Frobisher	0.06	4.5	0.96	0.03	4.5	0.85
Alida	0.01	2.9	0.62	0.01	2.9	0.61
Tilston	0.01	3.1	0.57	4.0E-03	3.1	0.54
Souris Valley	0.06	3.9	0.89	0.06	2.8	0.78
Bakken	0.02	3.6	0.68	0.02	3.4	0.60
Birdbear	0.06	3.9	0.81	0.06	3.7	0.73
Duperow	0.06	3.3	0.75	0.05	3.3	0.64
Manitoba	0.03	5.0	0.83	0.02	4.7	0.67
Winnipegosis	0.05	3.1	0.77	0.02	2.5	0.58
Ordo-Silurian	0.13	4.4	0.93	0.11	4.4	0.72
Yeoman	0.11	4.4	0.88	0.10	3.7	0.68
Cambro-Ordovician	0.09	3.8	0.86	0.06	3.5	0.61

Table 4.2. Hydraulic and water driving force gradients in the aquifers.

The Figures 4.1 to 4.19 (pages 96 to 114) have been removed at the request of the Faculty of Graduate Studies and Research at the University of Alberta. These tabloid sized maps will not be included in the microfilming version of this dissertation.

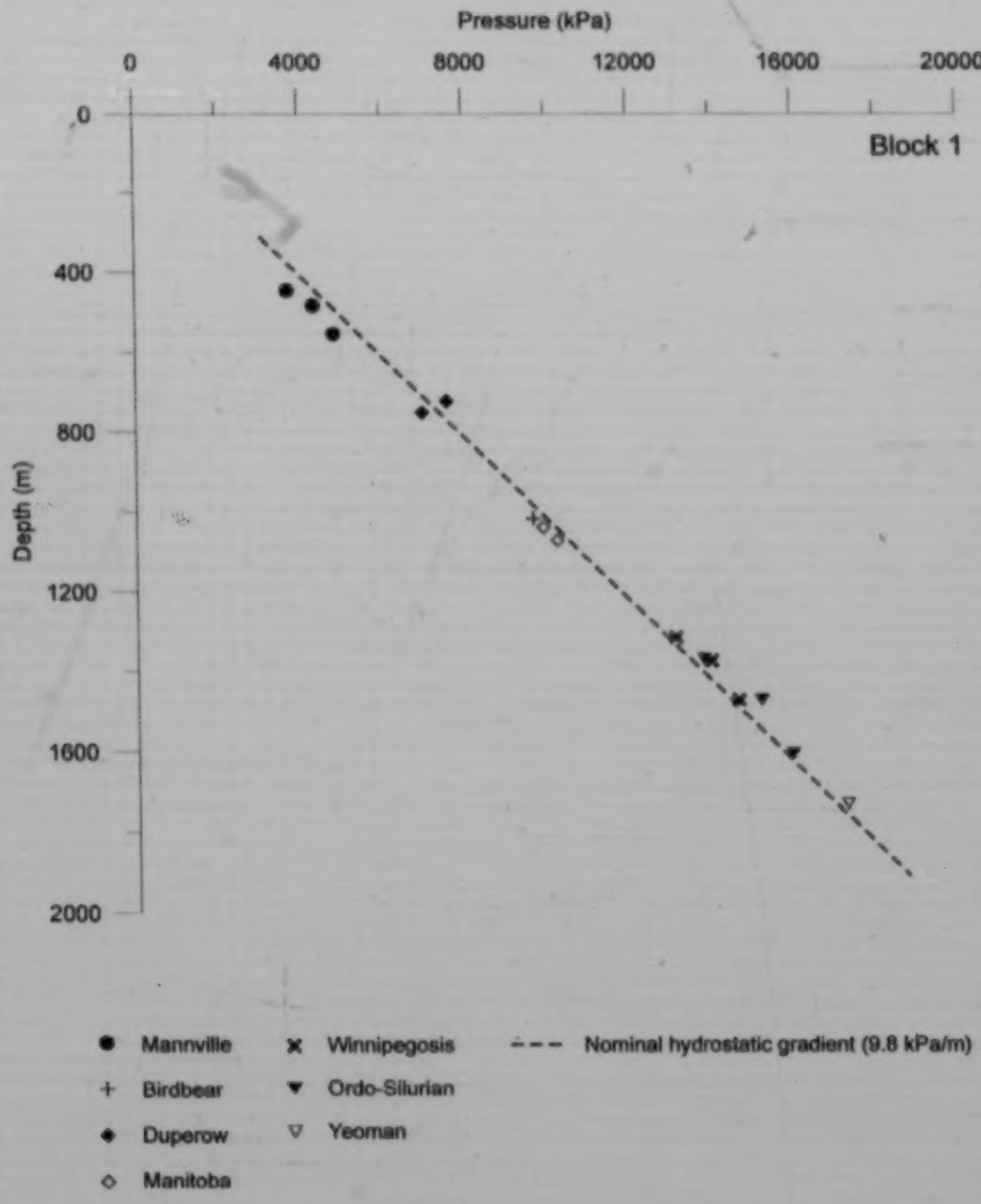

Figure 4.20. Pressure versus depth profile for block 1. Locations of the areas used for construction are shown in Figure 4.19.

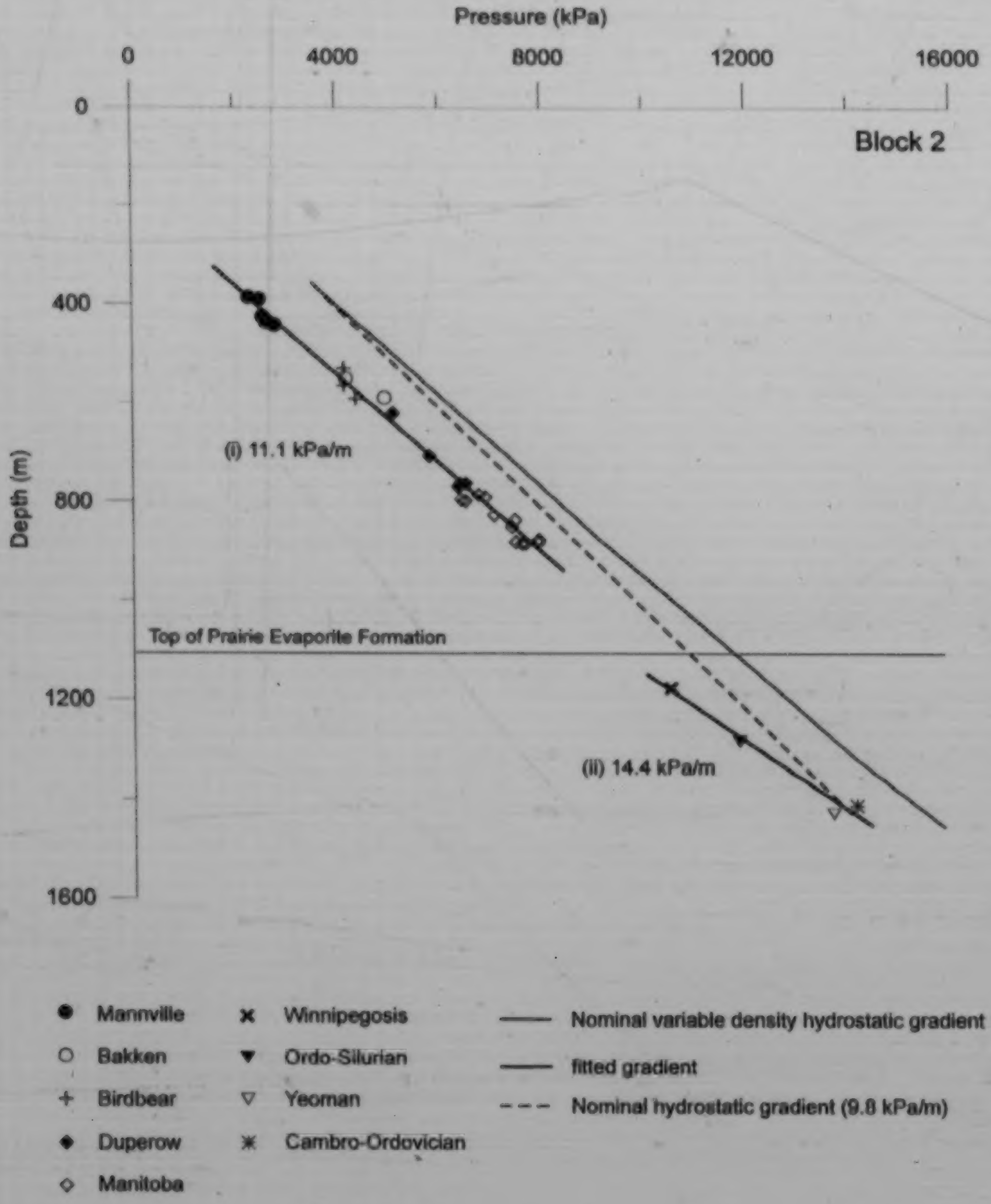

Figure 4.21. Pressure versus depth profile for block 2. Locations of the areas used for construction are shown in Figure 4.19.

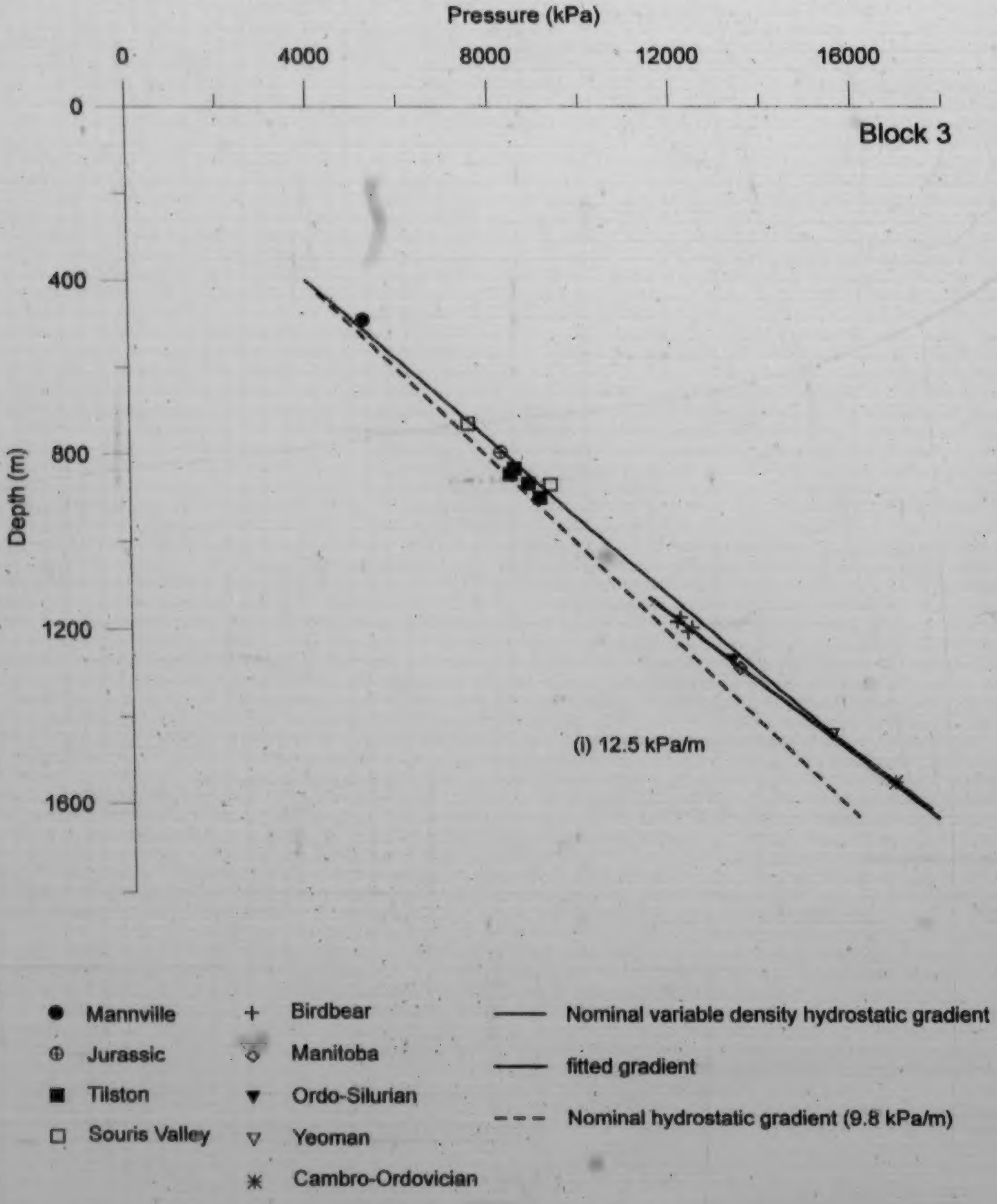

Figure 4.22. Pressure versus depth profile for block 3. Locations of the areas used for construction are shown in Figure 4.19.

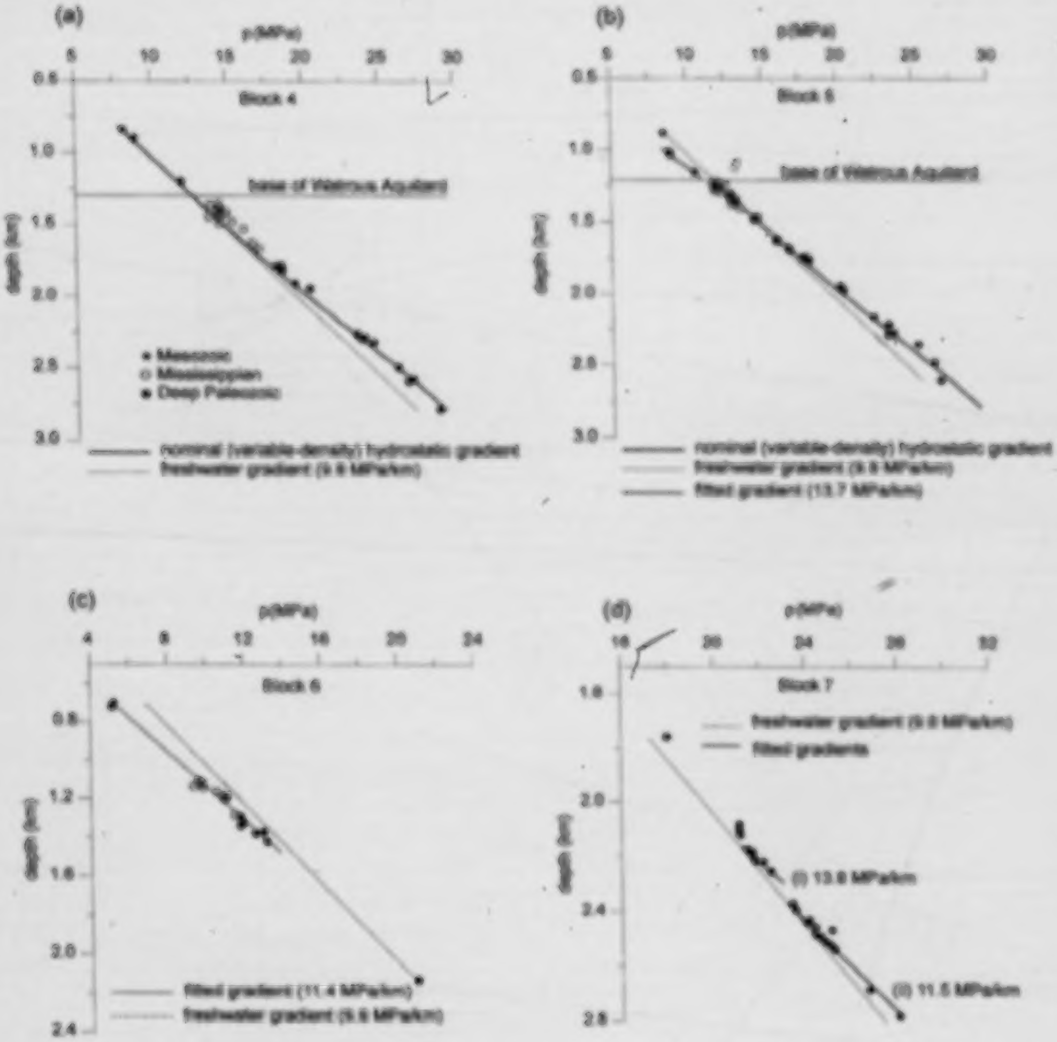

Figure 4.23. Pressure vs. depth profiles (after Khan, 2006): a) Block 4; pressure data fall along the nominal hydrostatic gradient despite some overpressures observed in the Mississippian; b) Block 5; pressure data fall along the nominal hydrostatic gradient except in the Mesozoic Jurassic and Mannville aquifers, which are underpressured and fit a superhydrostatic gradient; c) Block 6; underpressuring is observed between the Lower Paleozoic to Mesozoic aquifers with pressure data falling along a common superhydrostatic gradient; and d) Block 7; data from the Lower Paleozoic aquifers plot along superhydrostatic pressure gradients. Locations of the areas used for construction are shown in Figure 4.19.

5.0 REGIONAL HYDROGEOLOGICAL SYNTHESIS

A revised distribution of the hydrochemistry and fluid flow for the aquifers across Saskatchewan and Manitoba has been shown in Chapters 2 to 4. This updated hydrogeological model made use of the geological framework recently completed for the northeastern corner of the Williston Basin. The regional gravity-driven flow field has been analyzed using hydrochemistry and groundwater flow of formation waters.

To synthesize and interpret this characterization, first, the composition, distribution and origin of the formation waters are discussed (Section 5.1). Second, the consistent correlation between mapped salt dissolution edges and water chemistry are highlighted (Section 5.2). Third, the overall hydrodynamics are discussed and the effects of density-induced flows on the formation waters are summarized (Section 5.3). The last section examines and links this work to that postulated for subglacial recharge effects on the Williston Basin (Section 5.4).

5.1 REGIONAL HYDROCHEMISTRY IN THE NORTHEASTERN CORNER OF THE WILLISTON BASIN

Different events and processes acting within a sedimentary basin and in particular the Williston Basin, can be represented in, and inferred from the chemical signature of the formation waters (Hanor, 1994). A large variation of formation waters are found both within and across the aquifers.

5.1.1 Overall Water Types

Previous research has proposed five water types in the Williston Basin (Iampen, 2003, Khan, 2006), and four of them are found within the northeastern corner.

Sodium-chloride (Type 2) waters are the most dominant formation waters found within the Williston Basin (Figures 5.1-5.3). Type 2 waters span the complete range of

TDS mapped in this study (Table 3.1). The Ca and SO_4 concentrations account for less than 10% of their respective cationic and anionic fractions and TDS is greater than 100 g/L. Basinal brines have two main evolutionary pathways (Hanor, 1994; Lowenstein et al., 2003); 1) Salt dissolution occurs when fresher groundwaters percolate through the rock framework and dissolve, in addition to becoming saturated with, mineral phases defined by a series of complex chemical reactions (Chebotarev, 1955), 2) Seawater, representative of the seawater composition of that geological time period (Lowenstein and Timofeeff, 2008), can evaporate sub-aerially or at surface and become enriched in species such as magnesium or calcium (enrichment in Ca produces calcium chloride brines – Ca-Cl). Differentiating between the two end-member compositions is most frequently performed using Na-Cl-Br systematics (Iampen and Rostron, 2000) as well as major and minor ion chemistry (Carpenter, 1978).

Sodium-chloride and Ca-Cl brines can be distinguished by comparing the cationic fraction of calcium. Calcium-chloride brines differ from Na-Cl brines in that calcium occurs in excess of 40% of the dissolved cations, TDS is frequently above 300 g/L, and other major cations represent significantly smaller fractions of the TDS (Carpenter, 1978; Khan, 2006). Khan (2006) identified Ca-Cl brines in the Weyburn area, but those were exclusively in the US portion of the basin. Iampen and Rostron (2000) also concluded that only mixed end-members of Na-Cl and Ca-Cl brines have been found in the Canadian portion of the basin. No end-member Ca-Cl brines were identified based on major ion chemistry (Section 3.3) in the study area Type 2 brines are interpreted to be of halite dissolution origin in the Canadian portion of the Williston Basin (Iampen, 2003). Brines derived from halite dissolution were found in every aquifer with the exception of the uppermost Mannville and Newcastle aquifers (Section 3.2 and 3.3).

Calcium-sulphate (Type 1) freshwaters are found in all major stratigraphic subdivisions of the Lower Paleozoic, Mississippian, and Mesozoic aquifer systems and in particular the Duperow, Birdbear, Ratcliffe, Poplar and Jurassic aquifers (Section

3.4.1). This type water is characterized by Ca in excess of 40% the total cations, SO_4 having greater than 50% of the total anions, and a TDS that is less than 10 g/L. Type 1 waters are only located in the southwestern corner of the map area (Figure 5.1-5.3). Calcium-sulphate type waters in this freshwater zone have been interpreted, using stable isotopes, as having a meteoric origin (Rostron and Holmden, 2003). In a basinal context (Benn and Rostron, 1998), this water is interpreted to be a large freshwater plume originating from the southwestern corner. The waters coming from this recharge zone could have preferentially invaded specific aquifers as it flooded the western margin following the Laramide Orogeny.

Sodium-bicarbonate waters (Type 3) have TDS less than 10 g/L, HCO_3 levels greater than 20% of total anions, and the Ca component less than approximately 10% total cations (Section 3.4). Type 3 waters have been identified in the Cambro-Ordovician, Yeoman, Ordo-Silurian, Mannville and Newcastle aquifers (Section 3.4.1). For the three basal aquifers (Cambro-Ordovician, Yeoman and Ordo-Silurian aquifers), Type 3 waters have all been found in northern Saskatchewan (Figure 5.1). In contrast, the Mannville and Newcastle aquifers have Na-HCO_3 waters located in the southwestern and southeastern corners, and around TWP 40 (Figure 5.3 and Section 3.2). Type waters of this composition in Manitoba have been linked to Pleistocene meltwater recharge into the Williston Basin south of Lake Manitoba and this phenomenon is discussed in Section 5.4 (Ferguson et al., 2007). Moreover, formation waters have been sampled around Lake Manitoba and stable isotopes indicate that the origin is Pleistocene meltwater (Rostron and Holmden, 2003; Grasby and Chen, 2005).

As for the Mannville and Newcastle aquifers, the presence of Na-HCO_3 waters (Type 3) indicates that meteoric recharge has occurred in both the western, northern and eastern margins, displacing more saline waters (Figure 5.3). The presence of Na-HCO_3 type waters suggests that ion-exchange between Ca and Na, during the influx of meteoric water, is occurring. Ferguson et al. (2007) make the observation that in the Winnipeg Formation, modern recharge zones in the Sandilands area (Figure 4.19;

south-southeast of Lake Winnipeg) show Ca-HCO$_3$ transitioning into Na-HCO$_3$ waters and westward into more brackish waters. This is also consistent where freshwater recharge into saline coastal aquifers has occurred and resulted in Na-HCO$_3$ type groundwater (Appelo, 2005; Edmunds, 1994; Lambrakis and Kallergin, 2001).

Sodium-sulphate (Type 4) waters have an intermediate and mixed composition that correlates to the chemistries found in the brackish water zone (Figure 5.1-5.3; Section 3.2). These waters occur approximately between the TDS contours of 25-100 g/L but never exceeding 100 g/L. This composition of water is interpreted to be a result of hydrodynamic mixing (advective and diffusive transport processes) between meteoric freshwater (precipitation and/or glacial meltwater) and Na-Cl brines. It has been shown on a local scale within "The Carbonate Rock Aquifer" of Manitoba, using major/minor ion chemistry and isotopes, that mixing of saline brines with both meteoric waters and Pleistocene meltwater in the northeastern margin of the Williston Basin can yield Na-SO$_4$ compositions (Grasby and Betcher, 2002). The detailed hydrochemical mapping completed here specifies the geographical region where mixing of basinal brines, meteoric recharge and/or Pleistocene meltwater has taken place (Figure 5.1-5.3).

5.1.2 Spatial Distribution of Water Types

Lower Paleozoic Aquifers

Hydrochemical distributions in the Lower Paleozoic aquifers exhibit similarities and differences as evidenced in the TDS mapping (Figures 3.2-3.9) and major ion chemistries (Figure 3.20).

For the Lower Paleozoic aquifers, the interpretation of the brackish water mixing zone (Na-SO$_4$) on the northeastern margin is a direct result of the Wisconsin Glaciation and Pleistocene glacial meltwater recharging into the basin's edge (Figure 5.1). Near the end of the Wisconsin Glaciation, several glaciofluvial complexes were formed in the vicinity of the boundary between the Canadian Shield and the Williston Basin sediments, including the Sandilands Interlobate Moraine shown in Figure 4.19 (Ferguson et al., 2007). These glaciofluvial landforms provide present-day recharge into the eastern margin of the Williston Basin. Direct subglacial recharge is a result of this brackish water transition zone whereby Pleistocene meltwater has preferentially recharged into the Lower Paleozoic aquifers and mixed with basinal brines (Grasby and Betcher, 2002; Grasby and Chen, 2005).

Mississippian Aquifers

The Mississippian succession of aquifers are characterized by Type 2 (Na-Cl), Type 4 (Na-SO_4) and Type 1 (Ca-SO_4) compositions (Figure 5.2). Sodium-chloride brines dominate the south and southeastern map areas with Ca-SO_4 waters invading from the western margin. Hydrodynamic mixing of Type 1 (Ca-SO_4) and Type 2 (Na-Cl) waters is evident in the distribution of TDS (Figures 3.10-3.16), and major ion chemistry (Figure 3.21).

Mississippian aquifers are different from the Lower Paleozoic aquifers when comparing the hydrochemistry. Major-ion chemistry of the two aquifer groups (Figures 3.20, 3.21) indicates that relative proportions of sodium and calcium are characteristically different. Overall, in the Mississippian a significant reduction in the presence of high TDS brines is evident combined with lower Na concentrations (Figure 3.21a). Also, percent cationic calcium concentrations are lower in the Mississippian (Figures 3.20d, 3.20d; Lowenstein et al., 2003).

In the Mississippian aquifers, the relative amount (based on TDS) of freshwater incursion increases up the stratigraphic section and the SO_4 concentrations also increase (Figures 3.10-3.16, Appendix B). The TDS of the Souris Valley Aquifer (Figure 3.10) for example, has a fresh-brackish water plume that extends across the majority of the formation. Plus, it also appears that paleo-basin boundary conditions would have forced brines further up-dip (as noticed in the Souris Valley Aquifer) to eventually become displaced by later freshwaters. This phenomenon is present for the entire study area where recharge waters mix in an attempt to re-equilibrate the chemical and pressure potentials induced.

Mesozoic Aquifers

Hydrochemical distributions (Figures 3.17-3.19) and major ion chemistry (Figure 3.22) demonstrate the similarities and differences between the Mesozoic aquifers to the underlying Mississippian and Lower Paleozoic aquifers. Compositions and TDS distributions of formation waters indicate that the Jurassic, Mannville and Newcastle aquifers are different than all underlying aquifers but also in comparison to each other.

The Jurassic Aquifer has some similarities to the underlying Poplar, Ratcliffe, Birdbear and Duperow aquifers. In the western portion of the study area, the presence of $Ca\text{-}SO_4$ (Type 1) waters and the indication that vertical hydraulic communication exists between the formations (Section 4.3; Khan, 2006) supports that the Jurassic Aquifer is not completely isolated. This interpretation is supported by the TDS distribution of the Jurassic Aquifer where higher salinities are found (Figure 3.17). The Jurassic Aquifer has evidence of Na-Cl brines in the northern and eastern margins of the study area.

Hydrocarbon migration trends in the lower Mesozoic of the northern Williston Basin have been extensively studied (Christopher, 1964, 1966, 1987; Christopher et al., 1971). Migration of Paleozoic fluids into the Jurassic reservoirs forming regional oil pools are known to exist because petroleum source beds are not present in the Jurassic system (van Delinder, 1984). Christopher (1987) interpreted that migration and trapping of Paleozoic fluids into the Jurassic reservoirs occurred during Early Cretaceous uplifts with subsequent basin subsidence leading to the eventual isolation of the Mississippian and Mesozoic strata of southern Saskatchewan. Saline waters (with TDS greater than 100 g/L) found within the Jurassic Aquifer are interpreted to be a result of vertical mixing between the Lower Paleozoic aquifers likely sourced from the Duperow and/or Birdbear aquifers.

5.2 SALT DISSOLUTION

There are four main areas in the northeastern Williston Basin whereby evaporites correlate with formation water compositions. In most instances they correlate with precision and in others the shape is parallel but slightly offset.

The first example is in the Yeoman Aquifer (Figure 3.3). This aquifer contains the Lake Alma Anhydrite. There are three control points that lie along the trace of the anhydrite edge (TWP 24 R31 W1, TWP 8 R1 W1 and TWP 2 R10 W1). In north-central Saskatchewan, there is insufficient data that constrains the formation waters directly north of the Lake Alma Anhydrite edge above 100 g/L. However, in Manitoba the evidence is convincing that dissolution and the overall distribution of the Lake Alma Anhydrite correlates with the brackish water transition zone and the fresher waters south-southeast of Lake Manitoba (Figure 3.3). Therefore, it is possible to infer that the distribution of formation waters having a TDS greater than 100 g/L in the Yeoman Aquifer are bounded to the edge of the Lake Alma Anhydrite. It must be noted that formation waters with greater than 50 g/L are found in TWP 45 R 25 W1 adjacent to Lake Winnipegosis (Figure 3.3).

Secondly, in the Winnipegosis Aquifer the Prairie Evaporite Formations' dissolution edge is correlative with the brackish water transition zone (Figure 3.5). It is apparent that the dissolution edge forms a band around the basinal brines and with the freshwater recharge along the southwestern margin. Also, this dissolution edge is coincident with $Na\text{-}SO_4$ (Type 4) waters and is evidence of the effects that recharging waters into the basin margins had on the geology and hydrogeology of the basin.

The third example is from the Manitoba Aquifer and its Davidson Salt Member (Figure 3.6). While the exact alignment of dissolution and chemistry are offset in this example, it indicates that an association is noticed when formation fluids dissolve evaporite layers. In the Manitoba Aquifer, the Davidson Salt Member is completely absent around the freshwater plume in the southwest. The presence of the Davidson Salt Member also roughly aligns with the saline water distribution trending toward the northwest. There are two data points in the Manitoba Aquifer (TWP 27 R17 W2 and TWP 24 R10 W2) that appear to be control points for the dissolution edge of the Davidson Salt Member. There is evidence that the dissolution of the salt bed at these control points has increased the TDS of the formation waters within the Manitoba Aquifer.

In the Duperow Aquifer, the Flat Lake Salt Member mimics the distribution of saline waters where it is present and its shape also resembles that of the freshwater recharge zone to the west (Figure 3.7). However, the edge is slightly offset and does not correlate exactly as was noticed in the Winnipegosis Aquifer. Nevertheless, the association of freshwater recharge and evaporitic formations is recognized and can aid in paleohydrogeological and present-day interpretations for basin hydrogeology.

5.3 DRIVING FORCES ON FORMATION WATERS

A gravity-driven regional flow field, as defined by the classic model of Tóth (1963), is present in the Williston Basin (Downey, 1984a, b; Hannon, 1987; DeMis 1995; Bachu and Hitchon, 1996).

Lower Paleozoic Aquifers

Formation fluids in the Lower Paleozoic aquifers (Figures 4.1-4.8) are generally traveling up-dip towards the northeast outcrop and subcrop locations (Figure 5.6). The flow field is a direct result of the basin configuration imparted by the Laramide Orogeny (DeMis, 1995; Bachu and Hitchon, 1996).

Similarities between the Cambro-Ordovician, Yeoman, Ordo-Silurian and Manitoba aquifers is the occurrence of higher hydraulic gradients around Lake Manitoba (Figures 4.1-4.3; 4.5). While many aquifers have a "band" of higher gradients toward the basin margin or their own respective subcrop/outcrop edge, these aquifers have a strong correlation of having enhanced gradients around Lake Manitoba. These regions are frequently linked with the brackish water mixing zone (Section 5.1), recharge areas (western margin of the Ordo-Silurian and Manitoba aquifers; Figures 4.3, 4.5, 5.1), and/or some major salt dissolution edges (Section 5.2). Zones of hydrodynamic mixing, increased hydraulic gradients around the perimeter of the margins, and salt dissolution are directly related to recharge and the basin's transient adjustment to the denudation of the recharge areas (Tóth and Millar, 1983) to the south-southwest and/or the overburden and dynamics of the Wisconsin glaciers. Heterogeneity and geologic parameters, such as porosity and permeability can also cause increased hydraulic gradients; however, the correlation of the factors aforementioned and the spatial distribution along the perimeter of the basin point to the recharge interpretation.

Mississippian Aquifers

Hydrodynamics of the Mississippian aquifers, with the exception of the Souris Valley Aquifer (Figure 4.9), contrast the Lower Paleozoic aquifers in flow directions and hydraulic gradients. Overall, flow is from west to east in the Mississippian aquifers. The hydraulic heads in the Mississippian are larger than the underlying Lower Paleozoic aquifers and in south-central Saskatchewan there is evidence that it is also over-pressured (Figure 4.23; Khan, 2006). Hydraulic heads definitely increase up-section from the Souris Valley to Poplar aquifers (Section 4.2.2) but the origins of these over-pressures are still not definitively known. Khan (2006) speculated that the over-pressuring could be a result of minor hydraulic isolation measured in that location of the aquifer or likely the effects of nearly fifty years of water-flooding and injection operations for enhanced oil recovery. The determination of the origin of over-pressuring in the Mississippian aquifers was not an objective here and while still ambiguous, it could be added that the over-pressuring could be an effect of the recharge waters from the west.

Mesozoic Aquifers

The Mesozoic aquifers have two types of flows. First, the Jurassic Aquifer (Figure 4.16) has southwest-northeast flow directions comparable to the Lower Paleozoic aquifers. Inference of vertical hydraulic communication between the Lower Paleozoic aquifers up to the Mesozoic aquifers (Section 4.3) spatially correlates to areas of increased equipotential spacing (western and east-central areas of Jurassic Aquifer). Also, the presence of the Manitoba Escarpment on the aquifers can cause under-pressuring and preferential flow in the aquifer.

Second, the Mannville and Newcastle aquifers (Figures 4.17, 4.18) have considerably different flow fields. Large troughs across the Mannville Aquifer can be attributed to enhanced permeability (channel sands) and/or an under-pressuring signature as a result of outcrops located along the Manitoba Escarpment. The pressure drawdown effect can also be observed in the Newcastle Aquifer where two principal flow directions are observed (toward the northwest and northeast). The northeast flow direction has greater hydraulic gradients and could be a result of the outcrops along the Manitoba Escarpment edge.

5.3.1 Vertical Pressure Gradients

The presence of vertical variations in fluid potentials indicating upward or downward movement of groundwater and the existence of hydraulic continuity was assessed here. Whether the aquifers are under-pressured, normally-pressured, or over-pressured quantifies the vertical flow and hydraulic communication. This is summarized for each region below and in Figures 5.4 and 5.6. The locations of the pressure-depth profiles are found in Figure 4.19.

Block 1

The Paleozoic and Mesozoic aquifers have pore-pressures that are all nominally-pressured. In the west-central region there is predominantly horizontal flow. The Mannville Aquifer here is slightly under-pressured that is consistent with most samples above the Prairie Evaporite Formation (Figure 4.20).

Directly south of this region in Khan's (2006) investigation (Figure 4.19, Block 7) a significant upward component to flow in the Paleozoic aquifers was interpreted (Figures 4.23, 5.6; Block 7). The reason why in block 1 the vertical component to flow no longer exists is that the Prairie Evaporite Formation did not undergo dissolution and actually still is up to 185 m thick (Figure 4.19).

In the presence of the Prairie Aquitard the region is normally-pressured and dominated by horizontal flow.

Block 2

In this region, there is vertical hydraulic communication between the Cambro-Ordovician through Winnipegosis aquifers and a component of upward flow is present. The overlying aquifers (Manitoba, Duperow, Birdbear, Bakken and Mannville) fall along a super-hydrostatic gradient suggesting that there is vertical continuity and upward flow between these formations (Figure 5.6).

There is a hydraulic separation between these two groups of aquifers and this is explained by the competent Prairie Evaporite Aquitard (Figures 4.21, 5.6). In block 2, the Prairie Evaporite Formation is up to 80 m thick and forms the barrier between the lower and upper super-hydrostatic gradients depicted here.

Also of particular interest in block 2 is the under-pressuring of all the Mannville Aquifer samples along this hydrostatic gradient (Figure 4.21; 387 – 444 m depth). This was previously mentioned in the potentiometric surface analysis and is confirmed in the pressure-depth profile.

The Mannville Aquifer is under-pressured in this region as well and can be attributed to three potential factors: 1) The presence of high-permeability channel sands that trend longitudinally in the study area toward the Manitoba Escarpment, 2) At the Manitoba Escarpment portions of the Mannville Formation are exposed to atmospheric pressure and create an open aquifer system with pressure drawdown felt across the formation, and 3) The overburden pressure of up to 1500 m of ice over the Paleozoic outcrop belts has been interpreted to have caused more than 200 m of isostatic depression on the crust (Dyke and Prest, 1987). Given the short-lived residence time of the Laurentide ice-sheet over the Williston Basin (approximately 1000 years; Clayton and Moran, 1982), the unloading and rebound effect on the Mesozoic sediments could cause wide-spread under-pressuring.

Block 3

The Cambro-Ordovician through Birdbear aquifers fall on a super-hydrostatic gradient (Figure 4.22). This indicates that these formations are in vertical hydraulic communication and upward flow across the Lower Paleozoic and Devonian formations is occurring. This is contrasting what was observed in block 2 (Figure 4.21) where the Prairie Evaporite Formation created a hydraulic barrier to any vertical fluid potential. In block 3, the Prairie Evaporite Formation has been dissolved (Figure 4.19, orange line) providing the pathway for vertical continuity through the Lower Paleozoic and Devonian aquifers.

The Souris Valley, Tilston, Jurassic and Mannville aquifers have predominantly horizontal flow in this locality with the potential for upward flow. It is possible to fit one single normal to super-hydrostatic gradient (9.9 kPa/m) between them (Figure 4.22).

Southern Saskatchewan - Blocks 4-7

There does not appear to be any significant vertical flow throughout the entire hydrostratigraphic section in block 4 (Figures 4.23, 5.6). Horizontal flow is dominant with all aquifers plotting along the nominal hydrostatic gradient despite some over-pressures in the Mississippian.

Toward the east in block 5, there is an apparent hydraulic separation between the Mississippian and Mesozoic across the Watrous Aquitard (Figure 4.23). This indicates that there is a hydraulic discontinuity in this region between the Mississippian and Mesozoic aquifers. Also, upward flow from the under-pressured Jurassic to Mannville aquifers is recognized in block 5 with pressures fitting a super-hydrostatic gradient.

In block 6, all of the data spanning the interval between the Newcastle down to the Birdbear aquifers are under-pressured and plot along a super-hydrostatic gradient; thus, indicating that an upward flow of formation waters across the Watrous Aquitard is occurring (Figures 4.23, 5.6). This vertical hydraulic continuity between the Mesozoic, Mississippian and Paleozoic aquifers is supported here by the presence of saline brines in the northern Jurassic Aquifer.

Block 7 indicates that upward cross-formational flow in the Lower Paleozoic aquifers is occurring along the western margin (Figures 4.19, 4.23, 5.6). The absence of the Prairie Evaporite Formation in this region exemplifies that recharging waters dissolved the Prairie Aquitard and a significant component of upward flow exists. Therefore, in the absence of the Prairie Aquitard upward flow dominates in the northeastern corner of the Williston Basin.

5.3.2 Flow reversals in the northeastern margin of the Williston Basin

Buoyancy-driven formation water flow has been found to affect the overall net driving force on formation fluids in the Williston Basin (Alkalali, 2002; Khan, 2006). In a regional hydrogeological context, the water driving force analysis quantifies the magnitude and preferred direction of flow.

Previous authors (Alkalali, 2002; Khan, 2006) have not quantified density-dependent flows in the northeastern corner of the Williston Basin. Here and in previous regional hydrogeological characterizations in the Williston Basin (Downey, 1984a, b; 1986; Downey et al., 1987; Benn and Rostron, 1998; Khan, 2006) it has been identified that brines are displaced up-dip on the northeastern margin of the basin. The topographic gradient and boundary conditions set in place after the Laramide Orogeny displaced brines up-dip along the flank of the basin; however, continued erosion of the Black Hills, up to approximately 2100 m (Lisenbee and DeWitt, 1993) has significantly reduced the larger paleo-hydraulic gradients and near-equilibrium conditions are occurring.

The density-dependent analysis here provides an overview of the complete margin of the basin (Figure 5,5). The water driving force analysis quantifies where the present day hydraulic conditions are sufficient to counter the structural and buoyancy controlled forces preventing brines from flowing down-dip and rather slowly up-dip, quasi-stagnate, or completely stationary (Section 4.2).

Overall, down-dip flow reversals are only found in southern Saskatchewan (Figure 5.5). The interplay of high formation water densities, low hydraulic gradients (significant effective porosity and permeability), and sloping aquifers are required before the net driving force will be buoyancy dominated. Hydrodynamic conditions in the Mississippian aquifers support all of these criteria and that is why down-dip flow reversals are of a significant magnitude for these aquifers (Section 4.2). In the Lower Paleozoic and Devonian formations, local variations and down-dip flow directions are recognized as in the Mississippian but not near the same scale.

The Ordo-Silurian, Winnipegosis and Manitoba aquifers are the only units that display any density-dependent flow variations, or at least a greater than 30 degree azimuthal flow direction difference inferred by the hydraulic gradient alone, outside of southern Saskatchewan (Figure 5.5). These aquifers all have a southeast-northwest trending region where formation waters either are flowing parallel to the equipotentials, are quasi-stagnant, or moving down-dip. This vicinity also approximately corresponds to saline waters that are adjacent to the brackish water transition zone and a region of lower hydraulic gradients. In the Winnipegosis Aquifer, this same region can be roughly correlated to the dissolution edge of the Prairie Evaporite Formation in northern Saskatchewan.

The direct cause of the density-controlled flows is still largely ambiguous in these regions. The possibility exists that freshwaters recharging in the basin margin could alter the hydraulic gradients and facilitate the downward movement of fluids. Equally as plausible, these regions could have aquifer structural gradients and water densities that are larger and thus cause the formation fluids to preferentially sink versus traveling up-dip towards the margin. These brines are gravitationally instable in the present-day dynamics of the Williston Basin.

5.4 IMPLICATIONS FOR SUBGLACIAL RECHARGE IN THE BASIN

There has been an increasing amount of research since 1996 that has been targeted towards understanding the impacts and effects of Pleistocene glaciation on basin hydrodynamics. High fluid pressures at the base of continental ice-sheets are interpreted to cause recharge of subglacial meltwaters into sedimentary basins in Europe (Boulton et al., 1996; Piotrowski, 1997a, 1997b), the Illinois, Michigan and Appalachian Basins (Siegel, 1991; McIntosh et al., 2002; McIntosh and Walter, 2005), Atlantic continental shelf of New England (Person et al., 2003), western Ontario (Weaver et al., 1995), the Canadian Shield (Clark et al., 2000; Carlson et al., 2007), and in the Williston Basin (Remenda, 1993; Grasby et al., 2000; Grasby and Chen, 2005).

Researchers (Grasby and Chen, 2005) often pose the question: To what degree can modern-day pressure and geochemical distributions in high-latitude sedimentary basins be used to interpret past fluid flow histories if they have been significantly disrupted by Pleistocene glaciation? This question challenges the relevance of using present-day hydrodynamics to understand past migration events of basin brines, hydrocarbons, and mineral-bearing fluids.

In the northeastern corner of the Williston Basin there can be little doubt that subglacial recharge has taken place (supported by hydrochemistry here). First, it has been shown, using stable isotopes of oxygen and hydrogen, that in central Manitoba there is a mixing relationship between a dilute end-member brine (derived from salt dissolution) and a second original deep basinal brine (Rostron et al., 2002; Grasby and Chen, 2005). Second, the saline springs of central Manitoba (Grasby et al., 2000) originates from Pleistocene meltwaters that came into contact with and dissolved evaporite units on the northeastern margin of the basin (Grasby and Chen, 2005).

The hypothesis that the basin scale regional gravity-driven flow field was completely reversed during the Wisconsin glaciation (Grasby et al., 2000; Grasby and Betcher, 2000; Grasby and Chen, 2005) is not supported here. Further, that glacial effects were significant enough to render the use of modern-day fluid pressure distributions as not an accurate method of predicting past migration pathways of basin fluids.

The extent of the recharge into the basin has never been quantified on a regional scale. This work does not support the interpretation that the recharge was widespread causing a reversal of the flow field for two specific reasons: 1) the hydrochemistry analyzed here puts limits of the extent of subglacial recharge, and 2) there are no significant over-pressures in the northeastern corner of the Williston Basin. Furthermore, a recent study by Carlson et al. (2007) suggests that the extent of recharge was insufficient to reverse the regional scale flow fields in the Williston Basin.

5.4.1 Evaporite Dissolution

The argument that Pleistocene meltwater is responsible for dissolving the salt on the northeastern margin is not debated (Grasby and Chen, 2005). Rather, it should be clarified that the dissolution edge of the Prairie Evaporite Formation (Figure 4.19) marks the maximum glacial meltwater invasion limit into the Winnipegosis Formation of the northeastern margin. Using the hydrochemistry of the saline-meteoric mixing zone (Type 4) and the salt dissolution edges (Section 5.2), the maximum limit of subglacial recharge related to Pleistocene meltwaters can be constrained.

5.4.2 Basin Overpressures

Overpressures created by subglacial recharge during the Pleistocene are inferred to have generated "hydrodynamic blow-out structures" (Christiansen et al., 1982; Grasby and Chen, 2005). The location of a Pleistocene blow-out structure in east-central Saskatchewan called "Howe Lake" (Grasby and Chen, 2005) is roughly located around 103.4° W and 51.2° N (Figure 4.19).

Grasby and Chen (2005) infer that because hydrodynamic blowout structures exist and represent aquifer over-pressuring that the modern-day pressure distributions of the Western Canada Sedimentary Basin reflect the transient response of the basin trying to re-equilibrate. Therefore, pressure conditions are non-representative of Laramide-induced flow fields.

Vertical pore pressure gradients analyzed here for the Lower Paleozoic and Mesozoic aquifers are not deemed to be over-pressured (Figures 4.19-4.23). In block 1, the Paleozoic and Mesozoic aquifers are normally-pressured. Around blocks 2 and 3, the Lower Paleozoic aquifers are super-hydrostatic falling all on the same vertical pressure gradient. Block 2 indicates that all samples from the Ordo-Silurian through Mannville aquifers are under-pressured with respect to the nominal hydrostatic gradient for the location. In block 3, the Prairie Evaporite Formation is dissolved and no over-pressuring is evident.

In summary, if one of the effects of subglacial recharge were to create over-pressures in the aquifers and still have altering effects on present-day basin hydrodynamics, it would be expected that transient adjustment inferred by over-pressuring would still be evident. No evidence of significant modern-day over-pressuring throughout the northeastern margin of the Williston Basin is found here.

5.4.3 Water Driving Force and Mesozoic Under-pressuring

Further evidence of the unlikelihood for sub-glacial recharge significantly altering the basin hydrodynamics of modern-day pressure systems can be investigated using the Water Driving Force analysis (Section 4.2).

If Pleistocene waters had a long-term (greater than 10,000 years) effect on basin hydrodynamics, whereby today's pressure distributions represent a transient response to glacial boundary conditions, then potentially down-dip flows or at least relics would still be evident outside the basin centre. There is slight evidence of a southeast-northwest trending trough that roughly corresponds with the brackish water mixing zone in the Ordo-Silurian, Winnipegosis and Manitoba aquifers (Figures 4.3-4.5). Along this trend, WDF vectors show that gradients are quasi-stagnant and definitely lower in magnitude than the hydraulic gradients. However, no conclusive evidence of down-dip flows is apparent.

Further, the northern extent of brackish waters (greater than 50 g/L) in the Yeoman and Ordo-Silurian aquifers reaches are far north as TWP 25 R45 W1 (Figures 4.2, 4.3). This northerly extent verifies that pressure distributions have re-equilibrated and brines are still mixing and travelling up-dip with the regional-gravity driven flow field in place.

What could be inferred as a relict effect of the Wisconsin glaciation is the widespread under-pressuring of the Mannville Aquifer, the Mesozoic strata, and to some extent the entire Phanerozoic succession as shown in block 2 (Figures 4.19 and 4.21). The net unloading effect (Neuzil and Pollock, 1983) can cause significant under-pressuring and disequilibrium in pore-pressures as isostatic rebound takes effect. In all of the pressure-depth profiles the Mesozoic aquifers were either normally- or under-pressured (Figures 4.20-4.23). Glacial loading could have caused under-pressuring in the Mesozoic stratigraphy; however, the outcrops along the Manitoba Escarpment will also cause pressure drawdown.

5.4.4 Glacial Residence Time

Pleistocene glaciation has had a noticeable effect on the hydrogeology of the Williston Basin and it is also evident today. However, it is the magnitude and scale of its perturbation that is of recent research. Carlson et al. (2007) conducted a study on the James Lobe of the Laurentide ice-sheet. The James Lobe covers the entire northeastern margin of the Williston Basin and it is the westernmost distinctive lobe that drained the southern margin of this ice-sheet. Numerical simulations chose boundary conditions and parameters to reflect the hydrogeology of the Williston Basin as depicted by Downey (1986) and Downey and Dinwiddie (1988). Steady-state simulations in Carlson et al. (2007) accurately depicted the regional-scale flow field in the basin. Carlson et al. (2007) concluded that both their steady state and transient simulations suggest subglacial recharge under the James Lobe had little effect on the regional groundwater flow below the Quaternary. The two main factors as to why the flow fields were not significantly affected were: 1) Low permeability in the upper and lower Cretaceous strata acted as a regional aquitard for meltwater recharge and, 2) A 10,000 year transient simulation was insufficient to reverse flow fields, given the maximum extent of the James Lobe was less than 1000 years before retreating commenced (Clayton and Moran, 1982). The short-lived extent of the glacier was not capable of completely reversing the gradients altering the dominant northeast flow.

The results here and previous works (e.g. Carlson et al., 2007) contradict the prediction that significant flow reversals were experienced in the Williston Basin during glaciation. However, they do agree that in near-surface exposures (Carlson et al., 2007) and down to the brackish water mixing zone of Lower Paleozoic and Devonian aquifers, down-dip flow of Pleistocene meltwater occurred for a small amount of time (thousands of years).

Steep fluid salinity zones, that represent changes in major-ion chemistry, and variable amounts of halite dissolution from salt-bearing formations defines the regional extent to which meltwaters recharged into the Williston Basin. These Pleistocene glacial events occurred over relatively short times scales (thousands of years) as compared to the basinal-scale fluid migration events that are driven by tectonics, sediment compaction and topography that occurred over millions of years (McIntosh and Walter, 2005).

The primary understanding of regional hydrogeology and hydrochemistry in sedimentary basins are imperative to discern and comprehend the chemical evolution of basinal brines and the dynamics of brines during meteoric invasion. Characterization using a methodical approach to the geology and hydrogeology enables an integrative analysis of the saline-meteoric water mixing zone and the sources of salinity in sedimentary basins.

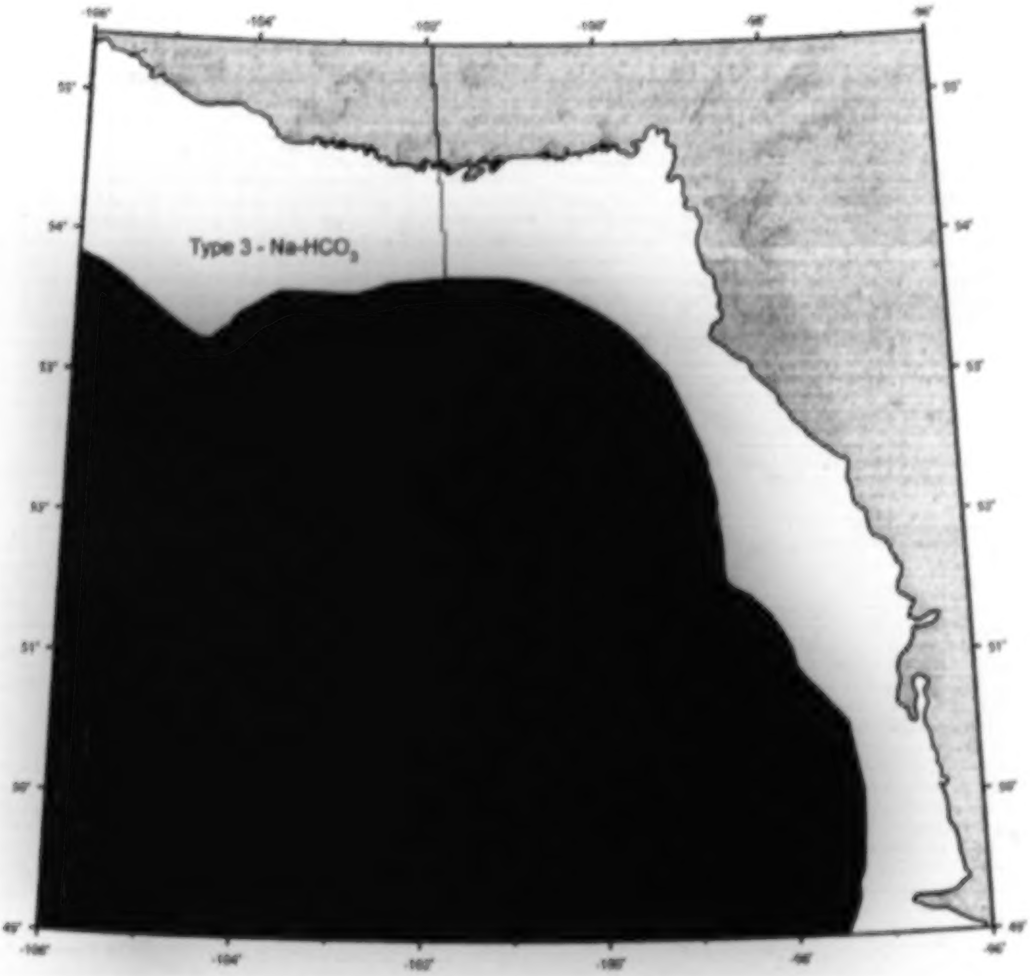
-106°
-104°
-102°
-100°
-98°
-96°
55°
54°
Type 3 - Na-HCO$_3$
53°
52°
51°
50°
49°

Figure 5.1. Schematic representation of the water types in the Lower Paleozoic aquifers.

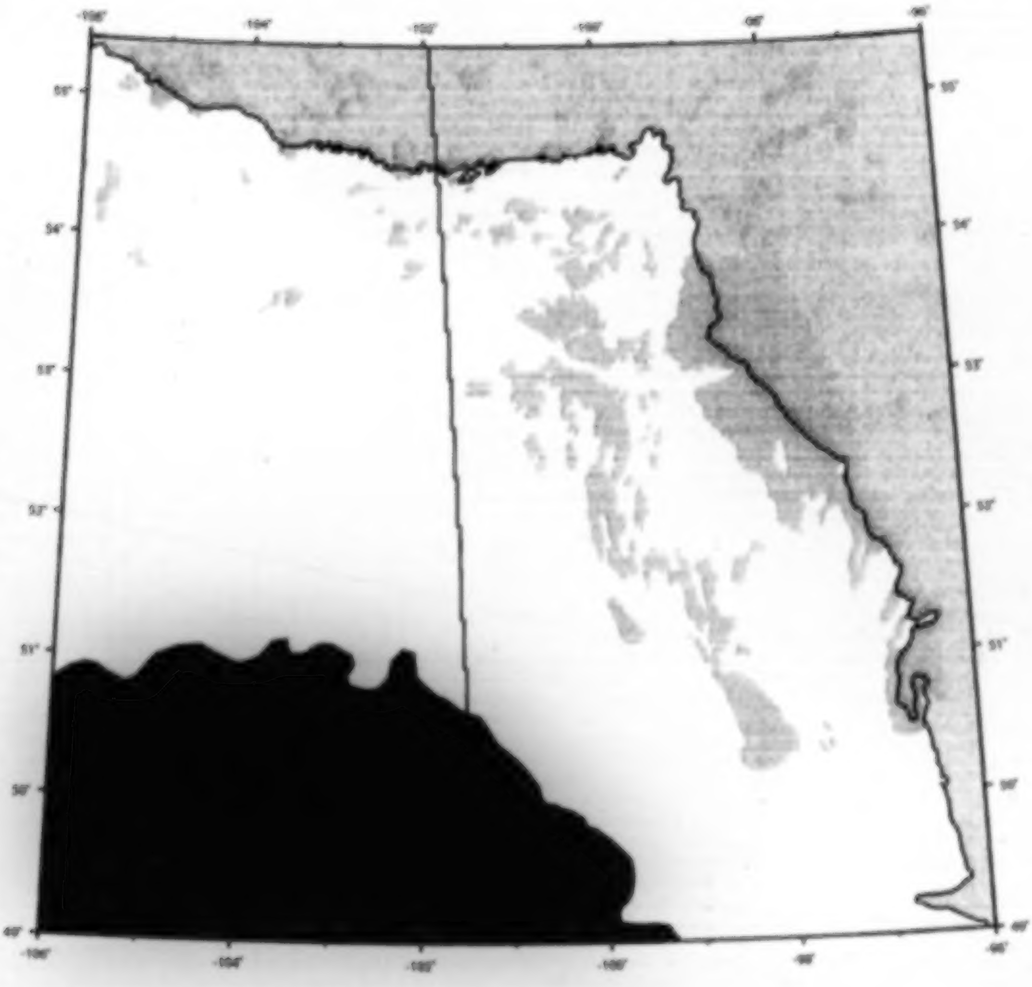

Figure 5.2. Schematic representation of the water-types in the Mississippian aquifers.

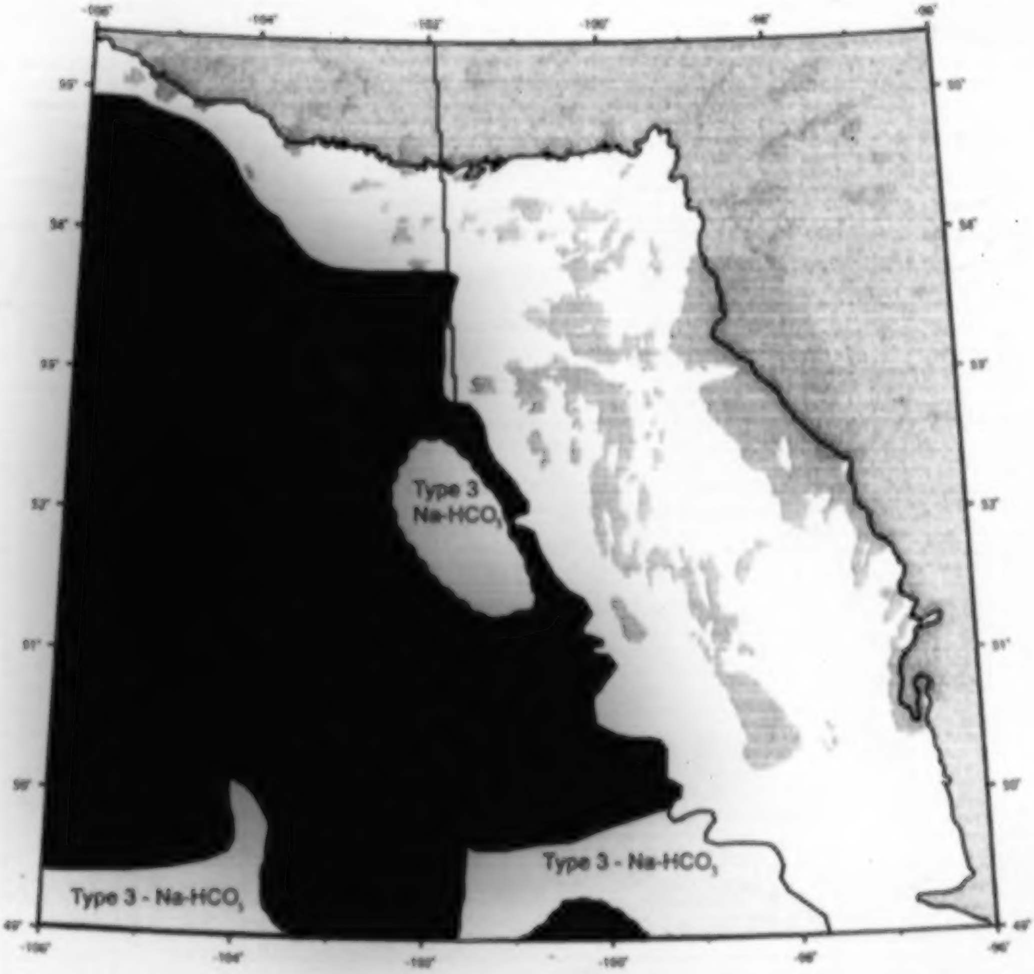
-106°
-104°
-102°
-100°
-98°
-96°
55°
54°
53°
52°
51°
50°
49°
SR
Type 3
Na-HCO$_3$
Type 3 - Na-HCO$_3$
Type 3 - Na-HCO$_3$

Figure 5.3. Schematic representation of the water types in the Mesozoic aquifers.

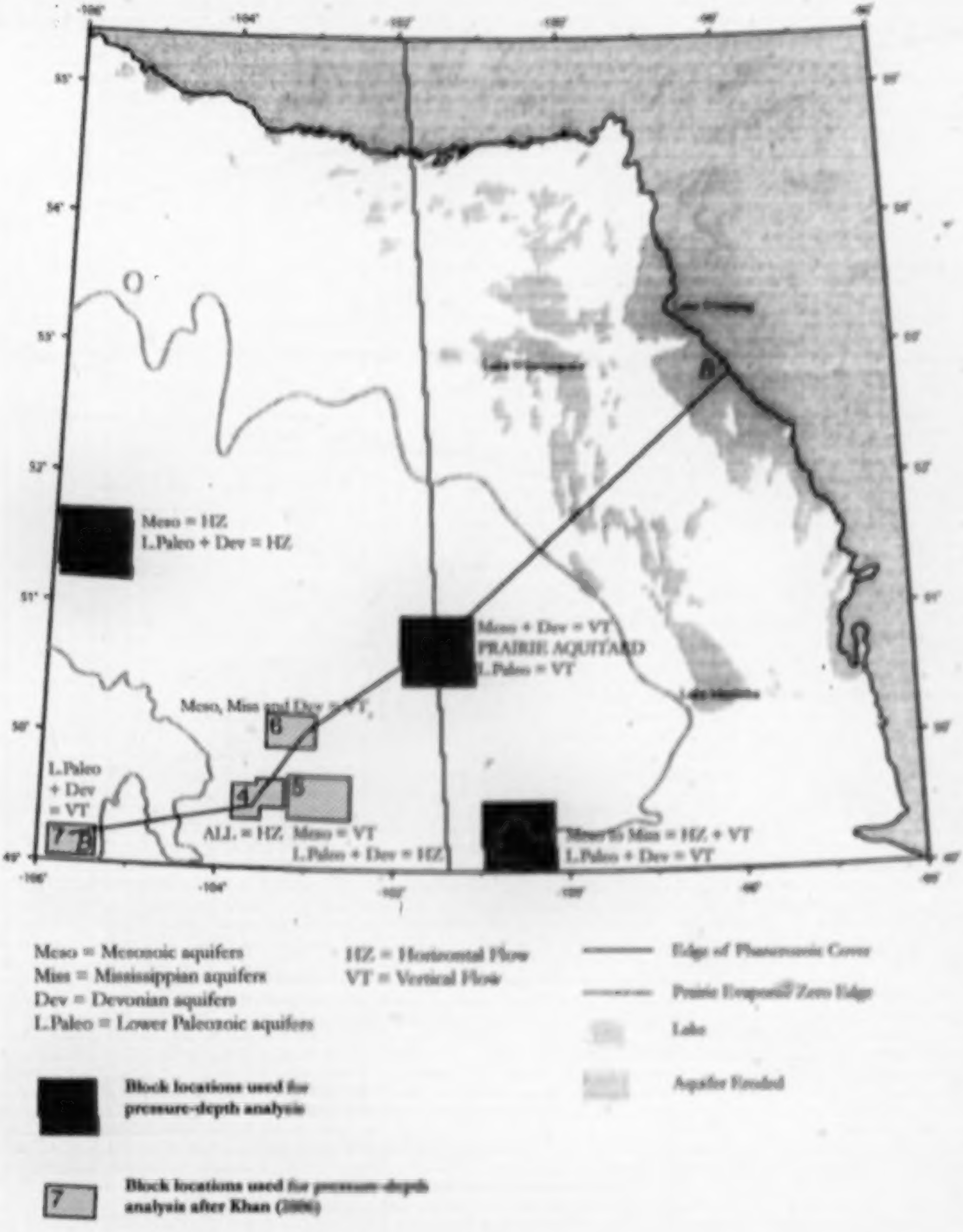
55°
54°
53°
52°
51°
50°
49°
-106°
-104°
-102°
-100°
-98°
B'
Meso = HZ
L.Paleo + Dev = HZ
Meso + Dev = VT
PRAIRIE AQUITARD
L.Paleo = VT
Meso, Miss and Dev = VT
6
L.Paleo
+ Dev
= VT
4
5
7
8
ALL = HZ
Meso = VT
L.Paleo + Dev = HZ
Meso to Miss = HZ + VT
L.Paleo + Dev = VT
Meso = Mesozoic aquifers
Miss = Mississippian aquifers
Dev = Devonian aquifers
L.Paleo = Lower Paleozoic aquifers
HZ = Horizontal Flow
VT = Vertical Flow
Edge of Phanerozoic Cover
Prairie Evaporite Zero Edge
Lake
Aquifer Eroded
Block locations used for pressure-depth analysis
7
Block locations used for pressure-depth analysis after Khan (2006)

Figure 5.4. Summary of the horizontal and vertical flow fields across the study area. The location of cross-section B to B' (Figure 5.6) is identified.

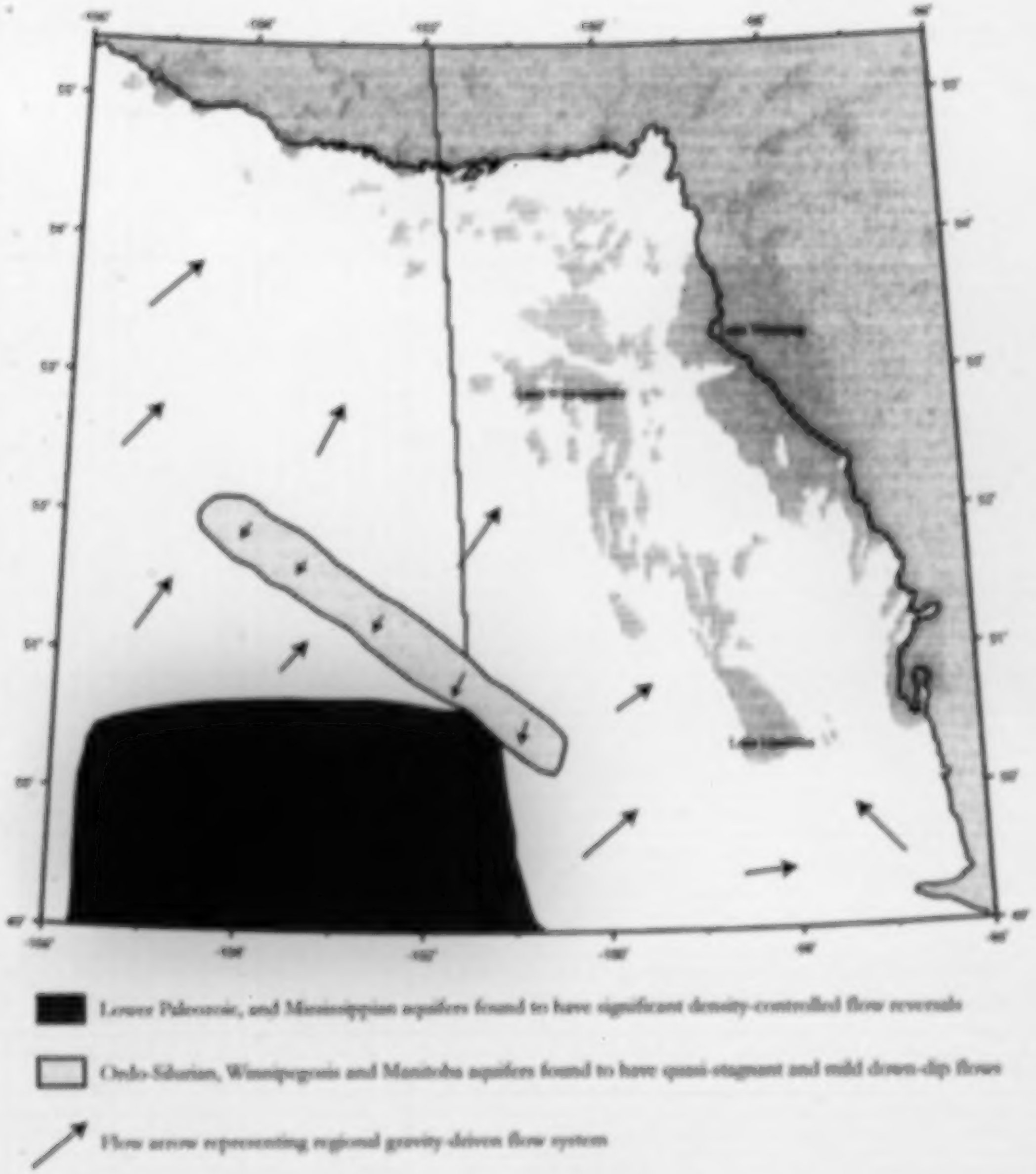
Lower Paleozoic, and Mississippian aquifers found to have significant density-controlled flow reversals
Ordo-Silurian, Winnipegosis and Manitoba aquifers found to have quasi-stagnant and mild down-dip flows
Flow arrow representing regional gravity driven flow system

Figure 5.5. Schematic representation of the regions in the Lower Paleozoic and Mississippian aquifers where density-flows are significant.

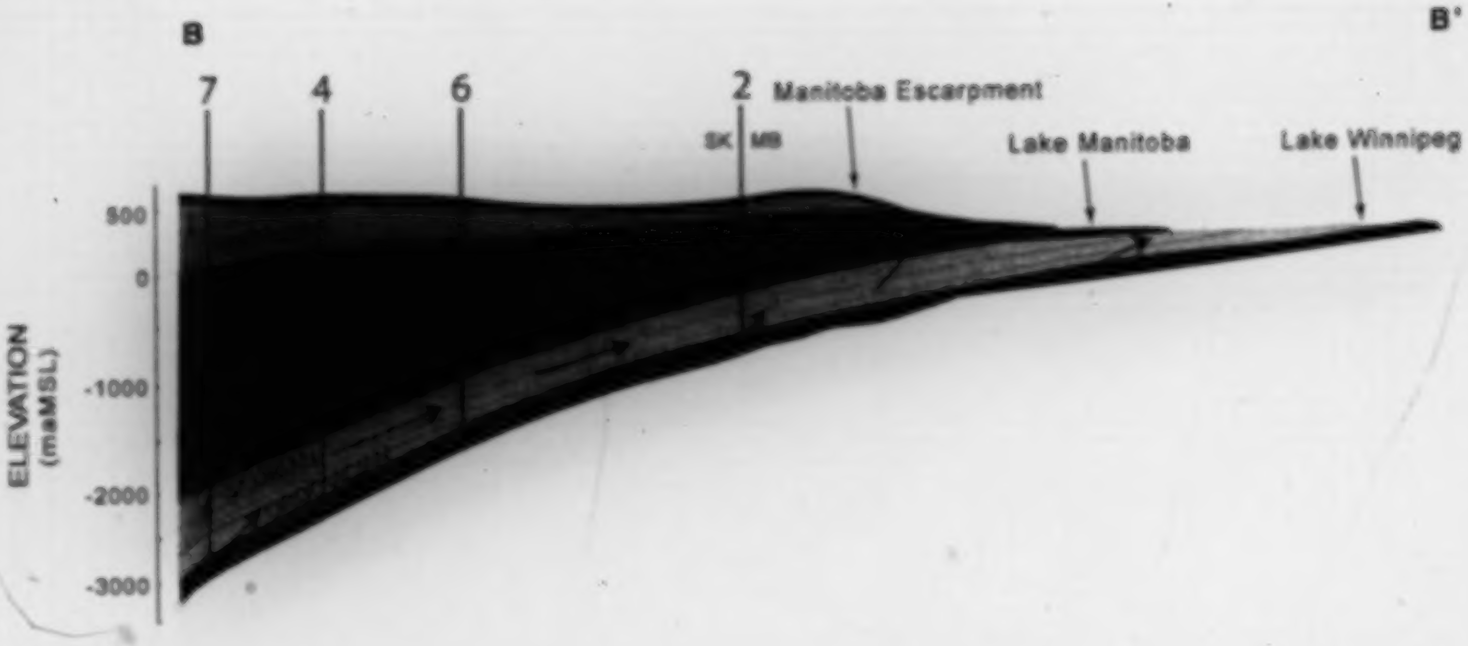
B
B'
7
4
6
2
Manitoba Escarpment
SK
MB
Lake Manitoba
Lake Winnipeg
500
0
-1000
-2000
-3000
ELEVATION
(maMSL)

Figure 5.6. Structural cross-section B to B' through the line of section shown in Figure 5.4. The conceptual flow field depicted here is aligned with the pressure-depth profiles identified.

6.0 CONCLUSIONS AND RECOMMENDATIONS

6.1 CONCLUSIONS OF THE REGIONAL HYDROGEOLOGICAL CHARACTERIZATION

1. A seamless hydrostratigraphic model for high-resolution hydrochemical and fluid flow analyses has been developed in the northeastern corner of the Williston Basin.

2. Significant compositional variations of formation waters are found both within and between individual aquifers. Four principal water chemistries and compositions were identified in the study area: (Type 1) - Ca-SO_4 freshwaters (TDS less than 10 g/L) characterize the recharging waters in the southwestern margin; (Type 2) – Na-Cl brines (span the complete range of TDS found) represent evolved formation waters derived from halite dissolution; (Type 3) - Na-HCO_3 freshwaters (TDS less than 10 g/L) denote meteoric or Pleistocene glacial meltwater recharge that originated as Ca-HCO_3 waters; and (Type 4) – Na-SO_4 brackish waters (TDS ranges from 25-100 g/L) are either formed by the mixing between Type 1 recharging waters and Type 2 brines or through recharge of Ca-HCO_3 freshwaters that evolve toward Na-HCO_3 facies and then mix with Type 2 brines in areas of high SO_4.

3. Type 1 (Ca-SO_4) waters have been identified in all major stratigraphic subdivisions of the Lower Paleozoic, Mississippian and Mesozoic aquifer systems in the southwestern corner of the study area. The origin of this recharge into the basin is attributed to topographic uplifts created from the Laramide Orogeny. Type 3 (Na-HCO_3) waters are found in the Lower Paleozoic and Mesozoic aquifer systems and represent partially evolved fresher water compositions from modern-day recharge and/or refluxing subglacial meltwater along the northeastern margin. Type 4 (Na-SO_4) waters are an intermediate and mixed composition between meteoric freshwater (precipitation and/or glacial meltwater) and Na-Cl brines. For the Lower Paleozoic aquifers, the interpretation of the Type 4 (Na-SO_4) brackish

water-mixing zone on the northeastern margin is a direct result of the Wisconsin Glaciation and subglacial recharge into the basin's edge.

4. Saline waters (greater than 100 g/L) are found within the Jurassic Aquifer as a result of vertical mixing between the Lower Paleozoic aquifers likely sourced from the Duperow and/or Birdbear aquifers. The Jurassic Aquifer is not completely isolated from the rest of the Paleozoic rocks. The Souris Valley and Tilston aquifers have vertical pressure gradients that would support an upward movement of formation waters across the Watrous Aquitard.

5. Formation waters in the Lower Paleozoic aquifers are generally flowing up-dip and northeast toward the outcrop and subcrop locations. This flow system is a direct result of the basin configuration imparted from the Laramide Orogeny.

6. Flow directions in the Mississippian aquifers are generally west to east. Significant differences between the aquifers exist and Mississippian aquifer segregation is important as both pressure and chemical variations are found laterally and vertically throughout.

7. Mesozoic flow directions are dominantly east-northeast with northward flow present in the Mannville and Newcastle aquifers. Pressure regimes are regionally under-pressured and flow systems are considerably affected by the outcrops along the Mesozoic Escarpment and the net unloading effect during isostatic rebound after the retreat of the Laurentide ice sheet. High transmissivity Mesozoic aquifers reflect efficient pressure drainage along the outcrops.

8. The central Williston Basin experiences primarily horizontal fluid flow traveling parallel to aquifer confining surfaces. Vertical flow and hydraulic continuity is evident towards the basin margin. Where present, the Prairie Evaporite Formation forms a competent barrier and hydraulic separation from any vertical flow

potentials between overlying/underlying formations. However, thinning of aquitards and complete salt removal promotes upward vertical flow.

9. Flow reversals are generally only found in southern Saskatchewan. This suggests that brine migration patterns are in a transient re-equilibration period following the Laramide peak energy boundary conditions. These brines are gravitationally unstable in the present-day dynamics of the Williston Basin.

10. Analysis of hydrochemistry incorporating the geological formation edges has identified geochemical signatures correlative with salt dissolution edges. There are four main occurrences whereby evaporite dissolution edges show a distinct correlation with formation water chemistry (Lake Alma Anhydrite, Prairie Evaporite Formation, Davidson and Flat Lake Salt Members).

11. The Prairie Evaporite Formation marks the maximum limit of glacial meltwater invasion into the Winnipegosis Formation of the northeastern margin. Using hydrochemistry of the saline-meteoric mixing zone and the salt dissolution edges, it is possible to put constraints on the limit of freshwater recharge related to Pleistocene meltwaters in the northeastern corner of the Williston Basin.

12. Pleistocene glaciation has had a noticeable effect on the hydrogeology of the Williston Basin and it is also evident today. However, the residence time of the ice-sheets was insufficient to cause long-term, regional-scale pressure distributions to be in disequilibrium today. Thus, modern-day pressure and geochemical distributions in the Williston Basin can be used to interpret past fluid flow events.

13. Primary understanding of regional hydrogeology and hydrochemistry in sedimentary basins are imperative to discern and comprehend the chemical evolution of basinal brines and the dynamics of brines during meteoric invasion.

6.2 RECOMMENDED AREAS OF FUTURE RESEARCH

The northeastern corner of the Williston Basin is of particular importance to Manitoba's groundwater resources. The methods and synthesis of this regional hydrogeology characterization must be further linked to the shallow-potable groundwater aquifers utilized by the City of Winnipeg. In southeastern Manitoba, freshwater portions of the Carbonate Rock Aquifer are heavy utilized for municipal, industrial, agricultural and residential water supply. The basin hydrodynamics will affect and govern, to some extent, the water supply capacity, threat of saline water intrusion, and the overall quality and dynamics of the groundwater system. The eastward movement of saline brines and especially the brackish water mixing zone would be detrimental to water quality and quantity in southeastern Manitoba.

Utilization of the detailed hydrostratigraphic model for the regional characterization needs to be carried over into local-scale hydrogeological analyses. Currently, the Carbonate Rock Aquifer is homogenized including the Yeoman through Manitoba aquifers as one. Completing an interval-testing procedure on these groundwater wells to determine their perforation intervals will greatly aid in integrating the regional and local-scale systems.

If the two systems are assimilated, then the dynamics of the regional-scale system on the near-surface regime, and ultimately the potential re-organizing of the shallow drinking water resources, could be determined.

Following this integrative approach, a regional numerical-model would quantify the flow and transport mechanisms of the saline-meteoric zone given excessive withdrawals from the shallow aquifer. The results of the regional hydrogeology model could then be used as initial conditions by which a fully coupled groundwater-surface model would evaluate groundwater resource management, as extraction will enhance the movement and mixing with the local groundwaters.

7.0 REFERENCES

Adams, J. J. and Bachu, S., 2002. Equations of state for basin geofluids: Algorithm review and intercomparison for brines. Geofluids, v. 2, p. 257-271.

Alkalali, A., 2002. Petroleum hydrogeology of the Nisku Aquifer. Unpublished M.Sc. thesis, Department of Earth and Atmospheric Sciences, University of Alberta, Edmonton, Alberta, Canada, 152 p.

Alkalali, A. I. and Rostron, B. J., 2003. Basin-scale analysis of variable-density groundwater flow: Nisku Aquifer, Western Canada Basin. Journal of Geochemical Exploration, v. 78-79, p. 313-316.

Appelo, C. A. J. and Postma, D., 2005. Geochemistry, groundwater and pollution, 2nd edition. A. A. Balkema, 649 p.

Bachu, S., 1995. Synthesis and model of formation water flow in the Alberta basin, Canada. American Association of Petroleum Geologists Bulletin, v. 79, p. 1159-1178.

Bachu, S. and Hitchon, B., 1996. Regional-scale flow of formation waters in the Williston Basin. American Association of Petroleum Geologists Bulletin, v. 80, p. 248-264.

Bachu, S. and Michael, K., 2002. Flow of variable-density formation water in deep sloping aquifers: Minimizing the error in representation and analysis when using hydraulic head distributions. Journal of Hydrology, p. 49-65.

Back, W., 1960. Origin of hydrochemical facies of ground water in the Atlantic Coastal Plain. 21st International Geological Conference, Copenhagen, p. 87-95.

Back, W., 1961. Techniques for mapping of hydrochemical facies. United States Geological Survey Professional Paper 424-D, p. 380-382.

Barchyn, D., 1982. Geology and hydrocarbon potential and the lower Amaranth Formation: Waskada-Pierson area, southwestern Manitoba. Manitoba Department of Energy and Mines Geological Report GR82-6. 30 p.

Barson, D. B., 1993. The hydrogeological characterization of oil fields in north-central Alberta for exploration purposes. Unpublished Ph.D. thesis, University of Alberta, Edmonton, Alberta, Canada, 301 p.

Batzle, M. and Wang, Z., 1992. Seismic properties of pore fluids. Geophysics, v. 57, p. 1396-1408.

Benn, A. A. and Rostron, B. J., 1998. Regional hydrochemistry of Cambrian to Devonian aquifers in the Williston Basin, Canada-U.S.A. *in*: J. E. Christopher, C. F. Gilboy, D. F. Paterson, and S. L. Bend, eds., Eighth International Williston Basin Symposium, Saskatchewan Geological Society Special Publication No. 13, p. 238-245.

Berg, R. R., DeMis, W. D., and Mitsdarffer, A. R., 1994. Hydrodynamic effects on Mission Canyon (Mississippian) oil accumulations. American Association of Petroleum Geologists Bulletin, v. 78, p. 501-518.

Bernatsky, R., 1998. Hydrogeochemistry of formation waters in southern Saskatchewan. Unpublished M.Sc. thesis, University of Regina, Regina, Saskatchewan, Canada, 206 p.

Betcher, R. N., Grove, G., and Pupp, C., 1995. Groundwater in Manitoba: Hydrogeology, quality concerns, management. National Hydrology Research Institute contribution CS-93017, Environment Canada, Saskatoon, 47 p.

Bethke, C. M. and Marshak, S., 1990. Brine migrations across North America - The plate tectonics of groundwater. Annual Reviews of Earth and Planetary Science, v. 18, p. 287-315.

Block, D., 2001. Water resistivity atlas of western Canada CSPG (abs.): Rock the Foundation, abstracts of technical talks, posters, and core displays. Canadian Society of Petroleum Geologists Annual Convention, p. 359-369.

Boulton, G. S., Caban, P. E., van Gijssel, K., Leijinse, A., Punkari, M., and van Weert, F. H. A., 1996. The impact of glaciation on the groundwater regime of Northwest Europe. Global and Planetary Change, v. 12, p. 397–413.

Bredehoeft, J. D., Neuzil, C. E., and Milly, P. C. E., 1983. Regional flow in the Dakota Aquifer: A study on the role of confining layers. United States Geological Survey Water-Supply Paper 2237, 45 p.

Brown, D. L. and Brown, D. L., 1987. Wrench style deformation and paleostructural influence on sedimentation in and around a cratonic basin. *in*: M. W. Longman, ed., Williston Basin: Anatomy of a Cratonic Oil Province, Rocky Mountain Association of Geologists, p. 57-70.

Busby, J. F., Kimball, B. A., and Downey, J. S., 1995. Geochemistry of water in aquifers and confining units of the Northern Great Plains in parts of Montana, North Dakota, South Dakota, and Wyoming. United States Geological Survey Professional Paper 1402-F, 146 p.

Carlson, A. E., Jenson, J. W., and Clark, P. U., 2007. Modeling the subglacial hydrology of the James Lobe of the Laurentide Ice Sheet. Quarterly Science Review, v. 26, p. 1384-1397.

Carpenter, A. B., 1978. Origin and chemical evolution of brines in sedimentary basins. Oklahoma Geological Survey Circular, v. 79, p. 60-77.

Chapman, R. E., 1987. Fluid flow in sedimentary basins: A geologist's perspective. *in*: J. C. Goff and B. P. J. Williams, Fluid Flow in Sedimentary Basins, Geological Society Special Publication, no. 34, p. 3-18.

Chebotarev, I. I., 1955. Metamorphism of natural water in the crust of weathering. Geochem, Cosmochim, Acta, v. 8, p. 22-48, 137-170, 198-212.

Chierici, G. L., 1994. Principles of petroleum reservoir engineering. Springer-Verlag, Berlin, New York, 430 p.

Chipley, D. and Kyser, T. K., 1991. Large scale fluid movement in the Western Canadian Sedimentary Basin as recorded by fluid inclusions in evaporites. *in*: J. E. Christopher and F. M. Haidl, eds., Sixth International Williston Basin Symposium, Saskatchewan Geological Society Special Publication, p. 265-269.

Christiansen, E. A., Gendzwill, D. J., and Meneley, W. A., 1982. Howe Lake: A hydrodynamic blowout structure. Canadian Journal of Earth Sciences, v. 19, p. 1122–1139.

Christopher, J. E., 1961. Transitional Devonian-Mississippian formations of southern Saskatchewan. Saskatchewan Department of Mineral Resources, Report 66. 103 p.

Christopher, J. E., 1964. The Middle Jurassic Shaunavon Formation of southwestern Saskatchewan. Saskatchewan Department of Mineral Resources, Report 95. 95 p.

Christopher, J. E., 1966. Shaunavon (Middle Jurassic) sedimentation and vertical tectonics in southwestern Saskatchewan. *in*: Jurassic and Cretaceous Stratigraphic Traps Sweetgrass Arch. Billings Geological Society, 17th Annual Field Conference Guidebook, p. 18-35.

Christopher, J. E., 1984a. Depositional patterns and oil field trends in the Lower Mesozoic of the northern Williston Basin, Canada. *in*: J. A. Lorsong and M. Wilson, eds., Oil and Gas in Saskatchewan, Saskatchewan Geological Society Special Publication No. 7, p. 83-102.

Christopher, J. E., 1984b. The Lower Cretaceous Mannville Group, northern Williston Basin region, Canada. *in*: D. F. Stott and D. J. Glass, eds., Mesozoic of Middle North America, Canadian Society of Petroleum Geologists Memoir 9. p. 109-126.

Christopher, J. E., 1987. Depositional patterns and oil field trends in the Lower Mesozoic of the northern Williston Basin, Canada, *in*: M. Longman, ed., 1987 Symposium of the Rocky Mountain Association of Geologists, p. 223-243.

Christopher, J. E., 2003. Jura-Cretaceous Success Formation and Lower Mannville Group of Saskatchewan. Saskatchewan Industry and Resources, 128 p.

Christopher, J. E., Kent, D. M., and Simpson, F., 1971. Hydrocarbon potential of Saskatchewan. Saskatchewan Department of Mineral Resources, Report 157, 47 p.

Christopher, J. E. and Yurkowski, M., 2005. The Upper Cretaceous (Turonian) Second White Specks Formation of eastern Saskatchewan. *in*: Summary of Investigations 2005, Volume 1, Saskatchewan Geological Survey, Saskatchewan Industry and Resources, Misc. Rep., 2005-4.1, CD ROM, Paper A-18, 12 p.

Christopher, J. E., Yurkowski, M., Nicolas, M., and Bamburak, J., 2006. The Cenomanian-Santonian Colorado Formation of eastern southern Saskatchewan and southwestern Manitoba. *in*: C. F. Gilboy and S. G. Whittaker, eds., Saskatchewan and Northern Plains Oil & Gas Symposium 2006, Saskatchewan Geological Society Special Publication 19, p. 299-318.

Clark, I. D., Douglas, M., Raven, K., and Bottomley, D., 2000. Recharge and preservation of Laurentide glacial melt water in the Canadian Shield. Ground Water, v. 38, p. 735–742.

Clayton, L. and Moran S. R., 1982. Chronology of late Wisconsinan ice-sheet influences on global climate change. Science, v. 286, p. 1104-1111.

Clayton, R. N., Friedman, I., Graf, D. L., Mayeda, T. K., Meents, W. F., and Shimp, N. F., 1966. The origin of saline formation waters 1. Isotopic composition. Journal of Geophysical Research, v. 71, p. 3869-3882.

Collins, A. G., 1975. Geochemistry of oilfield waters. Developments in Petroleum Science, Elsevier Science Publication Company, 496 p.

Cumming, G. L., Kyle, J. R., and Sangster, D. F., 1990. Pine Point: A case history of lead isotope homogeneity in a Mississippi valley-type district. Economic Geology, v. 85, p. 133-144.

Dahlberg, E. C., 1994. Applied Hydrodynamics in Petroleum Exploration, Second Edition. Springer-Verlag, 295 p.

Davies, P. B., 1987. Modeling areal, variable density, groundwater flow using equivalent freshwater head – analysis of potentially significant errors, in solving groundwater problems with models. Proceedings of the National Water Well Association, International Groundwater Modeling Center Conference, p. 888-903.

Davis, S., 1988. Where are the rest of the analyses? Groundwater, v. 26, p. 2-5.

DeMis, W. D., 1995. Effect of cross-basinal hydrodynamic flow on oil accumulations and oil migration history of the Bakken-Madison Petroleum System; Williston Basin, North America. *in:* L. D. V. Hunter and R. A. Schalla, eds., Seventh International Williston Basin Symposium, Billings, Montana, Geological Society, p. 291-301.

Downey, J. S., 1984a. Hydrodynamics of the Williston Basin in the Northern Great Plains. *in:* D. G. Jorgensen and D. C Signor, eds., Geohydrology of the Dakota Aquifer, National Water Well Association, Worthington, Ohio, United States, p. 92-98.

Downey, J. S., 1984b. Geohydrology of the Madison and associated aquifers in parts of Montana, North Dakota, South Dakota, and Wyoming. United States Geological Survey Professional Paper 1273-G, 47 p.

Downey, J. S. 1986. Geohydrology of Bedrock aquifers in the Northern Great Plains in parts of Montana, North Dakota, South Dakota, and Wyoming. United States Geological Survey Professional Paper 1402-E, 87 p.

Downey, J. S., Busby, J. F., and Dinwiddie, G. A., 1987. Regional aquifers and petroleum in the Williston Basin region of the United States. *in:* M. W. Longman, ed., Williston Basin: Anatomy of a Cratonic Oil Province, Rocky Mountain Association of Geologists, p. 299-312.

Downey, J. S. and Dinwiddie, G. A., 1988. The regional aquifer system underlying the northern Great Plains in parts of Montana, North Dakota, South Dakota, and Wyoming – summary. United States Geological Survey Professional Paper 1402-A, 63 p.

Dunn, C. E., 1975. The Upper Devonian Duperow Formation in southeastern Saskatchewan. Saskatchewan Department of Mineral Resources, Report 179, p. 151.

Dyke, A. S. and Prest, V. K., 1987. Paleogeography of northern North America, 18,000-5000 years ago. Geological Survey of Canada, Map 1703A, Scale 1:12.500,000.

Edie, R. W., 1958. Mississippian sedimentation and oil fields in southeastern Saskatchewan. Bulletin of the American Association of Petroleum Geologists, v. 42, p. 94-126.

Edmunds, N. R., 1994. Palaeowaters in European coastal aquifers – the goals and main conclusions of the PALAEAUX project. *in*: W. M. Edmunds and C. J. Milne, eds., Palaeowaters in Coastal Europe: Evolution of Groundwater since the Late Pleistocene, Geological Society of London, Special Publications 189, p. 1-16.

Ferguson, G. A. G., Betcher, R. N., and Grasby, S. E., 2007. Hydrogeology of the Winnipeg Formation in Manitoba, Canada. Hydrogeology Journal, v. 15, p. 573-587.

Freeze, R. A. and Cherry, J. A., 1979. Groundwater. Prentice-Hall, 604 p.

Fuller, J. G. C. M., 1956. Mississippian rocks and oilfields in southeastern Saskatchewan, Saskatchewan Department of Mineral Resources, Report 19, 72 p.

Fuzesy, L. M., 1975. Geology and hydrocarbon potential of the Winnipegosis Formation in southeastern Saskatchewan. *in*: Summary of Investigations 1975, Saskatchewan Geological Survey, Saskatchewan Department of Mineral Resources, p. 66-70.

Fuzesy, L. M., 1980. Geology of the Winnipegosis Formation in southeastern Saskatchewan. *in*: Summary of Investigations 1980, Saskatchewan Geological Survey, Saskatchewan Department of Mineral Resources, Misc. Rept. 80-4, p. 165.

Garven, G., 1985. The Role of Regional Fluid Flow in the Genesis of the Pine Point Deposit, Western Canada Sedimentary Basin. Economic Geology, v. 80, p. 307-324.

Garven, G., 1995. Continental-scale groundwater flow and geological processes. Annual Reviews Earth and Planetary Science, v. 23, p. 89-117.

Ge, S. and Garven, G., 1989. Tectonically induced transient groundwater flow in foreland basin. *in*: R. A. Price, ed., Origin and Evolution of Sedimentary Basins and their Energy and Mineral Deposits, Monograph 48, American Geophysical Union, Washington, D.C., United States, p. 145-157.

Gerhard, L. C., Anderson, S. B., LeFever, J. A., and Carlson, C. G., 1982. Geological development, origin, and energy mineral resources of the Williston Basin, North Dakota, American Association of Petroleum Geologists Bulletin, v. 66, p. 989-1020.

Gerhard, L. C. and Anderson, S. B., 1988. Geology of the Williston Basin (United States portion). *in*: L. L. Sloss, ed., Sedimentary Cover - North American Craton, U.S. Geological Society of America, p. 221-241.

Grasby, S. E., 2000. Saline spring geochemistry, west-central Manitoba. *in*: Report of Activities 2000, Manitoba Industry, Trades and Mines, Manitoba Geological Survey, p. 214-216.

Grasby, S. E., Betcher, R. N., and McDougall, W. J., 1999. Water quality of the Carbonate Rock Aquifer, southern Manitoba. Geological Survey of Canada, Open File 3725, 166 p.

Grasby, S. E., Osadetz, K., Betcher, R., and Render, F., 2000. Reversal of the regional-scale flow system of the Williston Basin in response to Pleistocene glaciation. Geology, v. 28, p. 635-638.

Grasby, S. E. and Betcher, R. N., 2002. Regional hydrogeochemistry of the Carbonate Rock Aquifer, southern Manitoba. Canadian Journal of Earth Science, v. 39, p. 1053-1063.

Grasby, S. E. and Chen, Z., 2005. Subglacial recharge into the Western Canada Sedimentary Basin – Impact of Pleistocene glaciation on basin hydrodynamics. Geological Society of America Bulletin, v. 117, no. 3/4, p. 500-514.

Haidl, F. M., 1987. Stratigraphic and lithologic relationships, Interlake Formation (Silurian), southern Saskatchewan. *in*: Summary of Investigations 1987, Saskatchewan Geological Survey, Misc. Rep. 87-4, p. 187-193.

Haidl, F. M., 1988. Lithology and stratigraphy of lower Paleozoic strata: New information from cores in the Cumberland Lake area, east-central Saskatchewan. *in*: Summary of Investigations 1988, Saskatchewan Geological Survey, Misc. Rep. 88-4, p. 202-210.

Haidl, F. M., Kreis, L. K., and Dancsok, E. F. R., 1996. New oil discoveries in Ordovician Red River strata, southeastern Saskatchewan. *in*: Summary of Investigations 1996, Saskatchewan Industry and Resources, p. 136-144.

Haidl, F., Nimegeers, A., and Marsh, A., 2006. Stratigraphy and Hydrocarbon Potential of Silurian Interlake Strata, Southeastern Saskatchewan. *in*: C. F. Gilboy and S. G. Whittaker, eds., Saskatchewan and Northern Plains Oil & Gas Symposium 2006, Saskatchewan Geological Society Special Publication 19, p. 74-91.

Halabura, S., 1982. Depositional environments of the Upper Devonian Birdbear Formation, Saskatchewan. Fourth International Williston Basin Symposium, Saskatchewan Geological Society Special Publication, p. 113-124.

Halabura, S., 2006. The Mississippian of southeastern Saskatchewan: Regional considerations. *in*: C. F. Gilboy and S. G. Whittaker, eds., Saskatchewan and Northern Plains Oil & Gas Symposium 2006, Saskatchewan Geological Society Special Publication 19, p. 146-164.

Hannon, N., 1987. Subsurface water flow patterns in the Canadian sector of the Williston Basin. *in*: M. W. Longman, ed., Williston Basin: Anatomy of a Cratonic Oil Province, Rocky Mountain Association of Geologists, p. 299-312.

Hanor, J. S., 1994. Origin of saline fluids in sedimentary basins. Geological Society Special Publication. *in*: J. Parnell, ed., Geofluids: Origin, Migration and Evolution of Fluids in Sedimentary Basins, p. 151-174.

Hitchon, B., 1996. Rapid evaluation of the hydrochemistry of a sedimentary basin using only 'standard' formation water analyses: Example from the Canadian portion of the Williston Basin. Applied Geochemistry, v. 11, p. 789-795.

Hitchon, B. and Brulotte, M., 1994. Culling criteria for "standard" formation water analyses. Applied Geochemistry, v. 9, p. 637-645.

Horner, D. R., 1951. Pressure build-up in wells. Proceeding Third World Petroleum Congress, Section 2, p. 503-521.

Hubbert, M. K., 1940. The theory of groundwater motion. Journal of Geology, v. 48, p. 785-944.

Hubbert, M. K., 1953. Entrapment of petroleum under hydrodynamic conditions. American Association of Petroleum Geologists Bulletin, v. 37, p. 1954-2026.

Iampen, H. T., 2003. The genesis and evolution of pre-Mississippian brines in the Williston Basin, Canada-U.S.A. Unpublished M.Sc. thesis, Department of Earth and Atmospheric Sciences, University of Alberta, Edmonton, Alberta, Canada, 124 p.

Iampen, H. T. and Rostron, B. J., 2000. Hydrogeochemistry of pre-Mississippian brines, Williston Basin, Canada-USA. Journal of Geochemical Exploration, v. 69-70, p. 29-35.

Jensen, G. K. S., 2007. Fluid flow and geochemistry of the Mississippian aquifers in the Williston Basin, Canada-U.S.A. Unpublished M.Sc. thesis, Department of Earth and Atmospheric Sciences, University of Alberta, Edmonton, Alberta, Canada, 123 p.

Jensen, G. K. S., Rostron, B. J., Duke, M. J. M., and Holmden, C., 2006. Bromine and stable isotopic profiles of formation waters from potash mine-shafts, Saskatchewan, Canada. Journal of Geochemical Exploration, v. 89. p. 170-173.

Kendall, A. C., 1975. The Ashern, Winnipegosis and Lower Prairie Evaporite formations of the commercial potash areas. Summary of Investigations 1975, Saskatchewan Geological Survey, Saskatchewan Department of Mineral Resources, p. 61-65.

Kendall, A. C., 1976. The Ordovician carbonate succession (Bighorn Group) of southern Saskatchewan. Saskatchewan Department of Mineral Resources, Report 180, 185 p.

Kent, D. M., 1968. The geology of the Upper Devonian Saskatchewan Group and equivalent rocks in western Saskatchewan and adjacent areas. Saskatchewan Department of Mineral Resources, Report 99, 224 p.

Kent, D. M., 1994. Paleogeographic evolution of the cratonic platform – Cambrian to Triassic. *in*: G. Mossop and I. Shetson (compilers), Geological Atlas of the Western Canada Sedimentary Basin, Canadian Society of Petroleum Geologists and Alberta Research Council, p. 69-86.

Kent, D. M. and Christopher, J. E., 1994. Geological history of the Williston Basin and Sweetgrass Arch. *in*: G. Mossop and I. Shetson (compilers), Geological Atlas of the Western Canada Sedimentary Basin, Canadian Society of Petroleum Geologists and Alberta Research Council, p. 421-429.

Kent, D. M., Thomas, P., and Heck, T., 2004. Geological mapping of the Mississippian strata in southeastern Saskatchewan, northwestern North Dakota, and northeastern Montana. Summary of Investigations 2004, Volume 1, Regina, Saskatchewan, Canada, Saskatchewan Industry and Resources, 22 p.

Khan, D. K., 2006. Hydrogeological characterization of the Weyburn CO_2 project area and gradient-free inverse conditioning of heterogeneous aquifer models to hydraulic head data. Unpublished Ph.D. thesis, Department of Earth and Atmospheric Sciences, University of Alberta, Edmonton, Alberta, Canada, 238 p.

Khan, D. K. and Rostron, B. J., 2004. Regional hydrogeological investigation around the IEA Weyburn CO_2 monitoring and storage project site. *in:* E. S. Rubin, D. W. Keith, and C. F. Gilboy, eds., Proceedings of the Seventh International Conference on Greenhouse Gas Control Technologies, Sept 5-9, 2004, Vancouver, Canada, Volume 1: Peer-Reviewed Papers and Plenary Sessions, Elsevier, UK, p. 741-750.

Kreis, L. K., Gent, M., and Vigrass, L. W., 1991. Subsurface brines in southern Saskatchewan. *in:* J. E. Christopher, C. F. Gilboy, D. F. Paterson, and S. L. Bend, eds., Sixth Annual Williston Basin Symposium, Saskatchewan Geological Society Special Publication, p. 283-292.

Kreis, L. K., Thomas, P. L., Burke, R. B., and Whittaker, S. G., 2003. Devonian isopach and structure maps: Initial results of the IEA Weyburn CO_2 Monitoring and Storage Project area. Summary of Investigations 2003, Volume 1, Saskatchewan Geological Survey, Saskatchewan Industry and Resources, Misc. Rep. 2003-4.1, Paper A-5, 6 p.

Kreis, L. K., Beauchamp, B., Bezys, R., Martiniuk, C., and Whittaker, S., 2004. Williston Basin architecture and hydrocarbon potential in eastern Saskatchewan and western Manitoba. *in:* Summary of Investigations 2004, Volume 1, Saskatchewan Geological Survey, Saskatchewan Industry Resources, Misc. Rep. 2004-4.1, CD-ROM, Paper A-3, 5 p.

Kreis, L. K. and Costa, A. L., 2005. Hydrocarbon potential of Bakken and Torquay formations, southeastern Saskatchewan. Saskatchewan Geological Society Core Workshop Volume, Special Publication Number 17, 13th International Williston Basin Symposium, p. 3-36.

Kreis, L. K., Costa, A. L., and Osadetz, K. G., 2006. Hydrocarbon potential of Bakken and Torquay formations, southeastern Saskatchewan. *in:* C. F. Gilboy and S. G. Whittaker, eds., Saskatchewan and Northern Plains Oil & Gas Symposium 2006, Saskatchewan Geological Society Special Publication 19, p. 118-137.

Lambrakis, N. and Kallergin, G., 2001. Reaction of subsurface coastal aquifers to climate and land use changes in Greece: Modelling of groundwater refreshening patterns under natural recharge. Journal of Hydrology, v. 245, p. 19-31.

Langmuir, D., 1997. Aqueous Environmental Geochemistry. Prentice-Hall, New Jersey, United States, 600 p.

LeFever, R. D., Thompson, S. C., and Anderson, D. B., 1987. Earliest Paleozoic history of the Williston Basin in North Dakota. *in:* C. G. Carlson and J. E. Christopher, eds., Fifth International Williston Basin Symposium, Saskatchewan Geological Society and North Dakota Geological Society Special Publication No. 9, p. 22-36.

Lefever, R. D., 1998. Hydrodynamics of formation waters in the North Dakota Williston Basin. *in:* J. E. Christopher, C. F. Gilboy, D. F. Paterson, and S. L. Bend, eds., Eighth Annual Williston Basin Symposium, Saskatchewan Geological Society Special Publication No. 13, p. 229-237.

Lisenbee, A. L. and DeWitt, E., 1993. Laramide evolution of the Black Hills uplift. *in:* A. W. Snoke, J. R. Steidtmann, and S. M. Roberts, eds., Geology of Wyoming, Geological Survey of Wyoming Memoir, v. 5, p. 374-412.

Lowenstein, T. K., Hardie, L. A., Timofeeff, M. N., and Demicco, R. V., 2003. Secular variation in seawater chemistry and the origin of calcium chloride basinal brines. Geology, v. 31, p. 857-860.

Lowenstein, T. K. and Timofeeff, M. N., 2008. Secular variations in seawater chemistry as a control on the chemistry of basinal brines: Test of the hypothesis. Geofluids, v. 8, p. 77-92.

McCabe, H. R., 1980. Stratigraphic mapping and core hole program, southwest Manitoba. Manitoba Department of Energy and Mines, Mineral Resources Division, Report of Field Activities, p. 70-73.

McCabe, H. R., 1983. Lower Paleozoic Formation water analyses Bakken to Precambrian December, 1971: Including supplement to December 1983. Manitoba Energy and Mines Petroleum, 27 p.

McIntosh, J. C., Walter, L. M., and Martini, A. M., 2002. Pleistocene recharge to mid-continent basins: Effects on salinity structure and microbial gas generation. Geochemica et Cosmochemica Acta, v. 66, p. 1681-1700.

McIntosh, J. C. and Walter, L. M., 2005. Volumetrically significant recharge of Pleistocene glacial meltwaters into epicratonic basins: Constraints imposed by solute mass balances. Chemical Geology, v. 222, p. 292-309.

Miller, C. and Krause, F., 2006. Waulsortian Lithofacies of the Mississippian Souris Valley Beds (Lodgepole Formation), Williston Basin, southeastern Saskatchewan, Canada. *in*: C. F. Gilboy and S. G. Whittaker, eds., Saskatchewan and Northern Plains Oil & Gas Symposium 2006, Saskatchewan Geological Society Special Publication 19, p. 173-183.

Mossop, G. D. and Shetson, I., 1994. Geological atlas of the Western Canada sedimentary basin. Canadian Society of Petroleum Geologists and Alberta Research Council, 510 p.

Neuzil, C. E., Bredehoeft, J, D., and Wolff, R. G., 1982. Leakage and fracture permeability in the Cretaceous shales confining the Dakota Aquifer in South Dakota. *in*: D. G. Jorgensen and D. C. Signor, eds., Geohydrology of the Dakota Aquifer, National Water Well Association, Worthington, Ohio, United States, p. 113-120.

Neuzil, C. E. and Pollock, 1983. Erosional unloading and fluid pressures in hydraulically 'tight' rocks. Journal of Geology, v. 91, p. 179-193.

Nicolas, M., 2006. Petroleum geology of the Devonian Three Forks Formation, Sinclair Field and surrounding area, southwestern Manitoba. Saskatchewan and Northern Plains Oil and Gas Symposium, Proceedings from the Core Workshop, 26 p.

Nicolas, M., 2007. Stratigraphic equivalencies table. Retrieved from: http://www.gov.mb.ca/stem/mrd/go/willistontgi.

Norford, B. S., Haidl, F. M., Bezys, R. K., Cecile, M. P., McCabe, H. R., and Paterson, D. F., 1994. Middle Ordovician to Lower Devonian strata of the Western Canada Sedimentary Basin. *in*: G. D. Mossop and I. Shetson, compilers, Geological Atlas of the Western Canada Sedimentary Basin, Canadian Society of Petroleum Geologists and Alberta Research Council, p. 109-127.

Osadetz, K. G. and Haidl, F. M., 1989. Tippecanoe Sequence: Middle Ordovician to Lowest Devonian: Vestiges of a great epeiric sea. *in*: B. D. Ricketts, ed., Western Canada Sedimentary Basin: A Case Study, Canadian Society of Petroleum Geologists, p. 121-137.

Palombi, D. D. and Rostron, B. J., 2006. Regional hydrochemistry of Lower Paleozoic aquifers in the northern portion of the Williston Basin, Saskatchewan-Manitoba. *in*: C. F. Gilboy and S. G. Whittaker, eds., Saskatchewan and Northern Plains Oil & Gas Symposium 2006, Saskatchewan Geological Society Special Publication 19, p. 201-209.

Paterson, D. F., 1988. Review of regional stratigraphy relationships of the Winnipeg Group (Ordovician), the Deadwood Formation (Cambro-Ordovician) and underlying strata in Saskatchewan. *in*: L. P. Beck, ed., Summary of Investigations 1988, Saskatchewan Geological Survey, p. 224-225.

Person, M., Dugan, B., Swenson, J. B., Urbano, L., Stott, C., Taylor, J., and Willett, M., 2003. Pleistocene hydrogeology of the Atlantic continental shelf, New England. GSA Bulletin, v. 115, p. 1324-1343.

Peterson, J. A., 1972. Jurassic System. *in*: W. Mallory, ed., Geologic Atlas of the Rocky Mountain Region, Rocky Mountain Association of Geologists, p. 177-189.

Peterson, J. A. and MacCary, L. M., 1987. Regional stratigraphy and general petroleum geology of the U.S. portion of the Williston Basin and adjacent areas. *in*: M. W. Longman, ed., Williston Basin: Anatomy of a Cratonic Oil Province, Rocky Mountain Association of Geologists, p. 9-44.

Piotrowski, J. A., 1997a. Subglacial hydrology in north-western Germany during the last glaciation: Ground-water flow, tunnel valleys and hydrological cycles. Quaternary Science Reviews, v. 16, p. 169–185.

Piotrowski, J. A., 1997b. Subglacial groundwater flow during the last glaciation in northwestern Germany. Sedimentary Geology, v. 111, p. 217–224.

Porges, R. E. and Hammer, M. J., 2001. The Compendium of Hydrogeology. National Groundwater Association, Ohio, 303 p.

Porter, J. W. and Fuller, J. G. C. M., 1959. Lower Paleozoic rocks of northern Williston Basin and adjacent areas. American Association of Petroleum Geologists Bulletin, v. 43, p. 124-189.

Potter, D., 2006. Relationships of Cambro-Ordovician stratigraphy to paleotopography on the Precambrian basement, Williston Basin. *in*: C. F. Gilboy and S. G. Whittaker, eds., Saskatchewan and Northern Plains Oil & Gas Symposium 2006, Saskatchewan Geological Society Special Publication 19, p. 63-73.

Poulton, T. P., 1984. The Jurassic of the Canadian western interior, from 49°N latitude to Beaufort Sea. *in*: D. E. Stott and D. J. Glass, eds., The Mesozoic of Middle North America, Canadian Society of Petroleum Geologists Memoir 9, p. 15-41.

Reinson, G. E. and Wardlaw, N. C., 1972. Nomenclature and stratigraphic relationships, Winnipegosis and Prairie Evaporite formations. Canadian Petroleum Geologists Bulletin, v. 2a, no. 2, p. 301-320.

Remenda, V. H., 1993. Origin and migration of natural groundwater tracers in thick clay tills of Saskatchewan and the Lake Agassiz clay plain. Unpublished Ph.D. thesis, University of Waterloo, Waterloo, Ontario, Canada, 289 p.

Rostron, B. J, 1994. A new method for culling pressure data used in hydrodynamic studies. American Association of Petroleum Geologists Annual Meeting Abstracts - American Association of Petroleum Geologists and Society of Economic Paleontologists and Mineralogists, p. 247.

Rostron, B. J., Kreis, L. K., and Holmden, C., 1999. The Saskatchewan brine sampling program. Summary of Investigations 1999, Saskatchewan Industry and Resources, v. 1, p. 85-86.

Rostron, B. J., Kelley, L. I., Kreis, L. K., and Holmden, C., 2002. Economic potential of formation brines: Interim results from the Saskatchewan brine sampling program. *in*: Summary of Investigations 2002, Volume 2, Saskatchewan Geological Survey, Saskatchewan Industry Resources, Misc. Rep. 2002-4.2, CD-ROM, Paper C-1, 29 p.

Rostron, B. J. and Holmden, C., 2003. Regional variations in oxygen isotopic compositions in the Yeoman and Duperow aquifers, Williston Basin (Canada-USA). Journal of Geochemical Exploration, v. 78-79, p. 337-341.

Sandberg, C. A. and Hammond, C. R., 1958. Devonian System in Williston Basin and central Montana. American Association of Petroleum Geologists Bulletin, v. 42, p. 2293-2334.

Seaber, P. R., 1988. Hydrostratigraphic units. Hydrogeology, Colorado, Geological Society of America, p. 9-14.

Siegel, D. I., 1991. Evidence for dilution of deep, confined groundwater by vertical recharge of isotopically heavy Pleistocene water. Geology, v. 19, p. 433–436.

Simpson, F., 1975. Marine lithofacies and biofacies of the Colorado Croup (middle Albian to Santonian) in Saskatchewan. *in*: W. G. E. Caldwell, ed., The Cretaceous System in the Western Interior of North America, Geological Association of Canada Special Paper 13, p. 553-537.

Simpson, F., 1979. Low-permeability gas reservoirs in marine, Cretaceous sandstones of Saskatchewan, 1. Project outline and rationale. *in*: J. E. Christopher and R. Macdonald, eds., Saskatchewan Geological Survey, Summary of Investigations, Saskatchewan Mineral Resources, Misc. Rept. 79-10, p. 174-180.

Simpson, F. and O'Connell, S., 1979. Low-permeability gas reservoirs in marine, Cretaceous sandstones of Saskatchewan, 2. Lower Colorado (middle Albian to Cenomanian) strata of southern Saskatchewan. *in*: J. E. Christopher and R. Macdonald, eds., Saskatchewan Geological Survey, Summary of Investigations, Saskatchewan Mineral Resources, Misc. Rept. 79-10, p. 181-185.

Sloss, L. L., 1987. The Williston Basin in the family of cratonic basins. *in*: M. W. Longman, ed., Williston Basin: Anatomy of a Cratonic Oil Province, Rocky Mountain Association of Geologists, p. 1-8.

Smith, D. L., 1964. A lithologic study of the Stony Mountain and Stonewall formations in southern Manitoba. Abst Min. J., v. 85, p. 114, 117.

Thomas, G. E., 1954. The Mississippian of the northeastern Williston Basin. Bull. C.I.M.M., v. 47, p. 136-142.

Toop, D. C., 1992. Petroleum hydrogeology and hydrochemistry of south-central Saskatchewan. Unpublished M.Sc. thesis, Department of Geology, University of Alberta, Edmonton, Alberta, Canada, 172 p.

Toop, D. C. and Tóth, J., 1995. Hydrogeological characterization of formation waters using ionic ratios, south-central Saskatchewan. *in:* L. D. V. Hunter and R. A. Schalla, eds., Seventh International Williston Basin Symposium, Montana Geological Society, p. 313-319.

Tóth, J., 1963. A theoretical analysis of groundwater flow in small drainage basins. Journal of Geophysical Research, v. 68, p. 4795-4812.

Tóth, J., 1978. Gravity-induced cross-formational flow of formation fluids, Red Earth region, Alberta, Canada: Analysis, patterns, evolution. Water Resources Research, v. 14, p. 805-843.

Tóth, J., 1984. The role of gravity flow in the chemical and thermal evolution of ground water. *in*: B. Hitchon and E. I. Wallick, eds., First Canadian/American Conference on Hydrogeology; Practical Applications of Groundwater Geochemistry, National Water Well Association, Banff, Alberta, Canada, p. 3-39.

Tóth, J., 1995. Hydraulic continuity in large sedimentary basins. Hydrogeology Journal, v. 3, p. 4-16.

Tóth, J. and Millar, R. F., 1983. Possible effects of erosional changes of the topographic relief on pore pressures at depth. Water Resources Research, v. 19, p. 1585-1597.

Tóth, J. and Corbet, T. F., 1986. Post-Paleocene evolution of regional groundwater flow-systems and their relation to petroleum accumulations, Taber area, southern Alberta, Canada. Bulletin of Canadian Petroleum Geology, v. 34, p. 339-363.

Tóth, J. and Almasi, I., 2001. Interpretation of observed fluid potential patterns in a deep sedimentary basin under tectonic compression: Hungarian Great Plain, Pannonian Basin. Geofluids, v. 1, p. 11-36.

Van Delinder, D. G., 1984. Source of oils in Cretaceous fields of southern Saskatchewan. *in*: J. A. Lorsong and M. A. Wilson, eds., Saskatchewan Geological Society Special Publication 6, p. 113-118.

Vigrass, L. W., 1971. Depositional framework of the Winnipeg Formation in Manitoba and eastern Saskatchewan. Geological Association of Canada, Special Paper No. 9, p. 225-234.

Weaver, T. R., Frape, S. K., and Cheery, J. A., 1995. Recent cross-formational fluid flow and mixing in the shallow Michigan Basin. Geological Society of America Bulletin, v. 107, p. 697–707.

Whittaker, S. and Gilboy, C., 2003. IEA Weyburn CO_2 Monitoring and Storage Project: Geoscience Framework Update. *in:* Summary of Investigations 2003, Volume 1, Saskatchewan Geological Survey, Saskatchewan Industry Resources, Misc. Rep. 2003-4.1, CD-ROM, Paper A-7, 9 p.

Whittaker, S., Rostron, B. J., Khan, D., Hajnal, Z., Qing, H., Penner, L., Maathuis, H., and Goussev, S., 2004. IEA GHG Weyburn CO_2 Monitoring & Storage Project Summary Report 2000-2004. *in:* M. Wilson and M. Monea, eds., Seventh International Conference on Greenhouse Gas Control Technologies, Petroleum Technology Research Centre, v. 1, 273 p.

Williams, G. D. and Burk, C. F. Jr., 1964. Upper Cretaceous. *in*: R. G. McCrossan and R. P. Glaister, eds., Geological History of Western Canada, Alberta Society of Petroleum Geologists, p. 169-189.

Wilson, J. L., 1967. Carbonate-evaporite cycles in Lower Duperow Formation of Williston Basin. Bulletin of Canadian Petroleum Geology, v. 15, p. 230-312.

APPENDIX A: WATER CHEMISTRY CULLING

Charge Balance Error

Charge balance error is the fundamental parameter in the true quality control of chemical analyses. Poor quality analyses are routinely detected by the simple procedure of calculating ion balances (Davis, 1988). The percent charge balance error (%CBE) is calculated (Freeze and Cherry, 1979) as:

$$\%CBE = \left[\frac{\sum Z \times m_c - \sum Z \times m_a}{\sum Z \times m_c + \sum Z \times m_a} \right] \times 100\% \qquad (A.1)$$

where: Z is the absolute value of the ion's charge; and m_c and m_a are molalities of the cationic and anionic species respectively.

In the Geofluids database, analytical error and incomplete analyses are identified. According to Freeze and Cherry (1979), overestimation of one cation (such as Na) and an equivalent underestimation of another does not ensure that the analysis is accurate. This compensation can create false chemical quantities and in particular the Geofluids database often calculates "sodium by difference", whereby this stoichiometric calculation is performed to evaluate non-reported species. Sodium by difference is calculated by taking the difference between the total dissolved solids (TDS) and the sum of the anions. For this study, irrespective of the Geofluids database, the charge balance errors are re-calculated for all samples and any analyses exceeding a plus or minus 10% CBE, are flagged and often subsequently culled from further mapping (including analyses where only Cl is reported).

Identification of Contaminated Samples

A number of criteria were implemented to identify potential contamination of the formation water by drilling completion fluids such as acid water, corrosion inhibitors, mud filtrates, and alcohols. These criteria were employed using a spreadsheet and a series of calculations simply identify the sample as satisfying the parameter or not (Alkalali, 2002; Khan, 2006). This true/false procedure was translated numerically into true equaling 1 and false equaling 0. With these numerical flags assigned, a summation of the parameters would result in a score indicating the quality of the sample. High scores relate to potentially poor quality contaminated samples and few to zero flags indicates the sample is likely to be representative of formation water.

The following list indicates the criteria applied to all water analyses in an attempt to identify contaminated samples (the ratios below are mass-based):

1) pH < 5 or > 8: The pH can be diagnostic of samples containing acid water completion fluid (pH < 5) or corrosion inhibitor completion fluid (pH > 8).
2) Hydroxide reported (OH^-): If OH is reported for the sample then a score of one is given because a substantial amount of mud may have been recovered during the test.
3) Carbonate reported (CO_3^{2-}): Phase equilibria for reactions involving carbon dioxide dissolved in water identify that CO_3 cannot exist in pH environments below 8.1 (Langmuir, 1997). For most subsurface brines the ionic species CO_3 will not exist naturally in solution unless the pH has been altered due to drilling fluids. Therefore, analyses were flagged and given a score of one if any CO_3 was reported (alkalinity in regional groundwater samples is reported as total HCO_3).
4) Density < 1 g/cm^3: If an alcohol was introduced into the drilling fluids the density of the sampled water maybe less than 1g/cm^3: this is uncharacteristic for formation brines.
5) Ca/Cl > 0.3 and pH < 5.7: This criterion is calculated to identify an acid water completion fluid.
6) Na/Ca < 1.2: If the ratio of sodium to calcium is not large then a flag is set to true as being possibly contaminated with acid water completion fluid.
7) Na/Ca < 5 and Na/Mg < 10 and pH < 6: This rarely encountered criterion is indicative of acid water completion fluid.

8) Na/K < 20: If the ratio of Na/K is small then a flag is set to true as a possible potassium chloride mud filtrate (KCL) used for "kill fluid" in drilling.

9) Na/Cl > 1: The anion Cl is often the dominant species dissolved in formation waters and when the ratio of Na/Cl is greater than one, a flag is set to true because this can often be characteristic of a large mud recovery.

10) Na/Cl > 3.5 and SO_4/Cl > 1.5: This criterion is rarely matched, although when found it is characteristic of the use of a corrosion inhibitor used in drilling fluids.

11) No interval: This is identified because it is not uncommon to find a water analysis where the testing interval is either missing, and must be assigned, or is not reported. When this occurred the water analysis was immediately highlighted and removed from subsequent mapping if the interval was not possible to determine.

12) Recovery < 100 metres (measured using drill pipe stands): The majority of water analyses in a regional mapping study are derived from historic oil and gas formation tests. These drill stem tests can recover water, oil, gas and mud. Therefore, the relative proportions of recovered fluids and recovery descriptions are important to determine what fluid was dominantly analyzed. This is often defined as the hydrodynamic factor and a letter designation is assigned to quantify the dominant fluid recovered. If in the event the recovery was low (less than 100 metres) then a flag is assigned because the lower the recovery often the less representative sample was attained from the formation.

In addition to these specific queries of the water constituents, a number of other variables can be used to determine the quality of the analyses. Sampling point location is one and often is used to identify where in the fluid column a sample has been taken. Locations in the drill pipe string range from the top, middle, and bottom of the fluid column, above the tool a certain distance, top of tool (above the down-hole sampler), and the down-hole sampler. The down-hole sampler is the preferred location, although representative samples can also be found at the top of the fluid column. Essentially, the lower in the fluid column the better the sample because a larger volume of formation fluids has entered the sampling points (a useful analogy is the procedure of purging a well volume from a water well in a shallower horizon). If the sample was taken from a DST then referring to the flow periods and DST chart can help to determine formation permeability and whether a sufficient sample was collected during the test.

APPENDIX B: PRESSURE DATA CULLING

A number of criteria were used to cull pressures examined for this study and they are as follows:

1) Interval length: The length of the test interval can often be too large for an accurate pressure reading and sometimes can be anomalously huge (over 50 metres).
2) Hydrofax quality code: Data vendors assign a code that signifies the test result as ranging from best quality (A), nearing stabilization (B), possible fluid plugging (C), misrun/questionable (D), low permeability and low pressure (E), low permeability and high pressure (F), and misrun (G).
3) Qualitative permeability: Similar to the hydrofax quality code, this code describes the permeability based on the shape of the shut-in curve. Permeabilities are assigned as excellent (EX) when the final flow pressure has stabilized with the final shut-in pressure; high (HI) corresponding to nearing stabilization of both flow and shut-in pressures; relatively high (RH) with flow and shut-in pressures still building slightly; average (AV) when the flowing and shut-in pressures are still building fairly rapidly; relatively low (RL) indicating that the flow pressures are low and shut-in pressures are building rapidly; low (LO) signifying poor flowing pressures and rapidly building shut-in pressures; and finally virtually none (VN) when flow pressures are nearly nil and shut-in pressures are building much too rapidly to accurately extrapolate.
4) Qualitative hydro factor: A simple calculation that is based on the total recovery during the DST. If water, mud, drilling fluid cushion, oil or gas were recovered the largest fluid recovery will be identified and denoted by W, M, CSH, O, or G respectively.
5) Flow and shut-in times: This is the length of time that the well is allowed to flow into the drill-pipe and subsequently closed-in for pressure build-up back to reservoir conditions. The longer the flow and shut-in times the more accurate a representation of the true formation pressure.

6) Recovery, gas blow and test comments: Another indication of what was recovered during the test, the gas blow description during the flow periods and overall the quality and mechanical description of the test.

7) DST chart: The visual inspection of the DST pressure-time chart gives an excellent indication and overview of exactly how the formation was responding during the test.

APPENDIX C: FRESHWATER HYDRAULIC HEAD MAPS

The Figures C.1 to C.19 (pages 175 to 193) have been removed at the request of the Faculty of Graduate Studies and Research at the University of Alberta. These tabloid sized maps will not be included in the microfilming version of this dissertation.

APPENDIX D: CALCULATING DRIVING FORCES ON FORMATION WATERS

Estimation of in-situ formation water densities

Khan (2006) used the equation of state developed by Chierici (1994) to accurately represent formation water densities in the Williston Basin. The Chierici (1994) equation of state underestimated the densities by less in comparison to the algorithm developed by Batzle and Wang (1992), and the review of various equations of state completed by Adams and Bachu (2002). The Chierici equation of state was used here based on the discussion found in Khan (2006).

Formation water densities according to Chierici's (1994) equation of state are calculated as follows:

$$\begin{aligned} p_w = {} & 730.6 + 2.025T - 3.8 \text{ x } 10^{-3} T^2 + \left[2.362 - 1.197 \text{ x } 10^{-2} T + 1.835 \text{ x } 10^{-5} T^2\right] P \\ & + \left[2.374 - 1.024 \text{ x } 10^{-2} T + 1.49 \text{ x } 10^{-5} T^2 - 5.1 \text{ x } 10^{-4} P\right] C \end{aligned} \tag{D.1}$$

where p_w is the formation water density, P is the pressure (in MPa) with the range of validity between 0-50 MPa, T is the temperature (K) applicable over 293-373 K, and C is the salinity that is valid for the range of brines within this study (Khan, 2006).

Calculation of Water Driving Force Vectors

The procedure to calculate the Water Driving Force (WDF) follows Khan (2006).

For variable density flow systems, Darcy's law in three-dimensions aligned along the coordinate axes can be represented as follows (Hubbert, 1953):

$$q_i = \frac{-k_{ij}}{u_o} \frac{u_o}{u} \left[\nabla h + \frac{p - p_o}{p_o} \nabla z \right], \; i = 1,2,3 \tag{D.2}$$

where: q is the specific discharge in the i^{th} direction, k is the rock absolute permeability tensor, u is the dynamic fluid viscosity, p is the fluid density, h is the hydraulic head, and z is the elevation. Subscript o refers to standard pressure and temperature conditions of the reference state.

Davies (1987) has written equation (D.2) for confined flow in a sloping aquifer as follows:

$$q(x,y) = \frac{-k}{u_o}\frac{u_o}{u}\left[\nabla h + \frac{p-p_o}{p_o}\nabla E\right] \tag{D.3}$$

where: *E(x,y)* represents the elevation of the underlying stratigraphic horizon forming the base of the confined aquifer. The net driving force on formation water at a particular point is achieved by the vectorial addition of the two terms within the brackets of equations (D.2) and (D.3) (Figure D.1). Therefore, the analytical solution for the Water Driving Force (WDF) is calculated as follows:

$$WDF = \nabla h + \frac{\Delta p}{p_o}\nabla E \tag{D.4}$$

where: h is the freshwater hydraulic head, Δp is the density difference between the calculated in-situ formation water and freshwater, p_o is the density of freshwater, and E is the elevation of the aquifer base.

The assumptions that Davies (1987) has made are the aquifer is confined, gently sloping, isotropic, and flow is parallel to the aquifer plane (strictly horizontal flow). In essence, the pressure-related driving force component is a function of the hydraulic gradient, while the density-related driving force is a product of the structural gradient and ratio of the difference in relative densities to that of freshwater (Figure D.1).

$$WDF = \nabla h + \frac{\Delta p}{p_o} \nabla E$$

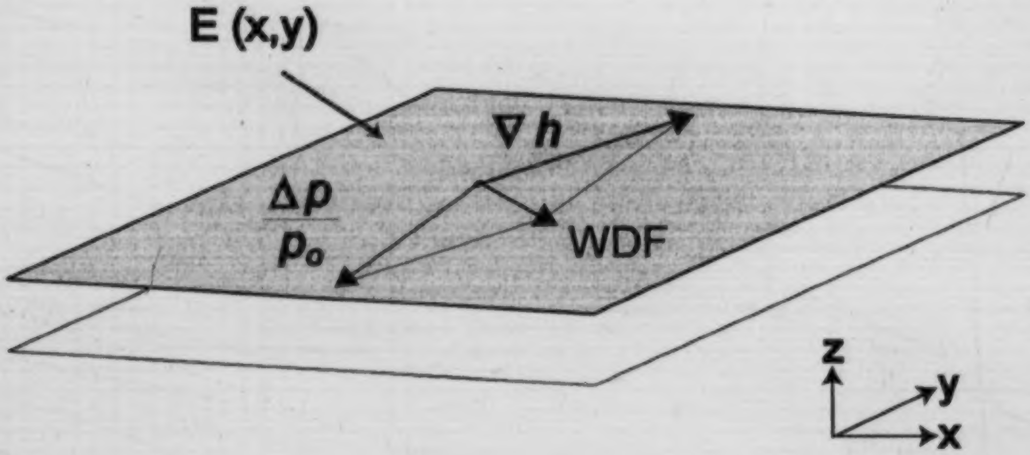

Figure D.1. Schematic representation of the Water Driving Force components in the analytical calculation of density-dependent water driving force (modified after Khan, 2006).